

# Antiviral Polymeric Drugs and Surface Coatings

by

Alyssa Maxine Larson

B.S. in Biochemistry  
University of California, Santa Barbara, 2008

Submitted to the Department of Chemistry  
in Partial Fulfillment of the Requirements of the Degree of

Doctor of Philosophy in Biological Chemistry

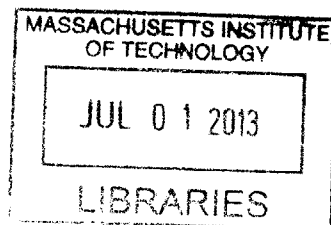
at the

MASSACHUSETTS INSTITUTE OF TECHNOLOGY

June 2013

© 2013 Massachusetts Institute of Technology  
All rights reserved

**ARCHIVES**



Signature of Author: \_\_\_\_\_  
Department of Chemistry  
April 26, 2013

Certified by: \_\_\_\_\_  
Alexander M. Klibanov  
*Firmenich Professor of Chemistry and Bioengineering*  
*Thesis Supervisor*

Accepted by: \_\_\_\_\_  
Robert W. Field  
*Haslam and Dewey Professor of Chemistry*  
*Chairman, Departmental Committee on Graduate Students*

This Doctoral Thesis has been examined by a committee of the Department of Chemistry as follows:

---

John M. Essigmann  
*William R. and Betsy P. Leitch Professor of Chemistry and Biological Engineering*  
*Thesis Committee Chair*

---

Alexander M. Klibanov  
*Firmenich Professor of Chemistry and Bioengineering*  
*Thesis Supervisor*

---

Elizabeth M. Nolan  
*Pfizer Laubach Career Development Assistant Professor of Chemistry*  
*Thesis Committee Member*

# Antiviral Polymeric Drugs and Surface Coatings

by

Alyssa Maxine Larson

Submitted to the Department of Chemistry on April 26, 2013, in Partial Fulfillment of the Requirements for the Degree of Doctor of Philosophy in Biological Chemistry

## Abstract

Viruses are a major cause of human morbidity and mortality in the world. New effective approaches to stop their spread are paramount. Herein, two approaches toward this goal are explored: (i) developing multivalent therapeutics (multiple copies of an antiviral agent covalently attached to a polymeric chain) with superior potency against their viral targets, and (ii) creating antiviral surface coatings that detoxify aqueous solutions containing various viruses on contact.

By harnessing the power of multivalency we endeavored to improve the potency of influenza inhibitors, as well as resurrect the potency of two FDA-approved influenza inhibitors for which widespread drug resistance now exists. In the former direction of research, we attached multiple copies of bicyclic naphthoquinone-like monomeric inhibitors to polymeric chains. When tested against the Wuhan strain of influenza, these multivalent conjugates were up to 240-fold more potent inhibitors than their monomeric predecessors. However, this improvement in potency was strain-dependent, as two other serotypically-different influenza strains were not inhibited nearly as well by multivalent inhibitors.

This strategy was also employed to restore inhibition for the adamantane class of influenza inhibitors against drug-resistant strains. The chemical modifications to the adamantane scaffold necessary for polymer attachment imposed deleterious steric constraints which resulted in poorer inhibitory effect. Even despite these drawbacks, however, the drug-polymer conjugates were up to 30-fold more potent against drug-resistant strains than their monomeric counterparts. These efforts made strides toward the ultimate goal of recovery of influenza virus inhibition for the adamantanes.

To diminish transmission of viral infections, we explored the action of antimicrobial PEI-based (PEI = polyethylenimine) hydrophobic polycations against both enveloped and non-enveloped viruses. When solutions containing herpes simplex viruses (both 1 and 2) were brought in contact with *N,N*-dodecyl,methyl-PEI coated on either polyethylene slides or latex condoms, they could be disinfected by up to 6-logs of viral titers. Our hydrophobic polycation also could be formulated into a suspension to disinfect herpes simplex virus-containing solutions, suggesting potential utility in a therapeutic modality.

We also investigated whether these findings were applicable to non-enveloped viruses, namely poliovirus and rotavirus. Aqueous solutions containing them indeed could be drastically disinfected by our hydrophobic polycation-coated slides; subsequent mechanistic studies suggested that this disinfection was due to adsorption of the viruses onto the coated surfaces from solution.

Thesis Supervisor: Dr. Alexander M. Klibanov

Title: Firmenich Professor of Chemistry and Bioengineering

## Acknowledgements

This PhD is the result of the support and love from many very special people, all of whom have contributed to my intellectual and personal growth for the past 5 years. I am grateful to my advisor, Alex Klibanov, who has taught me much more than how to be a scientist. Thank you for your “tough love” which helped me to develop “thick skin” as well as your endless jokes, stories, and anecdotes. Although you were not completely successful in “de-honeying” my voice, I believe you have made strides, and for that you should be proud. I am also appreciative to my thesis chair, Professor John Essigmann, for his intellectual guidance and help in getting into MIT by providing valuable feedback on my admissions essay. It was a joy to TA for you and I always cherished our several hour-long yearly meetings. Thank you to Professors Liz Nolan and Jianzhu Chen for their help in my research progress.

I am eternally grateful to my family and friends for keeping me sane these past 5 years. To my parents- thank you for your mental (and sometimes financial) support, for making many trips to the east coast, and for always being so excited about my research, even when I wasn't. To Lia- I am so glad we have been able to grow closer and enjoy many quick weekend trips since 2008 with good food, good wine, and excellent company. I can't wait to take you out once I get my first paycheck. To Pat- thank you for your love, support, and constant reminders that there is life outside buildings 56 and 78. Thanks for being my beeb. To Steph- you are my MIT chemistry soul mate. If we hadn't become friends I am nearly certain I wouldn't have made it through. Thank you for all the amazing times at Tommy Doyles, the hundreds of Magners we've consumed together, and for being such an amazing friend since August of 2008. You are my (hunter) hero! To Jeremy and Emily- Thank you both for your fantastic friendships. Jeremy- our multi-weekly Starbucks trips were a pivotal part of my coping mechanism for stress at MIT. Working with you on all of our non-lab related endeavors was a delight. I am so glad that we saw each other in the free stuff like at SidPac! Emily- I have adored our girls' nights, shopping trips to Marshalls, and our many Harpoon Brewery excursions. I am so glad that Jeremy shared you with us! To all my other friends at MIT and elsewhere- thanks for the fun times at the Muddy, Boston visits, phone calls, emails, etc. I truly cherish you all.

Thank you to all Klibanov and Chen lab members (past and present) for your help with science, career advice, and for your friendships. To Jen- thank you for all the lunch dates and advice you gave me my first two years. It was great working with you and your professionalism and poise were inspirational to me. To Alisha- thank you for teaching me how to run chemical reactions and to perform plaque assays, both of which were pivotal to my research.

I am also grateful for the guidance I received from my GW@MIT mentor Lynne Wilson, who has been an invaluable resource for me as I transition from student to scientist.

Thank you to all of the Professors, students, admins, technicians, collaborators, classmates, and student group leaders who I have had the privilege to work with over the past 5 years. It has been a great honor. MIT is a very special place, and although at times it can be overwhelming and stressful, I am glad that I had the love and support to make it through. It has provided me with opportunities that no other institution could and it enabled me to have a very unique PhD experience that I am both proud of and thankful for.

## Table of Contents

Abstract.....	3
Acknowledgements.....	4
Table of Contents.....	5
List of Figures.....	7
List of Tables.....	8
List of Abbreviations.....	9
<b>Chapter 1. Background, significance, and thesis overview</b>	
A. Introduction.....	12
B. References.....	17
<b>Chapter 2. Conjugating drug candidates to polymeric chains does not necessarily enhance anti-influenza activity</b>	
A. Introduction.....	22
B. Results and Discussion.....	23
C. Materials and Methods.....	37
D. References.....	42
<b>Chapter 3. Conjugation to polymeric chains of influenza drugs targeting M2 ion channels partially restores their inhibition of drug-resistant mutants</b>	
A. Introduction.....	48
B. Results and Discussion.....	49
C. Materials and Methods.....	61
D. References.....	66
<b>Chapter 4. Decreasing herpes simplex viral infectivity in solution by surface-immobilized and suspended <i>N,N</i>-dodecyl,methyl-polyethylenimine</b>	
A. Introduction.....	70
B. Results and Discussion.....	71
C. Materials and Methods.....	78
D. References.....	84
<b>Chapter 5. Hydrophobic polycationic coatings disinfect poliovirus and rotavirus solutions</b>	
A. Introduction.....	89
B. Results and Discussion.....	90
C. Materials and Methods.....	94
D. References.....	98
<b>Chapter 6. Biocidal packaging for pharmaceuticals, foods, and other perishables</b>	
A. Introduction.....	101
B. Active Biocide-releasing Packaging.....	103
C. Active Packaging Materials that Do Not Release a Biocide.....	111
D. References.....	120

**Appendix**

A. Selected NMR spectra from Chapter 2.....132  
B. Selected NMR spectra from Chapter 3.....137  
C. Selected NMR spectra from Chapter 4.....152  
**Curriculum Vitae**.....154

## List of Figures

Figure 1-1	Cartoon of influenza A virus	13
Figure 1-2	Structure of DMPEI	15
Figure 2-1	Chemical structures of 5-hydroxynaphthalene-1,4-dione and its analogs	23
Figure 2-2	Chemical structures of previously reported anti-hemagglutinin agents	24
Figure 2-3	Chemical structures of anti-influenza inhibitors attached to polymers	26
Figure 2-4	Docking results of hemagglutinin inhibitors on two representative influenza strain hemagglutinins	34
Figure 2-5	A cartoon depicting a multivalent vs. a monovalent interaction of an inhibitor with the influenza A virus	36
Figure 3-1	Chemical structures of the two FDA-approved adamantane-class M2 ion channel influenza A inhibitors	48
Figure 3-2	Synthetic route to generate amantadine-linker-azide for subsequent covalent attachment to poly-L-glutamate	49
Figure 3-3	Synthetic route to generate rimantadine-linker-azide compounds for subsequent covalent attachment to polymers	50
Figure 3-4	Chemical structures of poly-L-glutamate derivatized with amantadine or rimantadine at various degrees of loading	51
Figure 3-5	Chemical structures of poly-L-glutamate derivatized with rimantadine and various hydrophobic moieties	58
Figure 3-6	Chemical Structures of poly-L-glutamine, poly(acrylic acid Na salt), and carboxymethylcellulose Na salt derivatized with rimantadine	59
Figure 4-1	Reduction of viral titers of HSV-1 and -2 when incubated the presence of a DMPEI-coated polyethylene slide or a plain one	71
Figure 4-2	Reduction of viral titer of HSV-1 when incubated with PMPEI or PEI	72
Figure 4-3	Reduction of viral titer of HSV-1 when incubated in the presence of a DMPEI suspension	74
Figure 4-4	Reduction of viral titers of HSV-1 and -2 when incubated in PBS thickened with 1.5% HEC in which various concentrations of DMPEI were suspended	75
Figure 4-5	Reduction of viral titers of HSV-1 and -2 when incubated in the presence of piece of latex condom coated with DMPEI or a plain one	77
Figure 5-1	Reduction of viral titer of poliovirus when incubated the presence of a DMPEI-coated polyethylene slide, HMPEI-coated glass slide or plain slides	90
Figure 5-2	The time course of reduction in viral titer against rotavirus from a polyethylene slide coated with DMPEI or a plain one	93
Figure 6-1	Schematic depiction of various forms of biocidal active packaging	102
Figure 6-2	Schematic representation of the derivatization of polytetrafluoroethylene with the antibiotic ampicillin	112
Figure 6-3	Live-dead analysis of <i>S. aureus</i> cells after exposure to an underivatized amino-glass slide or of that covalently derivatized with HMPEI	115
Figure 6-4	Scanning electron microscopy images of <i>S. aureus</i> and <i>E. coli</i> cells after interaction with either plain silicon wafers or DMPEI-coated ones	117
Figure 6-5	Scanning electron microscopy images of influenza viral particles incubated with either plain silicon wafers or DMPEI-coated ones	118
Figure 6-6	Schematic mechanism of inactivation of influenza virus by DMPEI-coated surfaces	119

## List of Tables

Table 2-1	IC <sub>50</sub> values for both small molecule influenza inhibitors and their polymer-attached derivatives against the Wuhan strain of influenza A virus	27
Table 2-2	IC <sub>50</sub> values for both small molecule influenza inhibitors and their polymer-attached derivatives against the PR8 and turkey strains of influenza A virus.	30
Table 2-3	IC <sub>50</sub> values for 5-hydroxy-2-methyl-1,4-naphthalenedione, that attached to poly-L-glutamate, and that with a linker against three influenza A virus strains	31
Table 2-4	IC <sub>50</sub> values for 5-hydroxy-2-methyl-1,4-naphthalenedione conjugated to polymers of varying degrees of backbone charge against the Wuhan and turkey strains of influenza A virus.	32
Table 3-1	The IC <sub>50</sub> values for both monomeric amantadine and its poly-L-glutamate conjugates against the Wuhan, PR8, and WSN strains of influenza A virus	54
Table 3-2	The IC <sub>50</sub> values for monomeric rimantadine, 3-(1-aminoethyl)adamantan-1-ol, as well as for the latter's various polymer conjugates against the Wuhan, PR8, and WSN strains of influenza A virus	56
Table 4-1	Antiviral activity against HSV-1 and toxicity toward Vero cells of DMPEI suspensions	75
Table 5-1	The recovery of infectious poliovirus by washing uncoated and DMPEI-coated polyethylene slides with the detergents cetyltrimethylammonium chloride and Tween 80 after exposure to poliovirus solutions	92



## Abbreviations

Standard 1-letter codes are used for amino acids

ATCC	American type culture collection
BCS	bovine calf serum
CC <sub>50</sub>	50% cell cytotoxicity concentration
CMC	carboxymethylcellulose
CTAC	cetyltrimethylammonium chloride
DCC	<i>N,N'</i> -dicyclohexylcarbodiimide
DDTMAC	dodecyltrimethylammonium chloride
DIC	<i>N,N'</i> -diisopropylcarbodiimide
DMPEI	<i>N,N</i> -dodecyl,methyl-polyethylenimine
DMEM	Dulbecco's modified Eagle medium
DMAP	4-dimethylaminopyridine
DMF	dimethylformamide
DPTC	di(2-pyridyl)thionocarbonate
EMEM	Eagle's minimum essential medium
FBS	fetal bovine serum
FDA	Food and Drug Administration
Fmoc-Cl	fluorenylmethyloxycarbonyl chloride
HA	influenza hemagglutinin protein
HxNy	hemagglutinin(serotype#)neuraminidase(serotype#)
HBTU	<i>O</i> -(benzotriazol-1-yl)- <i>N,N,N',N'</i> -tetramethyluronium hexafluorophosphate
HEC	hydroxyethyl-cellulose
HMPEI	<i>N,N</i> -hexyl,methyl-polyethylenimine
HSV	herpes simplex virus
HSV-1	herpes simplex virus-1 KOS strain
HSV-2	herpes simplex virus-2 186syn <sup>+</sup> -1 strain
IC <sub>50</sub>	half-maximal inhibitory concentration
IgG	human immunoglobulin G
MDCK	Madin Darby canine kidney cells
MES	2-( <i>N</i> -morpholino)ethanesulfonic acid
MW	molecular weight
MTS	[3-(4,5-dimethylthiazol-2-yl)-5-(3-carboxymethoxyphenyl)-2-(4-sulfophenyl)-2H-tetrazolium
NHS	<i>N</i> -hydroxysuccinimide
NMR	nuclear magnetic resonance
PBS	phosphate-buffered saline
PEI	polyethylenimine
PFU	plaque forming units
PMPEI	per-methylated polyethylenimine
PR8	influenza strain A/PR/8/34 (human)
PTFE	polytetrafluoroethylene
SAR	structure-activity relationship
THF	tetrahydrofuran
Turkey	influenza strain A/turkey/MN/833/80 (avian)

Wuhan	influenza strain A/Wuhan/359/95 (human)
WSN	influenza strain A/WSN/33 (laboratory adapted, human)
X31	influenza strain A/X-31 (laboratory adapted, human)

## CHAPTER 1

Background, significance, and thesis overview

## **A. Introduction**

Viruses are ubiquitous in the environment and our lives. One cannot go more than a few days without seeing a news story about some viral strain, new or old, wreaking havoc on humans who encounter it. Because of their stealth nature, many viruses evade the immune system of their host and cause chronic illnesses or sometimes deadly acute infections.<sup>1</sup> Even for those viruses against which we are fortunate enough to have therapies, it is generally only a matter of time before resistance develops.<sup>2-6</sup> Vaccines, arguably one of the most important medical breakthroughs of the 20<sup>th</sup> century, can provide protection against a variety of viral pathogens; however, even with their overwhelming success against some viruses,<sup>7,8</sup> there are many others, for example, HIV or herpes simplex viruses, for which effective vaccines have yet to be developed.<sup>9-11</sup> Additionally, viruses like influenza mutate so often that new vaccines must be administered each year to combat them.<sup>1,12</sup> Furthermore, these vaccines are developed based on educated guesses as to what epitopes will be present on the following year's circulating influenza strains;<sup>1,13,14</sup> unfortunately, these guesses are not always accurate.

Transmission of many viruses from person to person often occurs through contaminated surfaces, also known as fomites.<sup>15</sup> In this case, an infected individual might cough or sneeze onto a surface after which a healthy person will touch it and potentially contract the virus. Other viruses, such as herpes simplex viruses and HIV, can be transmitted through sexual intercourse.<sup>16</sup> The limitations of our current arsenal against viral infections necessitate additional, novel methods to combat viruses, either through more potent and efficacious therapeutics or by reducing their spread.

In the Klibanov lab, we are investigating two alternative and distinct approaches utilizing polymeric materials to tackle these issues. The first involves exploring the effects of multivalent

inhibitors against influenza viruses. Influenza A virus (Figure 1-1) is a spherical, enveloped virus, with a segmented RNA genome.<sup>17</sup> The virus is decorated with many copies of three surface proteins. The first, hemagglutinin (HA), is a trimeric protein that is responsible for recognizing terminal sialic acid moieties on host cells and binding to them to initiate infection.<sup>17</sup> The Neuraminidase (NA) protein is involved in the final step of viral infection that allows progeny virions to escape the infected cell so that they may infect new cells.<sup>17</sup> Neuraminidase is the target of two of the four FDA-approved small molecule influenza inhibitors, namely Zanamivir and Oseltamivir.<sup>18</sup> The last surface protein, the M2 ion channel, is paramount in viral uncoating; that is, the release of influenza's segmented viral RNA genome into the cell during infection.<sup>17</sup> It is the target of the other two FDA-approved small molecule influenza inhibitors, amantadine and rimantadine.<sup>19</sup> Unfortunately, due to the occurrence of a variety of single-point mutations in the M2 ion channel, nearly all circulating influenza strains have developed resistance to amantadine and rimantadine. Therefore they are no longer recommended for use for treatment of influenza infection.<sup>20,21</sup>

## Influenza A virus

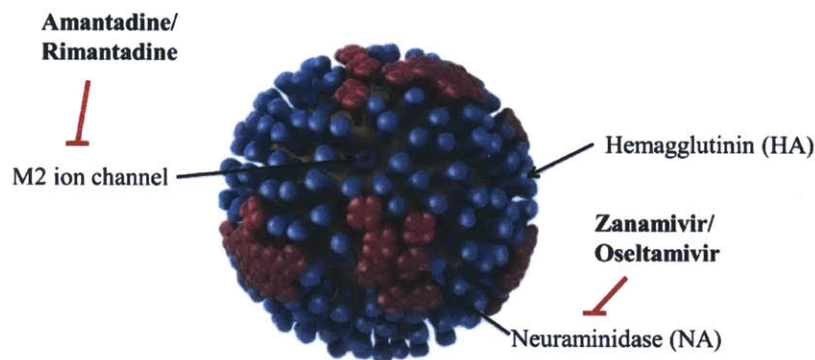


**Figure 1-1.** Cartoon depicting influenza A virus. Three surface proteins are shown. The hemagglutinin protein depicted in blue helps initiate infection while the neuraminidase protein in depicted in pink allows for progeny viral escape. The M2 ion channel depicted in purple aids in viral uncoating. Adapted from cdc.gov.

Previously, it has been shown by us and others that attachment of multiple copies of influenza surface protein ligands or inhibitors to flexible polymeric chains vastly improves their potency compared to that of their monomeric parents.<sup>18,22-26</sup> This improvement in potency is due to multivalency, whereby multiple simultaneous interactions between polymer-drug conjugates and receptors on the viral surface result in an enhanced binding avidity.<sup>24</sup> For the FDA-approved neuraminidase inhibitor zanamivir, we have recently discovered that this improvement in potency can also be attributed to an additional drug mechanism that is unique to the drug-polymer conjugate.<sup>23</sup> Importantly, the zanamivir-polymer conjugates are effective at potently inhibiting not only native influenza strains, but also zanamivir-resistant ones. This latter action is attributed to multivalency and likely the aforementioned alternative mechanism.<sup>18,23</sup>

In **Chapter 2** of this thesis, I will discuss a quest for multivalent inhibition by literature-predicted influenza inhibitors which target the hemagglutinin protein. Using the plaque reduction assay, relatively simple bicyclic quinone molecules, as well as multiple copies thereof covalently attached to a long polyglutamate-based polymeric chain, were examined as new inhibitors of various naturally-occurring strains of influenza A virus. The polymer-conjugated inhibitors were found to have a far greater potency (for some as high as two orders of magnitude when a long spacer arm was employed) than their corresponding parent molecules against the human Wuhan influenza strain. However, such polymeric inhibitors failed to exhibit higher potency compared to their small-molecule predecessors against the human PR8 and avian turkey influenza strains. These observations, further explored by means of molecular modeling, reveal the previously unrecognized unpredictability of the benefits of multivalency, possibly because of poor accessibility of the viral targets to polymeric agents.

**Chapter 3** also addresses multivalent influenza inhibitors; however, instead of attempting to improve new influenza inhibitors (as in Chapter 2) we endeavored to “resurrect” the inhibitory potency of the two FDA-approved adamantane-class M2 ion channel influenza inhibitors. As mentioned above, these drugs are no longer recommended for use to treat influenza infection because of widespread resistance to them. By attaching multiple copies of amantadine or rimantadine to polymeric chains we explored whether it was possible to recover their potency in inhibiting drug-resistant influenza viruses as previously seen in zanamivir examples. Depending on loading densities, as well as the nature of the drug, the polymer, and the spacer arm, polymer-conjugated drugs were up to 30-fold more potent inhibitors of drug-resistant strains than their monomeric parents. Although a full recovery of the inhibitory action against drug-resistant strains was not achieved, this study may be a step toward salvaging anti-influenza drugs that are no longer effective.

Though therapeutics are an excellent line of defense toward viral infection, it also would be valuable to eliminate the transmission of viruses before they cause disease in their host. By developing antimicrobial surface coatings, we have investigated reducing the transmission of bacteria and viruses from contaminated surfaces. Previously, our lab has developed

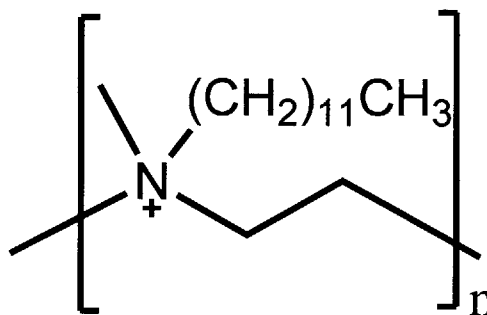


**Figure 1-2.** Chemical structure of *N,N*-dodecyl,methyl-polyethylenimine (DMPEI).

antimicrobial PEI-based (PEI = polyethylenimine) surface coatings which are lethal to *Staphylococcus aureus*, *Escherichia coli*, *Candida albicans*, and influenza.<sup>15,27-31</sup> In **Chapter 4** of this thesis, I discuss my studies characterizing our most efficacious antimicrobial coating, *N,N*-dodecyl,methyl-polyethylenimine (DMPEI) (Figure 1-2), against the previously untested herpes

simplex virus (HSV). In this chapter, surface-immobilized and suspended modalities of DMPEI are explored for their ability to reduce viral infectivity in aqueous solutions containing herpes simplex viruses (HSVs) 1 and 2. In our experiments, DMPEI coated on either polyethylene slides or male latex condoms dramatically decreased infectivity in solutions containing HSV-1 or HSV-2. Moreover, DMPEI suspended in aqueous solution markedly reduced the infectious titer of the HSVs. These results suggest potential uses of DMPEI for both prophylaxis (in the form of coated condoms) and treatment (as a topical suspension) for HSV infections.

Earlier work with our antimicrobially coated surfaces (whether covalently or non-covalently) involved bacteria, fungi, and enveloped viruses (namely, influenza and HSVs).<sup>15,16,28,31</sup> In **Chapter 5**, we explored whether our PEI-based hydrophobic polycations were active against the *non-enveloped* poliovirus and rotavirus. We discovered that covalently derivatizing glass surfaces with branched *N,N*-hexyl,methyl-PEI (HMPEI) or physically depositing (“painting”) linear DMPEI onto polyethylene surfaces enables the resultant coated materials to quickly and efficiently disinfect aqueous solutions containing poliovirus and rotavirus. Subsequent experiments revealed that washing these poliovirus-exposed DMPEI-coated surfaces with a detergent could recover the viruses in their infectious form. Therefore, HMPEI and DMPEI can disinfect solutions containing poliovirus and rotavirus by adsorption of viral particles.

In addition to the spread of disease via fomites as described above, many consumer goods must be protected from bacterial and fungal colonization to ensure their integrity and safety. By making these items’ packaging biocidal, the interior environment can be preserved from microbial spoilage without altering the products themselves. In **Chapter 6**, we briefly review this concept, referred to as “active packaging”, and discuss existing methods for constructing



active packaging systems, highlighting the work done in this regard in our lab. The methods described are based on either packaging materials that release biocides or those that are themselves intrinsically biocidal (or biostatic), with numerous variations within each category.

## **B. References**

1. Knipe DM, Howley PM. 2007. *Fields' Virology*. Philadelphia Wolters Kluwer Health/Lippincott Williams & Wilkins.
2. Gubareva LV. 2004. Molecular mechanisms of influenza virus resistance to neuraminidase inhibitors. *Virus Res.* 103(1):199-203.
3. Pielak RM, Schnell JR, Chou JJ. 2009. Mechanism of drug inhibition and drug resistance of influenza A M2 channel. *Proc Natl Acad Sci.* 106(18):7379-7384.
4. Piret J, Boivin G. 2011. Resistance of herpes simplex viruses to nucleoside analogues: mechanisms, prevalence, and management. *Antimicrob Agents Ch.* 55(2):459-472.
5. De Clercq E. 2006. Antiviral agents active against influenza A viruses. *Nat Rev Drug Disc.* 5(12):1015-1025.
6. Hayden FG, Pavia AT. 2006. Antiviral management of seasonal and pandemic influenza. *J Infect Dis.* 194(Supplement 2):S119-S126.
7. De Quadros CA, Andrus JK, Olive JM, de Macedo CG, Henderson DA. 1992. Polio eradication from the Western Hemisphere. *Annu Rev Publ Health.* 13(1):239-252.
8. Orenstein WA, Papania MJ, Wharton ME. 2004. Measles elimination in the United States. *J Infect Dis.* 189(Supplement 1):S1-S3.
9. Barouch DH. 2008. Challenges in the development of an HIV-1 vaccine. *Nature* 455(7213):613-619.

10. Johnston MI, Fauci AS. 2008. An HIV vaccine—challenges and prospects. *N Eng J Med.* 359(9):888-890.
11. Rajčáni J, Ďurmanová V. 2006. Developments in herpes simplex virus vaccines: old problems and new challenges. *Folia Microbiol.* 51(2):67-85.
12. Perez-Tirse J, Gross PA. 1992. Review of cost-benefit analyses of influenza vaccine. *Pharmacoeconomics.* 2(3):198-206.
13. Leroux-Roels I, Leroux-Roels G. 2009. Current status and progress of pre-pandemic and pandemic influenza vaccine development. *Expert Rev Vaccines.* 8(4):401-423.
14. Smith NM, Bresee JS, Shay DK, Uyeki TM, Cox NJ, Strikas RA. 2006. Prevention and control of influenza: recommendations of the Advisory Committee on Immunization Practices (ACIP). *Morbidity and Mortality Weekly Report.* 55(RR-10):1.
15. Klibanov AM. 2007. Permanently microbicidal materials coatings. *J Mat Chem.* 17(24):2479-2482.
16. Larson AM, Oh H, Knipe DM, Klibanov AM. 2013. Decreasing herpes simplex viral infectivity in solution by surface-immobilized and suspended *N,N*-dodecyl, methyl-polyethylenimine. *Pharm Res.* 30(1):25-31.
17. Lamb RA, Krug RM. 2007. Orthomyxoviridae: The viruses and their replication. In: *Fields' Virology.* Eds., Knipe DM, Howley PM. 5th ed. Philadelphia: Wolters Kluwer Health/Lippincott Williams & Wilkins.
18. Weight AK, Haldar J, Alvarez de Cienfuegos L, Gubareva LV, Tumpey TM, Chen J, Klibanov AM. 2011. Attaching zanamivir to a polymer markedly enhances its activity against drug-resistant strains of influenza A virus. *J Pharm Sci.* 100(3):831-835.

19. Kozakov D, Chuang G-Y, Beglov D, Vajda S 2010. Where does amantadine bind to the influenza virus M2 proton channel? *Trends Biochem Sci.* 35(9):471-475.
20. Bright RA, Shay DK, Shu B, Cox NJ, Klimov AI 2006. Adamantane resistance among influenza A viruses isolated early during the 2005-2006 influenza season in the United States. *JAMA.* 295(8):891-894.
21. Bright RA, Medina M-j, Xu X, Perez-Oronoz G, Wallis TR, Davis XM, Povinelli L, Cox NJ, Klimov AI 2005. Incidence of adamantane resistance among influenza A (H3N2) viruses isolated worldwide from 1994 to 2005: a cause for concern. *Lancet* 366(9492):1175-1181.
22. Haldar J, Alvarez de Cienfuegos L, Tumpey TM, Gubareva LV, Chen J, Klibanov AM. 2010. Bifunctional polymeric inhibitors of human influenza A viruses. *Pharm Res.* 27(2):259-263.
23. Lee CM, Weight AK, Haldar J, Wang L, Klibanov AM, Chen J. 2012. Polymer-attached zanamivir inhibits synergistically both early and late stages of influenza virus infection. *Proc Natl Acad Sci.* 109(50):20385-20390.
24. Mammen M, Choi S-K, Whitesides GM. 1998. Polyvalent interactions in biological systems: implications for design and use of multivalent ligands and inhibitors. *Angew Chemie Int Ed.* 37(20):2754-2794.
25. Sigal GB, Mammen M, Dahmann G, Whitesides GM. 1996. Polyacrylamides bearing pendant  $\alpha$ -sialoside groups strongly inhibit agglutination of erythrocytes by influenza virus: the strong inhibition reflects enhanced binding through cooperative polyvalent interactions. *J Am Chem Soc.* 118(16):3789-3800.

26. Choi S-K, Mammen M, Whitesides GM. 1997. Generation and in situ evaluation of libraries of poly (acrylic acid) presenting sialosides as side chains as polyvalent inhibitors of influenza-mediated hemagglutination. *J Am Chem Soc.* 119(18):4103-4111.
27. Park D, Wang J, Klivanov AM. 2006. One-step, painting-like coating procedures to make surfaces highly and permanently bactericidal. *Biotechnol Prog.* 22(2):584-589.
28. Haldar J, An D, Alvarez de Cienfuegos L, Chen J, Klivanov AM. 2006. Polymeric coatings that inactivate both influenza virus and pathogenic bacteria. *Proc Natl Acad Sci.* 103(47):17667-17671.
29. Haldar J, Chen J, Tumpey TM, Gubareva LV, Klivanov AM. 2008. Hydrophobic polycationic coatings inactivate wild-type and zanamivir- and/or oseltamivir-resistant human and avian influenza viruses. *Biotechnol Lett.* 30(3):475-479.
30. Haldar J, Weight AK, Klivanov AM 2007. Preparation, application and testing of permanent antibacterial and antiviral coatings. *Nat Protoc.* 2(10):2412-2417.
31. Hsu BB, Wong SY, Hammond PT, Chen J, Klivanov AM. 2011. Mechanism of inactivation of influenza viruses by immobilized hydrophobic polycations. *Proc Natl Acad Sci.* 108(1):61-66.

## CHAPTER 2

Conjugating drug candidates to polymeric chains does not necessarily enhance anti-influenza activity

The work presented in this chapter was published in the following manuscript and is reproduced with kind permission from Wiley Periodicals, Inc (Copyright © 2012):

Larson AM, Wang H, Cao Y, Jiang T, Chen J, Klivanov AM. 2012. Conjugating drug candidates to polymeric chains does not necessarily enhance anti-influenza activity. *J Pharm Sci.* 101(10):3896-905.

## A. Introduction

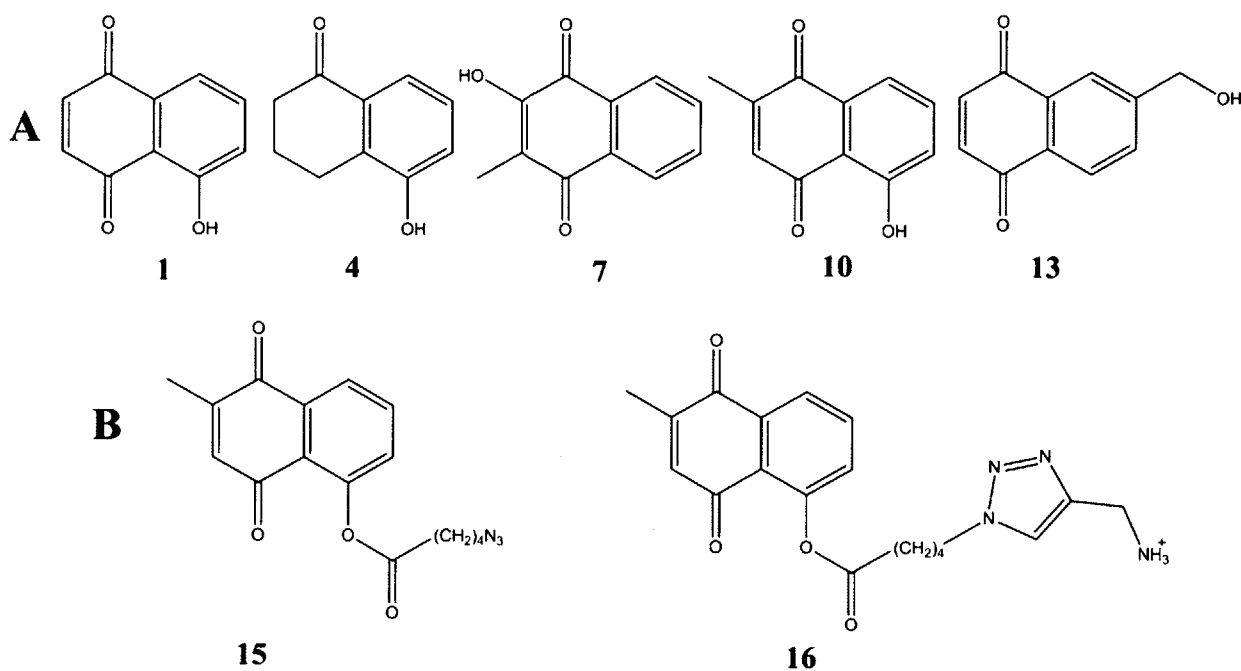
Influenza A virus is highly transmissible and kills over 250,000 people worldwide each year. In the United States alone, some 20% of the population contracts the virus annually, leading to countless missed days of work and school and tens of billions of dollars in associated costs.<sup>1,2</sup> Two of the FDA-approved drugs for the treatment of influenza infections, oseltamivir (Tamiflu™) and zanamivir (Relenza™), have fallen short of expectations due to their mediocre activity in reducing the symptoms and duration of the infection, as well as emerging resistance in clinical isolates.<sup>3-5</sup> Thus new and more effective anti-influenza therapeutic agents are greatly needed.

One proposed strategy for generating more potent inhibitors of influenza is to utilize the benefits of *multivalency*.<sup>2,4,6-11</sup> Conjugating multiple copies of influenza inhibitors to a flexible polymeric chain has been shown to result in multivalent interactions between the polymer-attached inhibitors and the viral surface receptor proteins.<sup>2,4,6-11</sup> These enhanced interactions, in turn, lead to a much stronger binding compared to that of the small-molecule parents stemming from favorable entropic factors; additionally, water-swollen polymeric chains may sterically hinder physical contacts between the virus and the target cell.<sup>6</sup>

The foregoing benefits of multivalency for binding to influenza virus have been demonstrated for viral surface proteins with the natural ligand of hemagglutinin, *N*-acetylneuraminic (sialic) acid, and with the neuraminidase inhibitor zanamivir.<sup>2,4,6-11</sup> However, both of these compounds are structurally complex, requiring many-step syntheses to become amenable to attachment to polymeric chains in order to investigate the effect of multivalency.<sup>2,4</sup> They are also difficult to modify selectively and thus not optimal for structure-activity relationship (SAR) studies. In the present work, we instead have employed simple organic

molecules<sup>12</sup> (Figure 2-1) with anti-influenza properties to investigate the SAR of multivalency. In particular, we have assessed whether the aforementioned potential benefits of multivalency invariably translate into greater anti-influenza activity.

**Figure 2-1.** Chemical structures of (A) 5-hydroxynaphthalene-1,4-dione (1) and its analogs 4, 7, 10, and 13 used in this study; (B) modified 10 with an azide-terminated spacer arm (15) for use in conjugating to propargylamine-derivatized poly-L-glutamate and 10 derivatized with a spacer arm (16) for investigation of the dependence of IC<sub>50</sub> on the presence of the spacer arm by itself with no polymer.



## B. Results and Discussion

Since the inherent structural complexities of zanamivir and sialic acid do not allow for easy manipulations, for our SAR studies we chose to investigate whether there were simpler molecules also possessing anti-influenza activity. In the scholarly study by Bodian *et al.*,<sup>12</sup> expanded by others,<sup>13</sup> docking simulations were performed to discover small organic molecules

that bind to the hemagglutinin protein on influenza A viral strain X31 (H3N2) and stabilize the protein in its native conformation. This stabilization was proposed to hinder the conformational changes necessary for cell-viral membrane fusion, which is an essential step in the influenza infection cycle.<sup>12</sup> Specifically, the binding site explored was a region approximately half-way between the most outer tip of the hemagglutinin protein and the viral membrane near the fusion peptide.<sup>12</sup> These docking studies resulted in a group of benzoquinones and hydroquinones as potential ligands to bind to hemagglutinin and inhibit the aforementioned conformational change.<sup>12</sup>

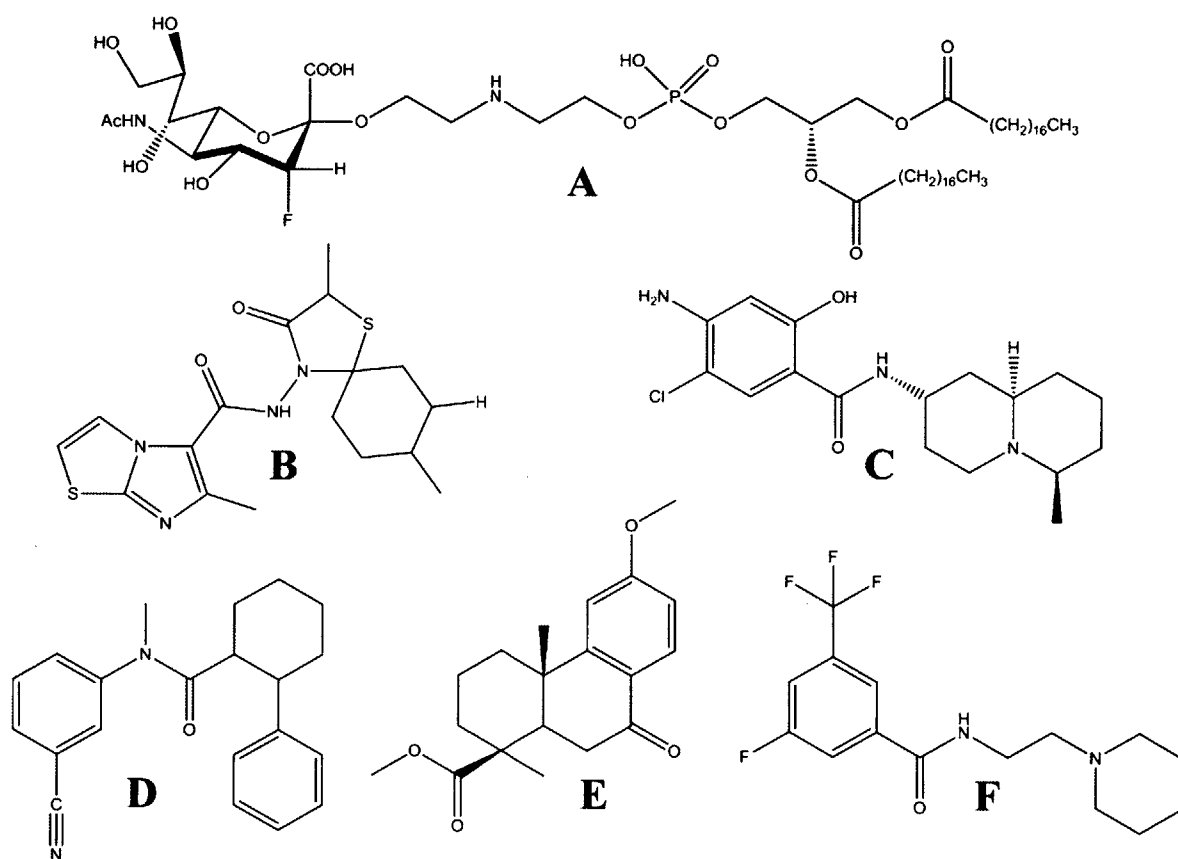


**Figure 2-2.** Chemical structures of anti-hemagglutinin agents previously described in the literature: (A) Neu5Ac3αF-DSPE;<sup>14</sup> (B) *N*-(2,8-dimethyl-3-oxo-1-thia-4-azaspiro[4.5]decan-4-yl)-6-methylimidazo [2,1-b]thiazole-5-carboxamide;<sup>15</sup> (C) 4-amino-5-chloro-2-hydroxy-*N*-((2*S*,6*R*,9*aR*)-6-methyloctahydro-1*H*-quinolizin-2-yl)benzamide;<sup>16</sup> (D) *N*-(3-cyanophenyl)-*N*-methyl-2-phenylcyclohexanecarboxamide;<sup>17</sup> (E) methyl-*O*-methyl-7-ketopodocarpate;<sup>18</sup> (F) 3-fluoro-*N*-(2-(piperidin-1-yl)ethyl)-5-(trifluoromethyl)benzamide.<sup>19</sup> It is worth noting that **1** is a more potent anti-influenza inhibitor than compound **F** (IC<sub>50</sub> of 315 μM),<sup>19</sup> on par with compounds **A**, **B**, and **C** (IC<sub>50</sub>'s of 5.6, 3-23, and 3-8 μM, respectively),<sup>14-16</sup> and less potent than compounds **D** and **E** (IC<sub>50</sub>'s of 98 and 31 nM, respectively).<sup>17,18</sup>



One of the foregoing compounds, 5-hydroxynaphthalene-1,4-dione (**1**), was selected as a starting point for our studies. Using the plaque reduction assay method to test **1** for putative anti-influenza activity against the Wuhan strain of the influenza A virus, we indeed found it to be a moderate inhibitor with an  $IC_{50}$  value of  $4.7 \pm 1.5 \mu\text{M}$  (Table 2-1, 1<sup>st</sup> entry). While other unnatural anti-hemagglutinin inhibitors exist (Figure 2-2),<sup>14-19</sup> all are structurally more complex than **1**. Therefore, we decided to continue our studies herein with compound **1**.

In light of the previous studies with polymer-attached zanamivir and sialic acid,<sup>2,4,6-11</sup> we next tested whether covalent conjugation of multiple copies of **1** to a polymeric chain would increase anti-influenza potency. To this end, **1** was attached to the physiologically benign and biodegradable polymer poly-L-glutamate at ~10% loading (*i.e.*, with approximately one tenth of all monomeric units being derivatized with the inhibitor). The resultant polymeric inhibitor **2a** (Figure 2-3) exhibited an over 10-fold better  $IC_{50}$  value compared to its monomeric counterpart **1** (Table 2-1, 2<sup>nd</sup> entry), presumably due to the phenomenon of multivalency. Interestingly, lowering the degree of loading of the inhibitor on the polymer from 10% to 5% (to yield **2b**) failed to improve the antiviral potency (Table 2-1), suggesting that the polymer-conjugated ligand molecules do not interfere with each other's ability to inhibit the virus at these loadings.

One can readily envisage how steric constraints imposed by the polymeric chain may hinder the ability of the inhibitor to bind to its viral receptor, thus masking the true power of multivalency. This hypothesis was verified by inserting a nine-atom spacer arm between the polymer and **1**, resulting in compound **3**. As seen in Table 2-1, this insertion indeed dramatically improved the  $IC_{50}$  value: 20-fold over **2a** and some 240-fold over **1**.

To examine the generality of these findings, several structural analogs of **1**, not previously identified as anti-influenza inhibitors,<sup>12</sup> were tested, along with their synthesized

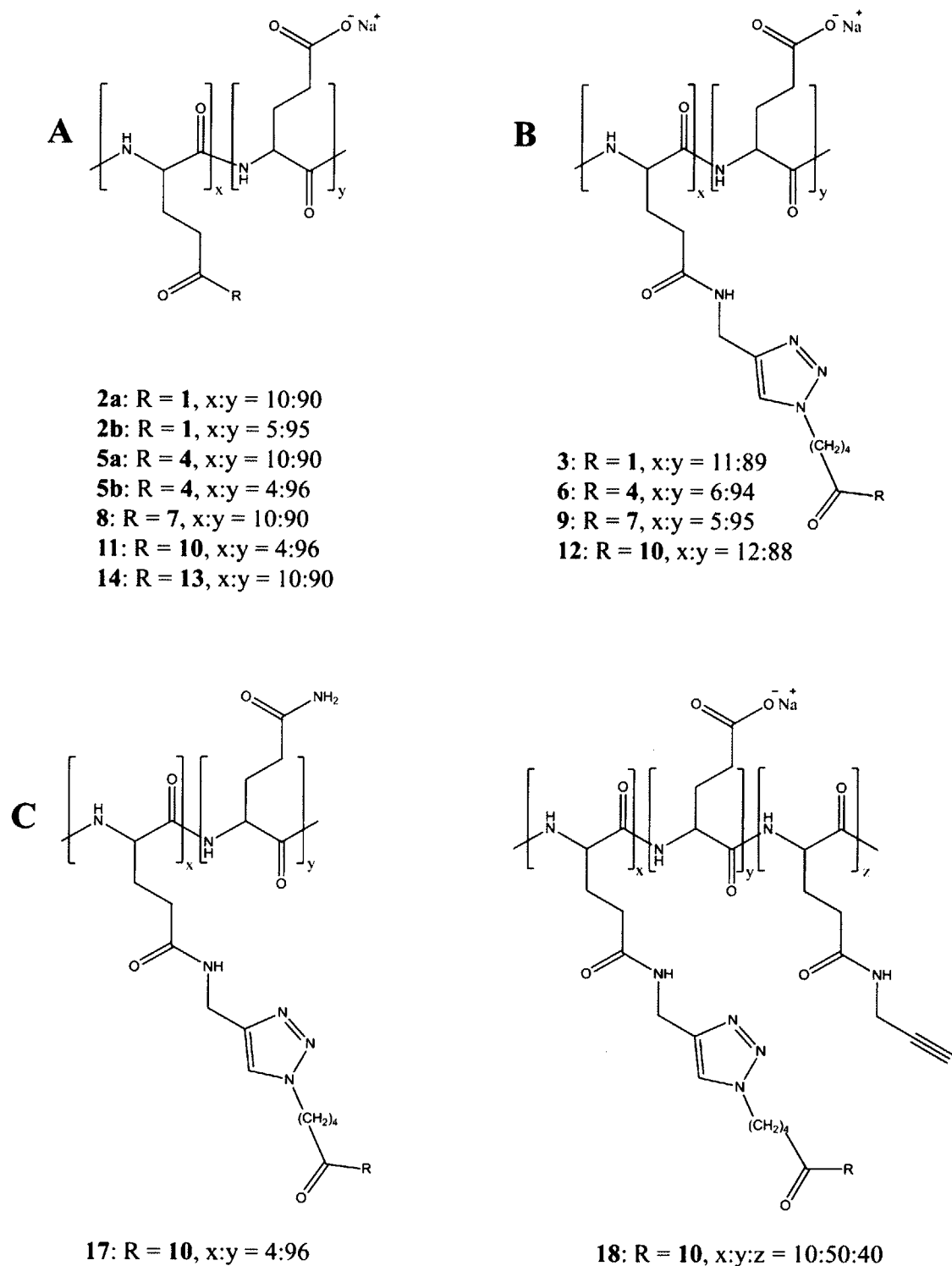


**Figure 2-3.** Chemical structures of anti-influenza inhibitors attached to poly-L-glutamate (**A**) with no spacer arm; (**B**) via a nine-atom spacer arm intended to reduce the putative steric hindrances imposed by the polymeric chains; (**C**) with the polymeric backbone of varying degrees of electrostatic charge.

**Table 2-1.** IC<sub>50</sub> values for both small molecules and their polymer-attached derivatives against the Wuhan strain of influenza A virus.

Inhibitor	IC <sub>50</sub> (μM) <sup>a</sup>
<b>1</b>	4.7 ± 1.5
<b>2a</b>	0.40 ± 0.20
<b>2b</b>	0.87 ± 0.14
<b>3</b>	0.020 ± 0.006
<b>4</b>	95 ± 22
<b>5a</b>	13 ± 7.2
<b>5b</b>	13 ± 2.7
<b>6</b>	2.5 ± 1.6
<b>7</b>	>100
<b>8</b>	33 ± 7.0
<b>9</b>	0.72 ± 0.21
<b>10</b>	5.7 ± 1.7
<b>11</b>	18 ± 10
<b>12</b>	0.11 ± 0.070
<b>13</b>	5.7 ± 0.70
<b>14</b>	0.18 ± 0.010

<sup>a</sup> The plaque reduction assay experiments were run at least in triplicate; the calculated mean and standard deviation values are presented in the table. The IC<sub>50</sub> values are expressed based on the concentration of the small-molecule inhibitor. The IC<sub>50</sub> value of bare poly-L-glutamate was found to exceed 1 mM and thus should not appreciably contribute to the extent of inhibition.

poly-L-glutamate conjugates, against the Wuhan influenza strain. 5-Hydroxy-3,4-dihydronaphthalene-1(2H)-one (**4**) and 2-hydroxy-3-methylnaphthalene-1,4-dione (**7**) both were found to be inhibitors, albeit much weaker ones than **1**. Conjugating them to the polymer directly, *i.e.*, with no spacer arm (to produce **5a** or **5b** depending on the degree of loading and **8**,

respectively) led to marked (7 and >3-fold, respectively) improvements in the antiviral potency (Table 2-1). Moreover, as seen in Table 2-1, when the nine-atom spacer arm was inserted to further distance the ligand from the polymeric chain (to form **6** and **9**, respectively), the inhibitory potency in both cases rose another several-fold to reach the overall improvement compared to those of the parents **4** and **7** of 38-fold and >140-fold, respectively.

The same general trend of a dramatically enhanced inhibitory potency upon attachment to the polymeric chain via the spacer arm was observed with yet another analog of **1** tested, namely 5-hydroxy-2-methyl-1,4-naphthalenedione (**10**). This compound, which differs from **1** only by a methyl substituent in the benzoquinone portion of the molecule, exhibited an IC<sub>50</sub> value comparable to that of **1**; converting it to **12** produced a 52-fold jump in inhibitory activity (Table 2-1). Interestingly, however, in the case of **10** attached to the polymer with no spacer arm (**11**), no increase (and, in fact, a sizeable decline) in the potency was observed (Table 2-1), illustrating how subtle the SAR is.

The poly-L-glutamate conjugate of **13** (in the absence of a nine-atom linker), **14**, exhibited a greater than 30-fold improvement over its monomeric counterpart (Table 2-1) demonstrating that attachment through the 6C position in the naphthoquinone moiety does not have a deleterious effect on the inhibitor improvement; in fact, it generated the most potent non-linker conjugated inhibitor.

In addition to a striking improvement in the inhibitory potency of the ligands upon conjugating them to poly-L-glutamate via the long spacer arm, their toxicity also diminished. In particular, both for **2a**, **2b**, and **3** vs. **1** and for **11** and **12** vs. **10** the cellular toxicity was at least an order of magnitude lower. For example, when compound **1** was used in the infection phase of the plaque reduction assay, cells that were incubated with the concentrations of inhibitor greater

than, or equal to, 30  $\mu\text{M}$  displayed obvious fatal demise. In contrast, cells incubated with even greater than 300  $\mu\text{M}$  concentrations of polymer-attached inhibitors **2a**, **2b**, and **3** were healthy and seemingly unaffected by the presence of inhibitor. Presumably, sequestering the toxic small molecules (50% cell cytotoxicity concentration,  $\text{CC}_{50}$ , of  $\sim 30$   $\mu\text{M}$  for **1**<sup>12</sup>) to the polymer prevents them from traversing the cellular membrane and exerting deleterious effects within the cell.

To determine to what extent the foregoing findings apply to other influenza A viruses, we selected two additional strains, namely the avian turkey and the human PR8 strains. Both strains have different serotypes of the hemagglutinin and neuraminidase proteins compared to Wuhan's, leading to subtle differences in the amino acid composition and structure of these proteins.<sup>20</sup> Using the plaque reduction assay, we tested the monomeric inhibitors **1**, **7**, **10**, and **13**, as well as those attached to poly-L-glutamate either via the nine-atom spacer arm (compounds **3**, **6**, and **12**) or directly (**14**). As in the case of the Wuhan strain, **1**, **10**, and **13** were substantial inhibitors of the viruses, whereas **7** was not (Table 2-2), suggesting similarities in the receptors' binding sites of all three strains. And yet, in stark contrast to the observations made with the Wuhan strain (Table 2-1), conjugation to the polymeric chains even via a long spacer arm not only failed to result in a significant improvement of the anti-influenza potency but, in the case of **1** and **10**, actually made it markedly worse, i.e., increased the  $\text{IC}_{50}$  values (Table 2-2). For **14**, conjugation of the inhibitor to the polymer through the C6 position in the naphthoquinone also caused a substantial deterioration in potency for both turkey and PR8 strains suggesting that the site of the linker's attachment is not entirely responsible for the reduction in inhibition.

We hypothesized that perhaps the addition of the linker group itself imposed new steric hindrances for binding of the inhibitor to the receptor sites on the turkey and PR8, but not

**Table 2-2.** IC<sub>50</sub> values for both small molecules and their polymer-attached derivatives against the PR8 and turkey strains of influenza A virus.

Inhibitor	IC <sub>50</sub> (μM) <sup>a</sup>	
	PR8	turkey
<b>1</b>	13 ± 1.6	4.7 ± 1.6
<b>3</b>	140 ± 45	84 ± 23
<b>7</b>	>100	>100
<b>9</b>	99 ± 16	100 ± 5
<b>10</b>	14 ± 1.6	17 ± 1
<b>12</b>	150 ± 10	53 ± 20
<b>13</b>	14 ± 1.0	5.3 ± 2.3
<b>14<sup>b</sup></b>	120 ± 19	>298

<sup>a</sup> The plaque reduction assay experiments were run at least in triplicate; the calculated mean and standard deviation values are presented in the table. The IC<sub>50</sub> values are expressed based on the concentration of the small-molecule inhibitor. The IC<sub>50</sub> values for compounds **4** and **6** exceeded 170 μM for both viral strains. Thus they were not included in this table because no definitive conclusions concerning the effect of attachment to the polymer can be made.

<sup>b</sup> All polymer conjugates characterized in this table contain the nine-atom spacer arm, except for **14** which comprises **13** conjugated directly to poly-L-glutamate.

the Wuhan, strains of the virus. This would inevitably lead to a diminished ability of the inhibitor to bind to its receptor when subsequently attached to poly-L-glutamate. To test this hypothesis, we focused on the compound **10** group of inhibitors and synthesized compound **16** containing the same chemical structure as the inhibitor plus the spacer arm portion of **12** but in the absence of

polymer. As seen in Table 2-3, **16** indeed exhibited a drastically poorer anti-influenza inhibition against all three viruses compared to the parent compound **10**.

Thus the deteriorated inhibition potency upon attachment of the nine-atom spacer arm indeed may account for at least some of the inferior inhibition observed for compounds **3**, **9**, and **12** compared to their monomeric precursors **1**, **7**, and **10**, respectively, against the turkey and PR8 strains. However, in order for **12** to exhibit the multivalency benefits over **16** of greater than 100-fold (as it did with Wuhan strain, Table 2-3), the IC<sub>50</sub> value of **16** would have to be at least 10<sup>4</sup> μM for the PR8 and turkey strains. The results of the plaque reduction assay suggest that this is not the case though: a reduction in plaque numbers for both of these strains upon incubation with 90 μM **16** indicated that the IC<sub>50</sub> was close to 100 μM (data not shown). The exact IC<sub>50</sub> for **16** was not measurable however, due to cytotoxicity of the compound.

**Table 2-3.** IC<sub>50</sub> values for compounds **10**, **12**, and **16** against three influenza A virus strains

Inhibitor	IC <sub>50</sub> (μM) <sup>a</sup>		
	Wuhan	PR8	turkey
<b>10</b>	5.7 ± 1.7	14 ± 1.6	17 ± 1
<b>12</b>	0.11 ± 0.070	150 ± 10	53 ± 20
<b>16</b>	45 ± 8	>100 <sup>b</sup>	>100 <sup>b</sup>

<sup>a</sup> The plaque reduction assay experiments were run at least in triplicate; the calculated mean and standard deviation values are presented in the table. The IC<sub>50</sub> values are expressed based on the concentration of the small-molecule inhibitor.

<sup>b</sup> Although the IC<sub>50</sub> values for the turkey and PR8 strains could not be conclusively determined because the 50% cell cytotoxicity concentration (CC<sub>50</sub>) for **16** only slightly exceeded 100 μM, there was a visible reduction in plaques upon incubation with 90 μM of **16**.

Next we investigated the role of the polymer's charge in antiviral activity. To this end, two new polymer conjugates with compound **10** attached via the nine-atom spacer arm (**17** and **18**) were prepared and tested against the Wuhan and turkey strains. Compound **17**, containing a neutral poly-L-glutamine backbone, showed modest improvements for the turkey strain over its negatively charged analog **12** but failed to exhibit a great enhancement over the monomer **10** (Table 2-4). Conversely, for the Wuhan strain, **17** demonstrated an almost 50-fold improvement over the monomer, similar to that afforded by compound **12** (Table 2-4). Likewise, compound **18** (containing a partly negatively-charged backbone) displayed no great enhancement for the turkey strain while exhibiting an almost 40-fold improvement over **10** for the Wuhan strain. These results indicate that the charge on the polymeric chain cannot account for the striking differences observed between the turkey and Wuhan strains for monomeric vs. polymer-attached inhibitors.

**Table 2-4.** Comparison of IC<sub>50</sub> values for 5-hydroxy-2-methyl-1,4-naphthalenedione (**12**) conjugated to polymers of varying degrees of backbone charge against the Wuhan and turkey strains of influenza A virus.

Inhibitor	IC <sub>50</sub> (μM) <sup>a</sup>	
	Wuhan	turkey
<b>12</b>	0.11 ± 0.070	53 ± 20
<b>17</b>	0.12 ± 0.061	7.4 ± 3.9
<b>18</b>	0.15 ± 0.035	35 ± 9.0

<sup>a</sup> The plaque reduction assay experiments were run at least in triplicate; the calculated mean and standard deviation values are presented in the table. The IC<sub>50</sub> values are expressed based on the concentration of the small-molecule inhibitor.



To determine whether the difference in improvements for polymer-attached conjugates over monomeric inhibitors between the Wuhan and turkey strains was an artifact of our biological assay, i.e., whether the inhibitor was brought into contact with the virus at the inappropriate time during infection, we performed an additional plaque assay with **10** and **12** present not only during the pre-incubation and binding (as is conventionally done) but also with the inhibitor in the agar overlay. This modality of the plaque reduction assay exposes cells and viruses to the inhibitor for the entirety of the first and subsequent infection phases leaving the inhibitor available for all steps in the viral cycle and not just for binding or endocytosis. In this experimental mode, the inhibitory effect of **10** and **12** for the Wuhan strain changed only modestly:  $IC_{50}$ 's of  $2.4 \pm 0.39 \mu\text{M}$  and  $0.061 \pm 0.045 \mu\text{M}$ , respectively, for incubation of inhibitor in the agar overlay vs.  $5.7 \pm 1.7 \mu\text{M}$  and  $0.11 \pm 0.070 \mu\text{M}$  for our conventional experiment. For the turkey strain, the inhibition by the monomer (**10**) improved more ( $IC_{50}$  of  $17 \pm 1.0 \mu\text{M}$  when not included in the agar and  $2.9 \pm 0.49 \mu\text{M}$  when included in the agar) but the polymer-attached inhibitor's (**12**'s)  $IC_{50}$  exceeded  $5 \mu\text{M}$ ; these observations confirm that the lack of improvement for polymer-attached inhibitors against the turkey strain was not an artifact of our biological assay.

We then hypothesized that the preferred binding sites of the monomeric vs. the polymer-attached inhibitors might be distinct between the strains, thus being responsible for their vastly different inhibitory properties. To explore this possibility, we ran *in silico* docking experiments to determine the preferred binding sites for the monomeric inhibitor **10** and the linker-attached inhibitor **16** for the PR8 strain and a Wuhan surrogate strain, X31 (both Wuhan and X31 are H3N2). Note that the X-31 strain has a 87% sequence identity for the HA1 strand of the hemagglutinin molecule compared to the Wuhan strain (the HA2 Wuhan sequence is

unavailable)<sup>21,22</sup> (for comparison, the PR8's HA1 strand has just a 33% sequence identity<sup>23</sup>). As seen in Figure 2-4A, for the X-31 strain both inhibitors bind in the same region of the hemagglutinin protein; this region coincides with the crystallographically determined binding site for *tert*-butyl hydroquinone (another fusion inhibitor described by Bodian et al.<sup>12,13</sup>). In stark contrast, for the PR8 strain, inhibitors **10** and **16** bind in vastly distinct locations on the hemagglutinin protein, with as much as 40 Å separating them (Fig. 2-4B). Note that **10** binds to a similar location on the PR8 strain's hemagglutinin as both **10** and **16** in the X-31's protein;

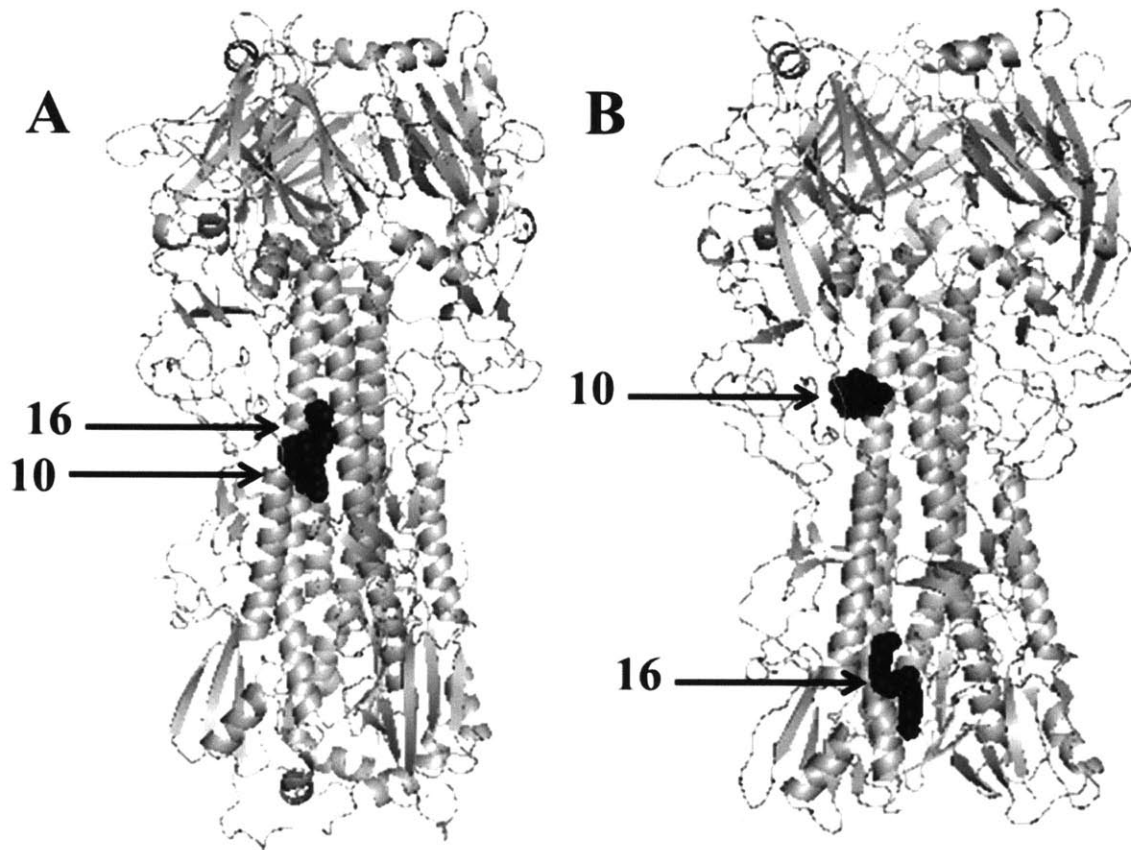


**Figure 2-4.** The docking results for inhibitors **10** and **16** (both black) on the hemagglutinin protein (grey) of the X-31 strain (a surrogate used to represent the Wuhan strain) (**A**, left panel) and of the PR8 strain (**B**, right panel) of influenza A virus. As seen in **A**, the binding sites on the protein for the two inhibitors overlap in the former case. In contrast, the distance between the binding sites for the two inhibitors in **B** is some 40 Å indicating that the molecules bind to the protein in vastly distinct locations. The images, generated in Pymol, depict only **10** and **16** docked on one hemagglutinin monomer for each viral strain.

however, **16** on the PR8 strain's hemagglutinin binds in a region that is closer to the viral envelope, thereby possibly hindering accessibility for the polymer-attached inhibitor.

One has to wonder why there are benefits of multivalency for all the compounds tested attached via a long spacer arm to a poly-L-glutamate for one strain of influenza, but not for the other two (Tables 2-1 and 2-2). It is unlikely that the observed differences in inhibition among viral strains are due to dissimilar spacing of hemagglutinin molecules along the viral surface among different strains. There are ~400 hemagglutinin molecules on a given viral particle of roughly the same size regardless of the influenza virus strain. Since the mechanism of viral particle formation is the same for different strains, the spacing among hemagglutinin molecules on average should be similar as well.<sup>20</sup> The binding of the first polymer-attached inhibitor molecule to hemagglutinin is also unlikely to prevent binding of all the others. Although the binding of the first inhibitor molecule indeed might make it sterically impossible for a second, nearby counterpart to bind to hemagglutinin, that cannot be the case for more distant polymer-attached inhibitor molecules. Since our (~10% derivatized) polymeric chain contains some 50 randomly distributed inhibitor molecules, most of them should be sufficiently remote from the first one bound to interact with another hemagglutinin molecule.

The three influenza strains undoubtedly have some differences in the binding site for these inhibitors;<sup>20</sup> in the case of the turkey and PR8 strains, these differences might interplay with the polymer and/or linker deleteriously to weaken the binding of the conjugated inhibitor to the virus. Additionally, the topology of the viral surface might introduce accessibility problems for the inhibitors once they are attached to the bulky, hydrated polymeric chain. In previous studies investigating the effect of multivalency on anti-influenza inhibitors, the receptor of the multivalent ligand was proximal to the solvent-exposed outer edge of the surface protein.<sup>2,4,6-11</sup>

Although the exact location of binding of **1** and its analogs to hemagglutinins in the strains studied herein is unknown, our docking studies (Fig. 2-4) predict that for **10** and **16** the site is located approximately half-way down the protein for the X-31 strain and close to the viral envelope for the linker-attached inhibitor (**16**) on the PR8 strain.<sup>12</sup> Perhaps while a small molecule readily accesses regions down the stock of the protein, conjugation to a bulky polymeric chain hampers the access below the dense canopy of proteins on the viral surface.

The concept of multivalency stipulates that several simultaneous interactions of ligands and receptors should result in a stronger, multipoint inhibitor-virus binding and hence give rise to

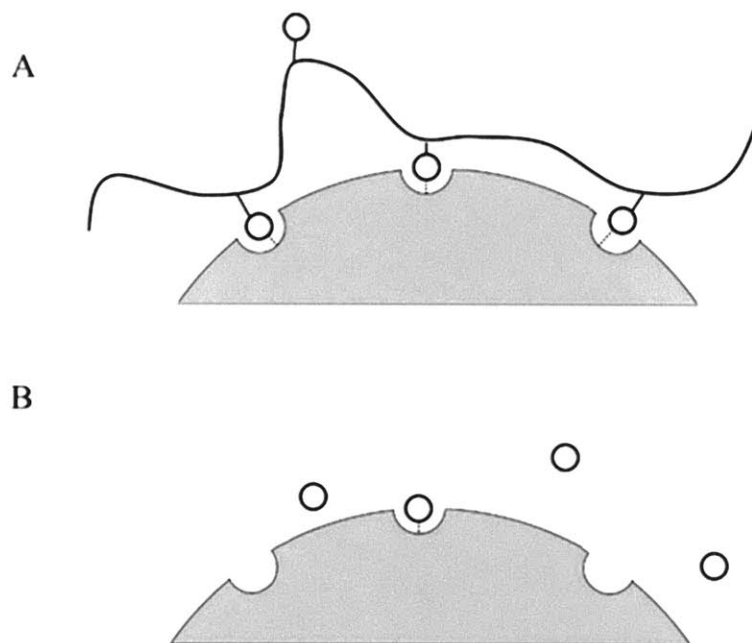


**Figure 2-5.** A cartoon depicting a multivalent vs. a monovalent interaction of an inhibitor with the virus. The top panel (A) depicts a polymer-attached inhibitor (polymer is black line, inhibitors are open circles) interacting with a viral envelope containing the receptors of the inhibitor (grey part-circle is the viral envelope, white open half-circles are receptors, dotted lines indicate a binding interaction). Attaching multiple copies of the inhibitor to a polymeric chain can result in a multivalent and hence much stronger interaction with the viral receptors. The bottom panel (B) depicts a monovalent interaction of parent inhibitor molecules with a viral receptor. In this case, the individual inhibitor molecules act independently of each other in binding to their receptors and hence do not benefit from entropically enhanced binding (i.e., from multivalency).

more potent inhibitors (Figure 2-5).<sup>6</sup> Our results herein suggest, however, that this is indeed the case only if attaching an inhibitor to a polymeric chain does not impose negative spatial constraints not outweighed by the inherent benefits of multivalency. Since it is unknown in advance whether this will be the case, our data illustrate that the superiority of multivalent inhibitors of a virus compared to their monovalent predecessors cannot be automatically assumed.

### **Acknowledgements**

I am thankful to Hongmei Wang for synthesizing compound **13**, to Yang Cao for performing the docking simulations, and to all coauthors for help in editing the manuscript that resulted in this chapter.

## **C. Materials and Methods**

### **Materials**

All small-molecule inhibitors except for **13**, poly-L-glutamate Na salt (50 -100 kDa), solvents, and reagents were purchased from Sigma-Aldrich Chemical Co. (St. Louis, MO) and used without further purification. Dialysis membranes (3,500 kDa molecular weight cutoff) were from Spectrum Labs (Rancho Dominguez, CA) and PD-10 desalting columns from GE Healthcare (Buckinghamshire, U.K.).

### **Syntheses**

**Synthesis of 6-(hydroxymethyl)naphthalene-1,4-dione (13)** was carried out as described by Antonini et al.<sup>24</sup>

**Synthesis of 2a, 2b, 5a, 5b, 8, 11, and 14:** Conjugation was carried out via a Steglich esterification with minor deviations from a reported procedure.<sup>25</sup> Specifically, poly-L-glutamate

Na salt was converted to poly(L-glutamic acid) by dissolution in double-distilled (dd) H<sub>2</sub>O, lowering the pH to 1, and washing with 0.10 M HCl to remove free salts before an overnight lyophilization. Lyophilized poly(L-glutamic acid) (20 mg, 0.16 mmol) was dissolved in 0.80 mL of dry dimethylformamide (DMF), followed by the addition of *N,N'*-dicyclohexylcarbodiimide (DCC) (4.3 mg (0.021 mmol) in 0.30 mL of DMF for a ~10% derivatization), an anti-influenza agent (0.050 mmol in 0.20 mL of DMF), pyridine (10  $\mu$ L, 0.12 mmol), and a catalytic quantity of 4-dimethylaminopyridine (DMAP) in 0.40 mL of DMF with vigorous stirring. The solution was stirred overnight at room temperature. The polymer was then isolated by precipitation in chloroform, washed with fresh chloroform to remove the unreacted anti-influenza agent, converted to the Na salt by dissolution in phosphate buffered saline (PBS), and dialyzed against ddH<sub>2</sub>O in a 3,500-Da MW cutoff dialysis membrane for 24 hr to remove free salts and other impurities. TLC using a 3:1 (v/v) ethyl acetate:hexanes mixture confirmed purity and demonstrated the disappearance of the anti-influenza agent's spot (for example, R<sub>f</sub> 0.68 for **10**). Percent conjugation of the anti-influenza agent was calculated by means of <sup>1</sup>H NMR in D<sub>2</sub>O using a Bruker 600 MHz instrument by comparing the ratio of the integration of a polymer peak with that of an anti-influenza agent's peak. In the case of a ~5% derivatization of the polymer with anti-influenza agent, 2.0 mg/0.010 mmol of DCC was added to the reaction mixture (**2b**, **5b**, and **11**). The NMR spectrum of **2a** appears in appendix A.

<sup>1</sup>H NMR (D<sub>2</sub>O)  $\delta$  (600 MHz) — for **2a** and **2b**: 1.6-2.0 (2H polymer, d, CH<sub>2</sub>), 2.1-2.5 (2H polymer, s, CH<sub>2</sub>), 4.0-4.4 (1H polymer, s, CH), 6.8-8.0 (5H, aromatics); for **5a** and **5b**: 1.8-2.1 (2H polymer, d, CH<sub>2</sub>), 2.1 (2H, m, cyclohexyl CH<sub>2</sub>), 2.2-2.4 (2H polymer, s, CH<sub>2</sub>), 2.6 (2H, m, cyclohexyl CH<sub>2</sub>), 2.8 (2H, m, cyclohexyl CH<sub>2</sub>), 4.2-4.4 (1H polymer, s, CH), 7.3-7.9 (3H, aromatics); for **8**: 1.6-2.0 (2H polymer, d, CH<sub>2</sub>, 3H, s, CH<sub>3</sub>), 2.1-2.5 (2H polymer, s, CH<sub>2</sub>), 4.0-

4.4 (1H polymer, s, CH), 7.5-8.0 (4H, aromatics); for **11**: 1.9-2.2 (2H polymer, d, CH<sub>2</sub>), 2.3 (3H, s, CH<sub>3</sub>), 2.4-2.5 (2H polymer, s, CH<sub>2</sub>), 4.0-4.4 (1H polymer, s, CH), 6.9-8.2 (4H, aromatics); for **14**: 1.6-2.0 (2H polymer, d, CH<sub>2</sub>), 2.0 (2H, s, CH<sub>2</sub>), 2.0-2.3 (2H polymer, s, CH<sub>2</sub>), 4.0-4.4 (1H polymer, s, CH), 6.7-8.0 (4H, aromatics).

**Synthesis of 3, 6, 9, and 12:** The conjugation of the anti-influenza agents to the polymer through a spacer arm was carried out via a Cu<sup>+</sup>-catalyzed [3+2] azide-alkyne cycloaddition in three steps. First, poly-L-glutamate Na salt was derivatized with propargylamine as described by Ochs et al.<sup>26</sup> Next, anti-influenza agents were derivatized with a linker terminating with an azide to be used in the subsequent cycloaddition. To this end, anti-influenza agent (0.30 mmol) was dissolved in 8 mL of dry dichloromethane, followed by the addition of azidopentanoic acid (50 μL, 0.40 mmol), *N,N'*-diisopropylcarbodiimide (DIC) (60 μL, 0.40 mmol), pyridine (50 μL, 0.60 mmol), and a catalytic quantity of DMAP. The reaction mixture was stirred overnight, concentrated by rotary evaporation, and purified by column chromatography (2:1 (v/v) hexanes:ethyl acetate) to generate such compounds as **15** (R<sub>f</sub> 0.6 for 15 visualized with UV irradiation). For the conjugation of anti-influenza agents to the polymer via cycloaddition, the alkyne-derivatized poly-L-glutamate Na salt (68 mg, 0.45 mmol) was dissolved in 1.5 mL of ddH<sub>2</sub>O. The above-mentioned purified linker-derivatized anti-influenza agent (0.10 mmol) was dissolved in 1.5 mL of *tert*-butanol and added to the water/polymer mixture. A 1.0 M aqueous solution of Na ascorbate (75 μL) and a 0.10 M aqueous solution of CuSO<sub>4</sub> (50 μL) were then added; the reaction mixture was incubated overnight,<sup>27</sup> concentrated via rotary evaporation, dissolved in PBS, run on a PD-10 desalting column, and dialyzed as above to remove unreacted starting material and reagents. Polymer conjugates were analyzed as outlined above to quantify derivatization. Examples of the NMRs spectra for **3** and **12** appear in Appendix A.

<sup>1</sup>H NMR (D<sub>2</sub>O) δ (600 MHz) — for **3**: 1.5 (2H, m, CH<sub>2</sub>), 1.7-2.1 (2H polymer, d, CH<sub>2</sub>, 4H, m, CH<sub>2</sub>), 2.1-2.5 (2H polymer, s, CH<sub>2</sub>), 4.0-4.5 (1H polymer, s, CH, 4H, m, CH<sub>2</sub>), 6.8-8.0 (6H, aromatics); for **6**: 1.7 (2H, m, CH<sub>2</sub>), 1.8-2.1 (2H polymer, d, CH<sub>2</sub>, 4H, m, CH<sub>2</sub>), 2.1 (2H, m, cyclohexyl CH<sub>2</sub>), 2.1-2.5 (2H polymer, s, CH<sub>2</sub>), 2.6 (2H, m, cyclohexyl CH<sub>2</sub>), 2.7 (2H, m, cyclohexyl CH<sub>2</sub>), 4.2-4.5 (1H polymer, s, CH, 4H, m, CH<sub>2</sub>), 7.2-8.0 (4H, aromatics); for **9**: 1.5 (2H, m, CH<sub>2</sub>), 1.7-2.1 (2H polymer, d, CH<sub>2</sub>, 4H, m, CH<sub>2</sub>, 3H, s, CH<sub>3</sub>), 2.1-2.5 (2H polymer, s, CH<sub>2</sub>), 4.2-4.5 (1H polymer, s, CH, 4H, m, CH<sub>2</sub>), 7.4-8.1 (4H, aromatics); for **12**: 1.6 (2H, m, CH<sub>2</sub>), 1.7-2.1 (2H polymer, d, CH<sub>2</sub>, 4H, m, CH<sub>2</sub>, 3H, s, CH<sub>3</sub>), 2.1-2.5 (2H polymer, s, CH<sub>2</sub>), 4.2-4.5 (1H polymer, s, CH, 4H, m, CH<sub>2</sub>), 6.5-8.0 (5H, aromatics).

**Synthesis of 1-(5-((6-methyl-5,8-dioxo-5,8-dihydronaphthalen-1-yl)oxy)-5-oxopentyl)-1H-1,2,3-triazol-4-yl)methanaminium (16)** was carried out similarly to the aforementioned cycloaddition. Briefly, 6-methyl-5,8-dioxo-5,8-dihydronaphthalen-1-yl 5-azidopentanoate (**15**) (33 mg, 0.10 mmol) was dissolved in 1.5 mL of *tert*-butanol. To that mixture, propargylamine (6.0 μL, 0.10 mmol) in 1.5 mL of ddH<sub>2</sub>O was added, followed by the addition of a 1.0 M aqueous solution of Na ascorbate (75 μL) and a 0.10 M aqueous solution of CuSO<sub>4</sub> (50 μL). The reaction was stirred overnight, concentrated by rotary evaporation, and dissolved in ddH<sub>2</sub>O. Following the addition of chloroform the aqueous fraction was recovered, dissolved in methanol, filtered, and concentrated for characterization by <sup>1</sup>H NMR and for further use in biological assays. The NMR spectrum for **16** appears in Appendix A.

<sup>1</sup>H NMR (MeOD) δ (400 MHz) for **16**: 1.6 (2H, m, CH<sub>2</sub>), 2.0 (2H, m, CH<sub>2</sub>, 3H, s, CH<sub>3</sub>), 2.7 (2H, m, CH<sub>2</sub>), 4.1 (2H, m, CH<sub>2</sub>), 4.4 (2H, m, CH<sub>2</sub>), 6.6 (1H, s, H3 aromatic), 7.3 (1H, d, H8 aromatic), 7.7 (1H, dd, H7 aromatic), 7.9 (1H, d, H6 aromatic), 8.1 (1H, s, NCHC).



**Synthesis of 17 and 18:** For **17**, poly-L-glutamate Na salt was activated with propargylamine as described above and then the remaining carboxylates were converted to their free acids by reducing the pH, followed by the removal of water by freeze-drying. The resultant compound (40 mg) was dissolved in 1.5 mL of DMF, then *N*-hydroxysuccinimide (NHS) (79 mg, 0.69 mmol) was added with stirring, and the temperature was reduced to 0 °C, followed by an addition of DIC (108  $\mu$ L, 0.69 mmol). The reaction mixture was stirred on ice for 30 min and at room temperature for 3 hr, after which time an excess of aqueous  $\text{NH}_4\text{OH}$  was added to displace the NHS-ester moieties resulting in a neutral poly-L-glutamine.<sup>4,28</sup> Conjugation of **15** to the propargylamine-derivatized poly-L-glutamine was carried out via a cycloaddition as described above. For **18**, poly-L-glutamate Na salt was derivatized with propargylamine in the same way as above, except that an excess of propargylamine (30  $\mu$ L, 0.47 mmol) was added. For derivatization with inhibitor, the reaction was performed as above, but only 0.1 mole-equivalents of **15** was used. The NMR spectrum for **17** appears in Appendix A.

<sup>1</sup>H NMR ( $\text{D}_2\text{O}$ )  $\delta$  (600 MHz) — for **17**: 1.6 (2H, m,  $\text{CH}_2$ ), 1.8-2.2 (2H polymer, d,  $\text{CH}_2$ , 4H, m,  $\text{CH}_2$ , 3H, s,  $\text{CH}_3$ ), 2.2-2.4 (2H polymer, s,  $\text{CH}_2$ ), 4.2-4.5 (1H polymer, s, CH, 4H, m,  $\text{CH}_2$ ), 6.4-8.0 (5H, aromatics); for **18**: 1.6 (2H, m,  $\text{CH}_2$ ), 1.9-2.2 (2H polymer, d,  $\text{CH}_2$ , 4H, m,  $\text{CH}_2$ , 3H, s,  $\text{CH}_3$ ), 2.2-2.5 (2H polymer, s,  $\text{CH}_2$ ), 2.6 (1H, s, CH), 3.9 (2H, s,  $\text{CH}_2$ ), 4.2-4.5 (1H polymer, s, CH, 4H, m,  $\text{CH}_2$ ), 6.3-7.9 (5H, aromatics).

### **Cells, Viruses, and Antiviral Assays**

Madin-Darby canine kidney (MDCK) cells were purchased from the American Type Culture Collection (ATCC) and maintained as described by Haldar et al.<sup>2</sup> The wild-type influenza A viruses Wuhan/359/95 (Wuhan) (H3N2) and turkey/MN/833/80 (turkey) (H4N2) were obtained from the U.S. Centers for Disease Control and Prevention (CDC), and the

influenza A strain PR/8/34 (PR8) (H1N1) was purchased from Charles River Laboratories (North Franklin, CT). The viruses were stored at -80°C and diluted in PBS prior to assays.

Plaque reduction assays with MDCK cells were conducted to determine the half-maximal inhibitory concentration (IC<sub>50</sub> value) for each compound tested using a literature methodology.<sup>2,4</sup> For plaque reduction assays investigating the effect of inhibitor in the solid growth agar, equal concentrations of the inhibitor were used during pre-incubation, infection, and in the nutrient agar formulation.

### **Docking simulations**

The hemagglutinin structures of the PR8 and X-31 strains of influenza A virus were obtained from the Protein Data Bank (PDB: 1RU7 and 2HMG, respectively). The docking studies for the hemagglutinin proteins and compounds **10** and **16** were performed with AutoDock Vina<sup>29</sup> and AutoDock Tools interface. All rotatable bonds in the ligands were allowed to rotate freely using the default settings. The search area, selected based on the previous studies with influenza small-molecule hemagglutinin inhibitors,<sup>12,13</sup> covered the majority of the grooves of the protein. The final results were selected based on the best binding modes.

### **D. References**

1. Graham-Rowe D. 2011. Epidemiology: Racing against the flu. *Nature*. 480(7376):S2-S3.
2. Haldar J, Alvarez de Cienfuegos L, Tumpey TM, Gubareva LV, Chen J, Klibanov AM. 2010. Bifunctional polymeric inhibitors of human influenza A viruses. *Pharm Res*. 27(2):259-263.
3. Palmer R. 2011. Drugs: lines of defence. *Nature*. 480(7376):S9-S10.

4. Weight AK, Haldar J, Alvarez de Cienfuegos L, Gubareva LV, Tumpey TM, Chen J, Klibanov AM. 2011. Attaching zanamivir to a polymer markedly enhances its activity against drug-resistant strains of influenza A virus. *J Pharm Sci.* 100(3):831-835.
5. Gubareva LV. 2004. Molecular mechanisms of influenza virus resistance to neuraminidase inhibitors. *Virus Res.* 103(1):199-203.
6. Mammen M, Choi SK, Whitesides GM. 1998. Polyvalent interactions in biological systems: Implications for design and use of multivalent ligands and inhibitors. *Angew Chem Int Ed.* 37(20):2754-2794.
7. Mammen M, Dahmann G, Whitesides GM. 1995. Effective inhibitors of hemagglutination by influenza-virus synthesized from polymers having active ester groups- Insight into mechanism of inhibition. *J Med Chem.* 38(21):4179-4190.
8. Choi SK, Mammen M, Whitesides GM. 1997. Generation and *in situ* evaluation of libraries of poly (acrylic acid) presenting sialosides as side chains as polyvalent inhibitors of influenza-mediated hemagglutination. *J Am Chem Soc.* 119(18):4103-4111.
9. Sigal GB, Mammen M, Dahmann G, Whitesides GM. 1996. Polyacrylamides bearing pendant  $\alpha$ -sialoside groups strongly inhibit agglutination of erythrocytes by influenza virus: the strong inhibition reflects enhanced binding through cooperative polyvalent interactions. *J Am Chem Soc.* 118(16):3789-3800.
10. Honda T, Yoshida S, Arai M, Masuda T, Yamashita M. 2002. Synthesis and anti-influenza evaluation of polyvalent sialidase inhibitors bearing 4-guanidino-Neu5Ac2en derivatives. *Bioorg Med Chem Lett.* 12(15):1929-1932.
11. Carlescu I, Scutaru D, Popa M, Uglea CV. 2009. Synthetic sialic-acid-containing polyvalent antiviral inhibitors. *Med Chem Res.* 18(6):477-494.

12. Bodian DL, Yamasaki RB, Buswell RL, Stearns JF, White JM, Kuntz ID. 1993. Inhibition of the fusion-inducing conformational change of influenza hemagglutinin by benzoquinones and hydroquinones. *Biochemistry*. 32(12):2967-2978.
13. Russell RJ, Kerry PS, Stevens DJ, Steinhauer DA, Martin SR, Gamblin SJ, Skehel JJ. 2008. Structure of influenza hemagglutinin in complex with an inhibitor of membrane fusion. *Proc Natl Acad Sci*. 105(46):17736-17741.
14. Guo C-T, Sun X-L, Kanie O, Shortridge KF, Suzuki T, Miyamoto D, Kazuya I-P, Wong C-H, Suzuki Y. 2002. An O-glycoside of sialic acid derivative that inhibits both hemagglutinin and sialidase activities of influenza viruses. *Glycobiol*. 12(3):183-190.
15. Vanderlinden E, Göktaş F, Cesur Z, Froeyen M, Reed ML, Russell CJ, Cesur N, Naesens L. 2010. Novel inhibitors of influenza virus fusion: structure-activity relationship and interaction with the viral hemagglutinin. *J Virol*. 84(9):4277-4288.
16. Luo G, Colonna R, Krystal M. 1996. Characterization of a hemagglutinin-specific inhibitor of influenza A virus. *Virol*. 226(1):66-76.
17. Tang G, Qiu Z, Lin X, Li W, Zhu L, Li S, Li H, Wang L, Chen L, Wu JZ. 2010. Discovery of novel 1-phenyl-cycloalkane carbamides as potent and selective influenza fusion inhibitors. *Bioorg Med Chem Lett*. 20(12):3507-3510.
18. Staschke K, Hatch S, Tang J, Hornback W, Munroe J, Colacino J, Muesing M. 1998. Inhibition of influenza virus hemagglutinin-mediated membrane fusion by a compound related to podocarpic acid. *Virol*. 248(2):264-274.
19. Plotch SJ, O'Hara B, Morin J, Palant O, LaRocque J, Bloom JD, Lang SA, DiGrandi MJ, Bradley M, Nilakantan R. 1999. Inhibition of influenza A virus replication by compounds interfering with the fusogenic function of the viral hemagglutinin. *J Virol*. 73(1):140-151.

20. Lamb RA, Krug RM. 2007. Orthomyxoviridae: The viruses and their replication. In: Fields' Virology. Eds., Knipe DM, Howley PM. 5th ed. Philadelphia: Wolters Kluwer Health/Lippincott Williams & Wilkins.
21. Russell CA, Jones TC, Barr IG, Cox NJ, Garten RJ, Gregory V, Gust ID, Hampson AW, Hay AJ, Hurt AC, Jong JC, Kelso A, Klimov AI, Kageyama T, Komadina N, Lapedes AS, Lin YP, Mosterin A, Obuchi M, Odagiri T, Osterhaus AD, Rimmelzwaan GF, Shaw MW, Skepner E, Stohr K, Tashiro M, Fouchier RA, Smith DJ. 2008. The Global Circulation of Seasonal Influenza A (H3N2) Viruses. *Science*. 320:340-346.
22. Ward C, Dopheide TA. 1981. Amino acid sequence and oligosaccharide distribution of the haemagglutinin from an early Hong Kong influenza virus variant A/Aichi/2/68 (X-31). *Biochem*. 193(3):953.
23. Winter G, Fields S, Brownlee GG. 1981. Nucleotide sequence of the haemagglutinin gene of a human influenza virus H1 subtype. *Nature*. 292(5818):72-75.
24. Antonini I, Lin TS, Cosby LA, Dai YR, Sartorelli AC. 1982. 2- and 6-Methyl-1, 4-naphthoquinone derivatives as potential bioreductive alkylating agents. *J Med Chem*. 25(6):730-735.
25. Li C, Yu DF, Newman RA, Cabral F, Stephens LC, Hunter N, Milas L, Wallace S. 1998. Complete regression of well-established tumors using a novel water-soluble poly(L-glutamic acid) paclitaxel conjugate. *Cancer Res*. 58(11):2404-2409.
26. Ochs CJ, Such GK, Staedler B, Caruso F. 2008. Low-fouling, biofunctionalized, and biodegradable click capsules. *Biomacromolecules*. 9(12):3389-3396.
27. Jia Z, Zhu Q. 2010. 'Click' assembly of selective inhibitors for MAO-A. *Bioorg Med Chem Lett*. 20(21):6222-6225.

28. Song YS, Goel A, Basrur V, Roberts PEA, Mikovits JA, Inman JK, Turpin JA, Rice WG, Appella E. 2002. Synthesis and biological properties of amino acid amide ligand-based pyridinioalkanoyl thioesters as anti-HIV agents. *Bioorg Med Chem.* 10(5):1263-1273.
29. Trott O, Olson AJ. 2010. AutoDock Vina: improving the speed and accuracy of docking with a new scoring function, efficient optimization, and multithreading. *J Comp Chem.* 31(2):455-461.

## CHAPTER 3

Conjugation to polymeric chains of influenza drugs targeting M2 ion channels partially restores their inhibition of drug-resistant mutants

The work presented in this chapter will be published in the following manuscript:

Larson AM, Chen J, Klibanov AM. Conjugation to polymeric chains of influenza drugs targeting M2 ion channels partially restores their inhibition of drug-resistant mutants. Submitted to the Journal of Pharmaceutical Sciences.

## A. Introduction

Influenza viruses commonly infect the respiratory tract in humans<sup>1</sup> and are a major cause of morbidity and mortality in the world.<sup>2,3</sup> Two of the four FDA-approved small-molecule anti-influenza drugs — the adamantane-class M2 ion-channel inhibitors amantadine (**1**) and rimantadine (**2**) (Fig. 1) — are no longer recommended as therapeutics because nearly every circulating influenza A strain has evolved resistance to them.<sup>2,4,5</sup> These drugs block the M2 ion channels on the surface of the virus,<sup>6-9</sup> thereby preventing the flow of protons into the viral core (an essential step in the viral infection cycle).<sup>2</sup> Resistance to **1** and **2** is due to point mutations in the M2 ion channel protein, with the most common being the S31N in the interior of the channel.<sup>2</sup>

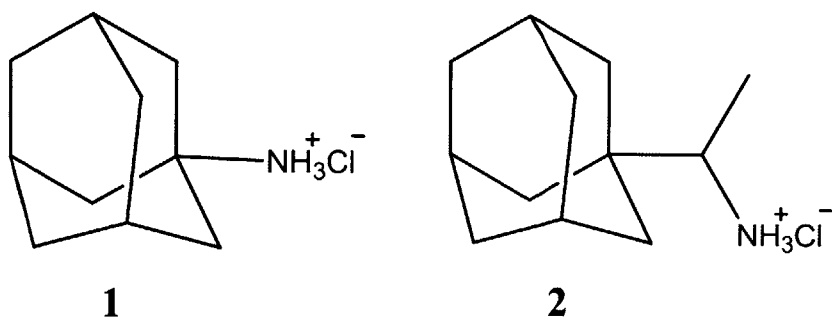


**Figure 3-1.** Chemical structures of both FDA-approved adamantane-class M2 ion channel influenza A inhibitors no longer recommended for therapeutic use: amantadine·HCl (**1**) and rimantadine·HCl (**2**).

Because of the daunting challenges in discovering new anti-influenza drugs, it would be of great benefit to salvage older FDA-approved drugs that are impotent against newly emerged mutants. Previously, we have demonstrated that the

attachment of multiple copies of the influenza neuraminidase inhibitor zanamivir to a flexible polymeric chain not only dramatically improves the potency against drug-sensitive strains, but also resurrects the inhibitory effect against zanamivir-resistant mutants.<sup>10,11</sup> This phenomenon appears to stem from two mechanisms. The first is multivalency, whereby several simultaneous interactions between polymer-attached zanamivir and its viral target result in a far greater avidity



compared to the monomer's binding constant,<sup>10,12,13</sup> while also generating an increased drug concentration in the vicinity of the virus.<sup>13</sup> The second contributor to the improved potency is a novel mechanism of inhibition, blocking earlier stages of the viral cycle, which monomeric zanamivir lacks.<sup>3</sup> Herein we explore whether the approach of attaching multiple copies of influenza drugs to polymeric chains can boost the adamantane inhibitors' prowess against drug-resistant influenza mutants (as it did with zanamivir<sup>10</sup>).

## B. Results and Discussion

To covalently attach multiple copies of amantadine (**1**) and rimantadine (**2**) to polymeric chains without chemically modifying the amine moieties (revealed by protein X-ray crystallography to be oriented toward interior of the virion upon binding<sup>6</sup> and hence presumably important), we sought structural analogs of **1** and **2** with readily functionalizable groups on the opposite side of the molecules. Since commercially available 3-amino-1-adamantanecarboxylic acid (**3**) and 3-(1-aminoethyl)adamantan-1-ol (**7**) fit this description, we employed these molecules as starting points.

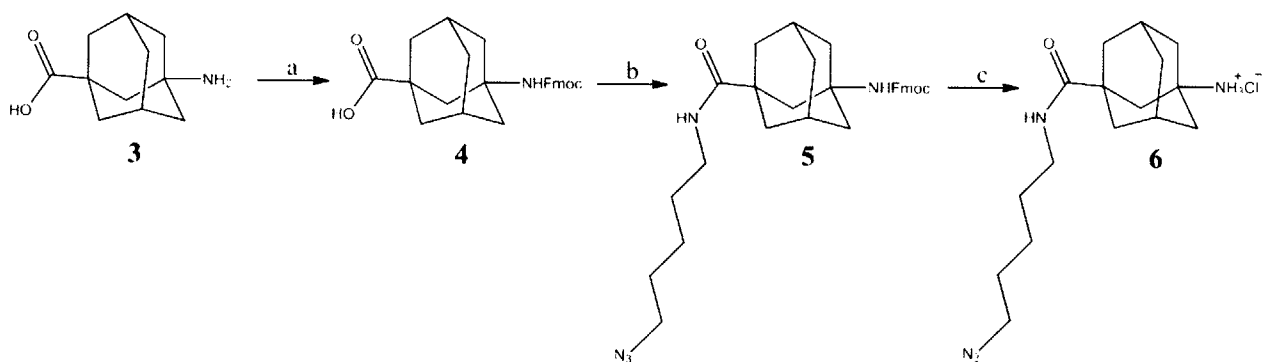


**Figure 3-2.** Synthetic route to generate the 1-linker-azide compound (**6**) for subsequent covalent attachment to poly-L-glutamate. Reagents employed: (a) Fmoc-Cl, Na<sub>2</sub>CO<sub>3</sub>, H<sub>2</sub>O/acetone; (b) HBTU, 5-azidopentan-1-amine, Hünig's base, THF; and (c) anhydrous acetonitrile/diethylamine. See Methods for details.

Both **3** and **7** were first derivatized for polymer attachment through a series of chemical reactions depicted in Figures 3-2 and 3-3. Since our previous studies (albeit with another influenza inhibitor-see chapter 2) demonstrated the benefits of a linker (spacer arm) between the drug and the polymeric backbone in reducing steric hindrances,<sup>14</sup> we also decided to insert a linker between **3** and **7** and the polymers used. As seen in Figs. 3-2 and 3-3, first the drugs' amino groups were protected by Fmoc and Boc groups, respectively, followed by linker attachment and amine deprotection to afford **1** and **2** with azide terminating linkers to be subsequently used for conjugation to polymers. Our initial studies herein utilized poly-L-

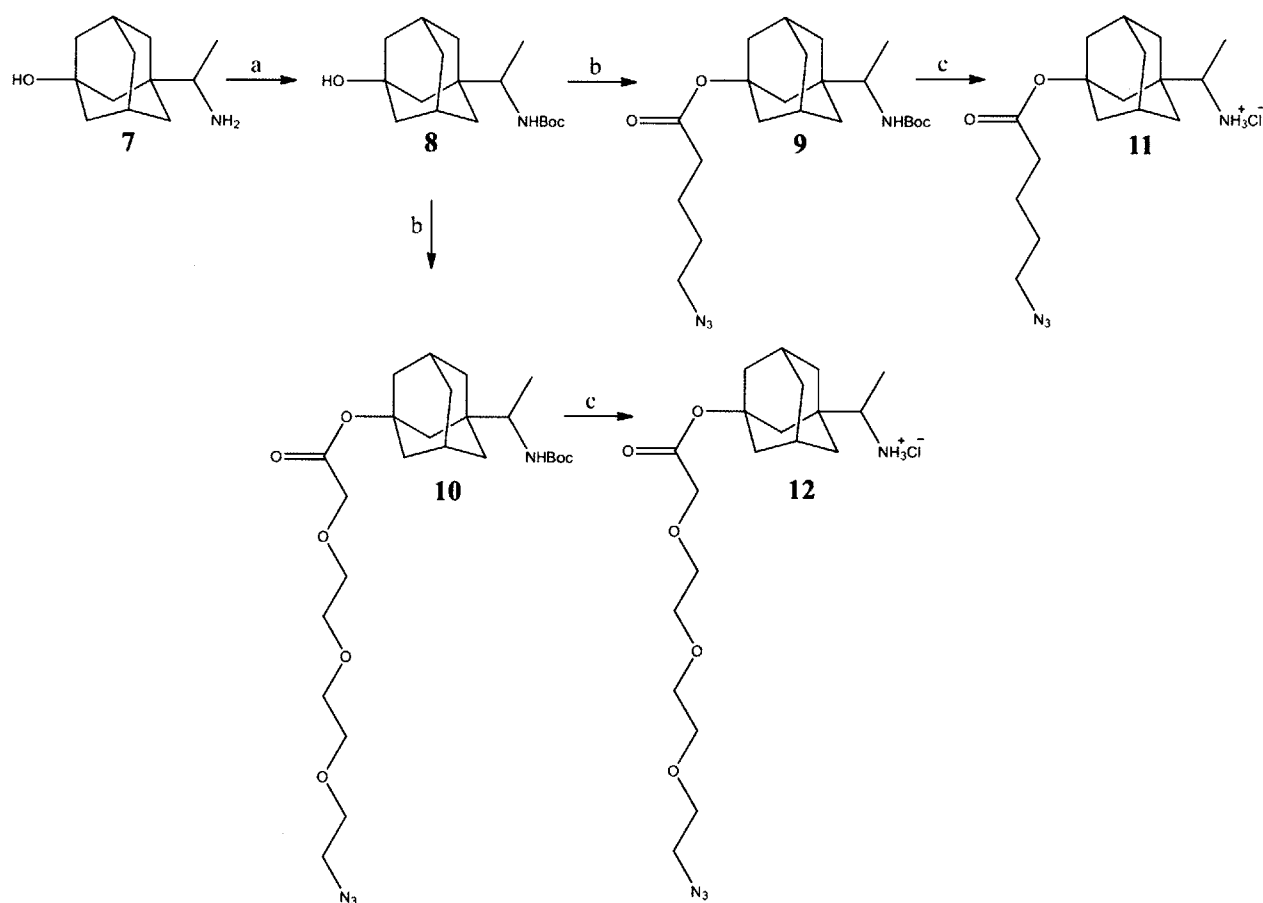


**Figure 3-3.** Synthetic route to generate the 2-linker-azide compounds (**11** and **12**) for subsequent covalent attachment to poly-L-glutamate and other polymers. Reagents employed: (a) di-*tert*-butyl dicarbonate, dichloromethane; (b) 5-azido-pentanoic acid or 11-azido-3,6,9-trioxaundecanoic acid, DPTC, DMAP, chlorobenzene (reflux); (c) 4 M HCl in dioxane. See Methods for details.

glutamate as a polymer because it is benign, freely water soluble, biodegradable, and non-immunogenic.<sup>10</sup>

To verify which strains were drug-resistant to the adamantane-class of inhibitors, we determined the IC<sub>50</sub> values for monomeric **1** against three representative influenza strains using the plaque reduction assay. They were A/Wuhan/359/95 (herein denoted as “Wuhan”), a human strain *with no known resistance* to the adamantane class of influenza inhibitors; A/PR/8/34 (herein denoted as “PR8”), a human strain *with documented resistance* to the adamantanes;<sup>15</sup> and A/WSN/33 (herein denoted as “WSN”), a laboratory-adapted human strain also *with known resistance* to the adamantanes.<sup>15</sup> As seen in the 1st line of Table 3-1 (the first three data

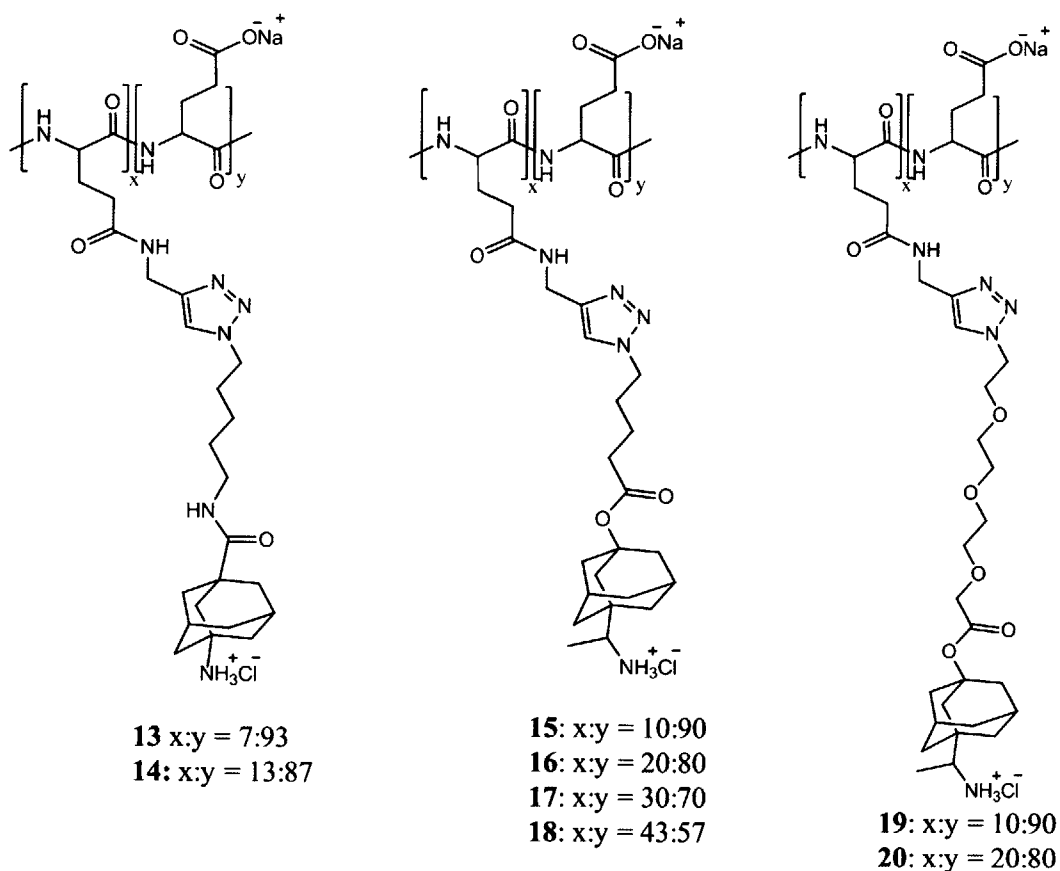


**Figure 3-4.** Chemical structures of poly-L-glutamate-attached conjugates of **1** and **2** at various degrees of loading (% of derivatization).

columns), the non-resistant Wuhan strain was quite sensitive to **1** with an  $IC_{50}$  of  $60 \pm 24 \mu\text{M}$ . In contrast, the drug-resistant PR8 and WSN strains were both far less sensitive toward the inhibitor with much poorer  $IC_{50}$  values of  $2.2 \pm 0.66 \text{ mM}$  and  $3.4 \pm 0.2 \text{ mM}$ , respectively, thus illustrating why **1** is no longer recommended for therapeutic use.

When **6** was attached to poly-L-glutamate at a ~7% loading (i.e., ~7% of all the monomeric units on the polymeric chain were drug-decorated), the inhibition for the resultant compound **13** (Figure 3-4) was nearly the same for the Wuhan and PR8 strains; for WSN, however, **13** was some 4-fold better inhibitor than **1** (Table 3-1, the first three data columns). When the degree of loading was roughly doubled (to yield compound **14** in Fig. 3-4), the inhibition for both the PR8 and WSN strains improved a few fold. Note that the original **1**'s precursor **3** could not be tested as a monomer in the plaque reduction assay to determine the effect of adding a  $-\text{COOH}$  to the structure because of its poor solubility in PBS, which is the medium used in our antiviral assays.

We then investigated whether an additional improvement in anti-influenza potency of our polymer-conjugates **13** and **14** over the monomeric **1** could be attained by lengthening the time of their contact with the viruses during the assay. In our standard plaque reduction assay (designated as "Not in Agar" in Table 3-1), compounds are incubated with the viruses for 1 h prior to infection and during the subsequent 1-h infection period. After that, the inhibitors are removed, and fresh nutrient agar replaces them for the duration of the assay (while plaque formation occurs). Therefore, in the next series of experiments, we decided to keep the inhibitors present not only during those initial steps of the assay but also in an equal concentration in the nutrient agar overlay to allow them to act on all subsequent steps in the viral cycle.

As seen in Table 3-1 (the “In Agar” data columns), including the inhibitor for the entire plaque reduction assay improved IC<sub>50</sub> values in most instances. With **13** and **14**, we observed no improvement in IC<sub>50</sub> values over **1** for the Wuhan strain but several-fold improvements for the PR8 and WSN strains. Thus although the inclusion in the agar results in *net* lower IC<sub>50</sub> values for most of the compounds tested, a greater *magnitude* of the improvement over the monomer (**1**) was seen when polymer conjugates were present only at initial steps of viral infection. Overall, however, these data show a marginal recovery in inhibitory potency toward drug-resistant strains when multiple copies of **1** are attached to poly-L-glutamate.

We next explored how the other FDA-approved M2 ion channel inhibitor, **2**, as well as its multiple copies attached to poly-L-glutamate, behaved against the aforementioned influenza strains. As in the case of **1**, the Wuhan strain was very sensitive to **2** with an even better IC<sub>50</sub> value of  $2.7 \pm 1.4 \mu\text{M}$ , while both the PR8 and WSN strains were far less sensitive with IC<sub>50</sub> values well into the low-single-millimolar range (Table 3-2), again confirming the reported drug resistance patterns.<sup>15</sup> We then tested the effect of the insertion of an OH group into the scaffold of **2** (to yield **7**, which was used in subsequent derivatization (Fig. 3-3)). Surprisingly, this small group greatly diminished the inhibitory potency against the Wuhan strain raising the IC<sub>50</sub> some ~90-fold (Table 3-2, first data column, 2nd line). The addition of an OH group also deleteriously, albeit less drastically, affected the already sub-optimal inhibition for the resistant strains (Table 3-2, second and third data columns, 2nd line).

Covalent attachment of **11** to poly-L-glutamate at a ~10% loading (compound **15**, Fig. 3-4) afforded a significant improvement for all three viral strains over **7** (Table 3-2, the first three

**Table 3-1.** The IC<sub>50</sub> values for both monomeric **1** and its poly-L-glutamate conjugates against the Wuhan, PR8, and WSN strains of influenza A virus.

Inhibitor	IC <sub>50</sub> (μM) <sup>a</sup>					
	“Not in Agar” <sup>b</sup>			“In Agar” <sup>c</sup>		
	Wuhan	PR8	WSN	Wuhan	PR8	WSN
<b>1</b>	(6.0 ± 2.4) x 10 <sup>1</sup>	(2.2 ± 0.6) x 10 <sup>3</sup>	(3.4 ± 0.2) x 10 <sup>3</sup>	(3.8 ± 0.7) x 10 <sup>1</sup>	>5 x 10 <sup>2</sup>	(1.8 ± 0.1) x 10 <sup>2</sup>
<b>13</b>	(8.5 ± 4.7) x 10 <sup>1</sup>	(1.4 ± 0.2) x 10 <sup>3</sup>	(7.8 ± 3.5) x 10 <sup>2</sup>	(3.3 ± 0.7) x 10 <sup>1</sup>	(1.2 ± 0.1) x 10 <sup>2</sup>	(8.3 ± 0.3) x 10 <sup>1</sup>
<b>14</b>	(4.4 ± 0.1) x 10 <sup>1</sup>	(8.9 ± 1.7) x 10 <sup>2</sup>	(8.6 ± 1.8) x 10 <sup>2</sup>	(4.9 ± 1.4) x 10 <sup>1</sup>	(2.2 ± 0.3) x 10 <sup>2</sup>	(7.7 ± 1.9) x 10 <sup>1</sup>

<sup>a</sup> The plaque reduction assay experiments were run in triplicate; the calculated mean and standard deviation values are presented in the table. All IC<sub>50</sub> values are expressed based on the concentration of **1**.

<sup>b</sup> “Not in Agar” refers to an inhibitor present only in initial steps of infection, i.e., during a 1-h pre-incubation and subsequent viral binding to MDCK cells.

<sup>c</sup> “In Agar” refers to an inhibitor present during all stages of viral infection, i.e., during a 1-h pre-incubation, subsequent viral binding to MDCK cells, and the rest of the 72-h plaque reduction assay.

data columns, 3rd line). When compared to the native inhibitor (**2**), however, the polymer conjugation did not fully overcome the negative effects of the OH addition for the Wuhan strain leaving the IC<sub>50</sub> value at 24 ± 5 μM, i.e., some 10-fold inferior to **2**'s. The attachment to poly-L-glutamate at a ~10% loading did little for the inhibitory effect against the PR8 strain but improved the IC<sub>50</sub> for WSN some 4-fold over **2**.

Since in our initial studies with **1** yielded an improvement when the loading of the inhibitor on the polymeric chain was increased (Table 3-1), we explored whether **2** also followed this trend. As seen in Table 3-2 (4<sup>th</sup> line, the first three data columns), increasing the loading to ~20% (compound **16**, Fig. 3-4) afforded some of the most potent poly-L-glutamate conjugates: although the IC<sub>50</sub> for **16** was still 10-fold worse than **2**'s for the Wuhan strain, for PR8 and WSN we saw 8-fold and 30-fold improvements over **2**, respectively. Interestingly, further increasing the degree of loading to ~30% and ~43% (compounds **17** and **18**, respectively, Fig. 3-4) gave little additional improvement or even yielded worse inhibitors (Table 3-2).

When testing the polymeric inhibitors **15**, **16**, **17**, and **18** for the duration of the plaque reduction assay (Table 3-2, the "In Agar" columns), patterns similar to those in the experiments with **1** were observed: the net IC<sub>50</sub> was improved in most cases, but the magnitude of improvement over the monomer (**2**) became smaller. The optimal degree of loading also became less clear for the PR8 strain because all compounds had nearly the same IC<sub>50</sub> values.

We next determined whether a longer and more hydrophilic spacer arm between **2** and poly-L-glutamate would be of benefit. Figure 3-3 depicts the synthetic route to compound **12** which contains a hydrophilic, poly(ethylene glycol), linker and six extra atoms between the drug and the polymeric chain. As seen in Table 3-2, when **12** is attached to poly-L-glutamate at

**Table 3-2.** The IC<sub>50</sub> values for monomeric **2** and **7**, as well as for the latter’s various polymer conjugates against the Wuhan, PR8, and WSN strains of influenza A virus.

Inhibitor	IC <sub>50</sub> (μM) <sup>a</sup>					
	“Not in Agar” <sup>b</sup>			“In Agar” <sup>c</sup>		
	Wuhan	PR8	WSN	Wuhan	PR8	WSN
<b>2</b>	2.7 ± 1.4	(1.3 ± 0.09) x 10 <sup>3</sup>	(2.4 ± 1.2) x 10 <sup>3</sup>	1.4 ± 0.5	(3.0 ± 0.6) x 10 <sup>2</sup>	(1.9 ± 0.8) x 10 <sup>2</sup>
<b>7</b>	(2.4 ± 0.5) x 10 <sup>2</sup>	(3.5 ± 0.8) x 10 <sup>3</sup>	>4.3 x 10 <sup>3</sup>	(1.2 ± 0.8) x 10 <sup>2</sup>	(8.6 ± 1.1) x 10 <sup>2</sup>	(5.0 ± 0.9) x 10 <sup>2</sup>
<b>15</b>	(2.8 ± 0.4) x 10 <sup>1</sup>	(1.5 ± 0.4) x 10 <sup>3</sup>	(6.4 ± 1.0) x 10 <sup>2</sup>	(8.0 ± 3.5) x 10 <sup>1</sup>	(1.1 ± 0.4) x 10 <sup>2</sup>	(4.2 ± 0.3) x 10 <sup>1</sup>
<b>16</b>	(2.5 ± 0.5) x 10 <sup>1</sup>	(1.5 ± 0.8) x 10 <sup>2</sup>	(7.7 ± 0.7) x 10 <sup>1</sup>	(4.8 ± 3.2) x 10 <sup>1</sup>	(1.4 ± 0.4) x 10 <sup>2</sup>	(5.0 ± 1.3) x 10 <sup>1</sup>
<b>17</b>	(1.4 ± 0.1) x 10 <sup>2</sup>	(9.3 ± 2.4) x 10 <sup>2</sup>	(3.9 ± 0.6) x 10 <sup>2</sup>	(1.5 ± 0.09) x 10 <sup>2</sup>	(1.7 ± 0.1) x 10 <sup>2</sup>	(1.8 ± 0.09) x 10 <sup>2</sup>
<b>18</b>	(8.0 ± 1.7) x 10 <sup>2</sup>	>1.4 x 10 <sup>3</sup>	>1.4 x 10 <sup>3</sup>	(1.5 ± 0.3) x 10 <sup>2</sup>	(1.2 ± 0.5) x 10 <sup>2</sup>	(1.8 ± 0.4) x 10 <sup>2</sup>
<b>19</b>	(1.9 ± 0.7) x 10 <sup>2</sup>	(1.1 ± 0.4) x 10 <sup>3</sup>	(9.2 ± 4.1) x 10 <sup>2</sup>	Tox >125 <sup>d</sup>	Tox >125 <sup>d</sup>	Tox >125 <sup>d</sup>
<b>20</b>	(4.9 ± 0.5) x 10 <sup>1</sup>	(1.0 ± 0.5) x 10 <sup>2</sup>	(1.8 ± 1.1) x 10 <sup>2</sup>	(7.3 ± 1.8) x 10 <sup>1</sup>	(1.1 ± 0.9) x 10 <sup>2</sup>	(8.8 ± 1.3) x 10 <sup>1</sup>
<b>21</b>	(4.7 ± 0.8) x 10 <sup>1</sup>	(7.6 ± 2.9) x 10 <sup>1</sup>	(1.5 ± 0.5) x 10 <sup>2</sup>	n.d.	n.d.	n.d.
<b>22</b>	(4.9 ± 0.2) x 10 <sup>1</sup>	(1.3 ± 0.5) x 10 <sup>2</sup>	(1.1 ± 0.5) x 10 <sup>2</sup>	n.d.	n.d.	n.d.
<b>23</b>	(6.4 ± 1.6) x 10 <sup>1</sup>	(6.0 ± 3.6) x 10 <sup>2</sup>	(2.0 ± 0.7) x 10 <sup>2</sup>	(1.2 ± 0.3) x 10 <sup>2</sup>	(9.9 ± 0.5) x 10 <sup>1</sup>	(5.0 ± 1.6) x 10 <sup>1</sup>
<b>24</b>	2.5 ± 0.4	(1.2 ± 0.5) x 10 <sup>2</sup>	(2.8 ± 0.5) x 10 <sup>2</sup>	n.d.	n.d.	n.d.
<b>25</b>	(7.6 ± 1.6) x 10 <sup>2</sup>	(1.2 ± 0.8) x 10 <sup>3</sup>	(7.8 ± 0.9) x 10 <sup>2</sup>	n.d.	n.d.	n.d.

<sup>a</sup> The plaque reduction assay experiments were run in triplicate; the calculated mean and standard deviation values are presented in the table. All IC<sub>50</sub> values are expressed based on the concentration of **2**; n.d. stands for “not determined”.

<sup>b</sup> “Not in Agar” refers to an inhibitor present only in initial steps of infection, *i.e.*, during a 1-h pre-incubation and subsequent viral binding to MDCK cells.

<sup>c</sup> “In Agar” refers to inhibitor present during all stages of viral infection, *i.e.*, during a 1-h pre-incubation, subsequent viral binding to MDCK cells, and the rest of the 72-h plaque reduction assay.

<sup>d</sup> The IC<sub>50</sub> value could not be determined because concentrations below 125 μM were below the IC<sub>50</sub> and concentrations above were toxic to the MDCK cells (*i.e.* no plaques could be visualized)



a ~10% loading to generate compound **19** (Fig. 3-4), there was little or no improvement in inhibition over **2** (some 70-fold worse for the Wuhan strain, no change for PR8, and approximately a 3-fold improvement for WSN). When the loading was increased to ~20% (compound **20**), which was the optimal loading for the shorter and more hydrophobic linker, the inhibition was improved compared to **19**: only a 18-fold worse inhibition for the Wuhan strain and a 13-fold improvements for both PR8 and WSN over **2** (Table 2-2).

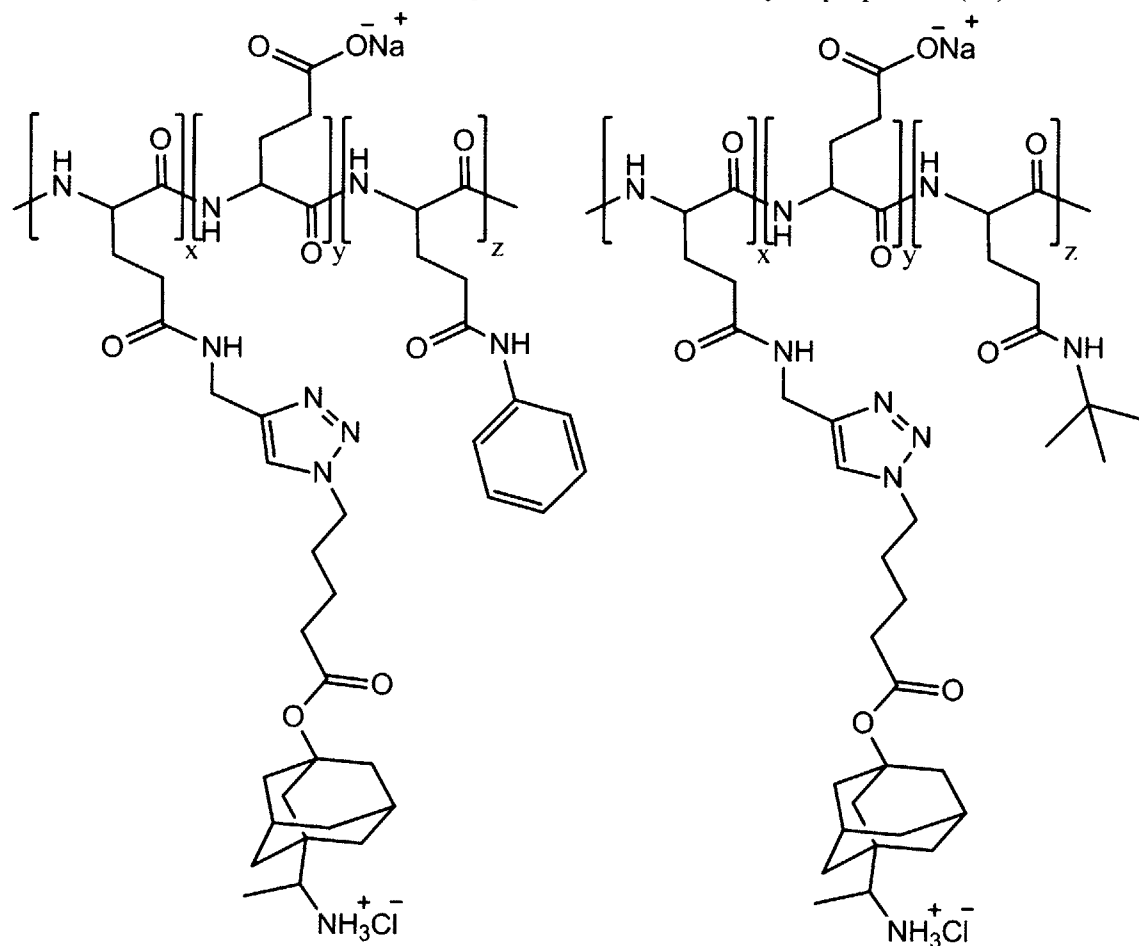
When assaying **19** and **20** for the duration of the assay (Table 3-2, “In Agar”), no sizable benefit to the longer incubation was observed and, in fact, **19** exhibited toxic effects in this modality. Since the longer and more hydrophilic linker failed to generate major improvements over the shorter and more hydrophobic linker, we decided to continue our studies with the latter.

To determine whether increasing hydrophobicity of the polymeric backbone by inserting extra aromatic or aliphatic hydrophobic moieties into it would improve inhibition, perhaps due to additional interactions between the polymer and the viral surface,<sup>12</sup> we synthesized **21** containing ~20% of benzyl rings in addition to a ~15% loading of **2**, as well as **22** containing ~25% of *tert*-butyl substituents in addition to ~20% of **2** moieties (Figure 3-5). When conjugate **21** was tested against all three influenza strains in the plaque reduction assay, we observed similar improvements over **2** compared to that afforded by poly-L-glutamate with ~20% loading and no additional hydrophobic moieties (**16**): some 18-fold weaker inhibition than the monomer for the Wuhan strain and 16/17-fold improvements for WSN and PR8 (Table 3-2). Similarly, for the *tert*-butyl-derivatized **2**-poly-L-glutamate conjugate **22**, we saw the same 18-fold decline in improvement over **2** for the Wuhan strain and some 10- and 22-fold improvements over **2** for PR8 and WSN, respectively. Therefore, although the addition of hydrophobic groups to the

polymer backbone in some cases led to a modest improvement, there was no compelling reason for their inclusion.

We also examined the role of the polymer characteristics in the conjugate's inhibitory potency. To this end, we first abolished the charge of the poly-L-glutamate backbone by transforming it into the neutral poly-L-glutamine (compound **23**, Figure 3-6). As seen in Table 3-2, the neutralization of the polymer resulted in no additional improvements and, in fact, over 20-fold weaker inhibition than with the monomeric **2** for the Wuhan strain. For PR8 and WSN, **23** afforded a 2-fold and 12-fold improvement, respectively, over **2**. When incubated with the

**Figure 3-5.** Chemical structures of poly-L-glutamate derivatized with ~15% of **2** of plus ~20% of benzylamine (**21**) and with ~20% of **2** plus ~25% of 2,2-dimethyl-1-propamine (**22**).



**21:**  $x:y:z = 15:20:65$

58

**22:**  $x:y:z = 20:25:55$

viruses for the duration of the assay, **23** exhibited improvements over the monomer for the PR8 and WSN strains, but not marked ones (Table 3-2, "In Agar"). Thus, putative electrostatic repulsions between the virus and polymer are not a significant factor in viral inhibition for our system (in contrast to observations in previous studies<sup>10,12</sup>).

To investigate how new, structurally-unrelated polymeric backbones would affect the inhibition of drug-resistant influenza viruses by polymer-conjugated **2**, the dissimilar linear polymers poly(acrylic acid Na salt) and carboxymethylcellulose Na salt (CMC). Since each of these polymers, like poly-L-glutamate, contained carboxylate moieties, the same conjugation chemistry could be carried out.

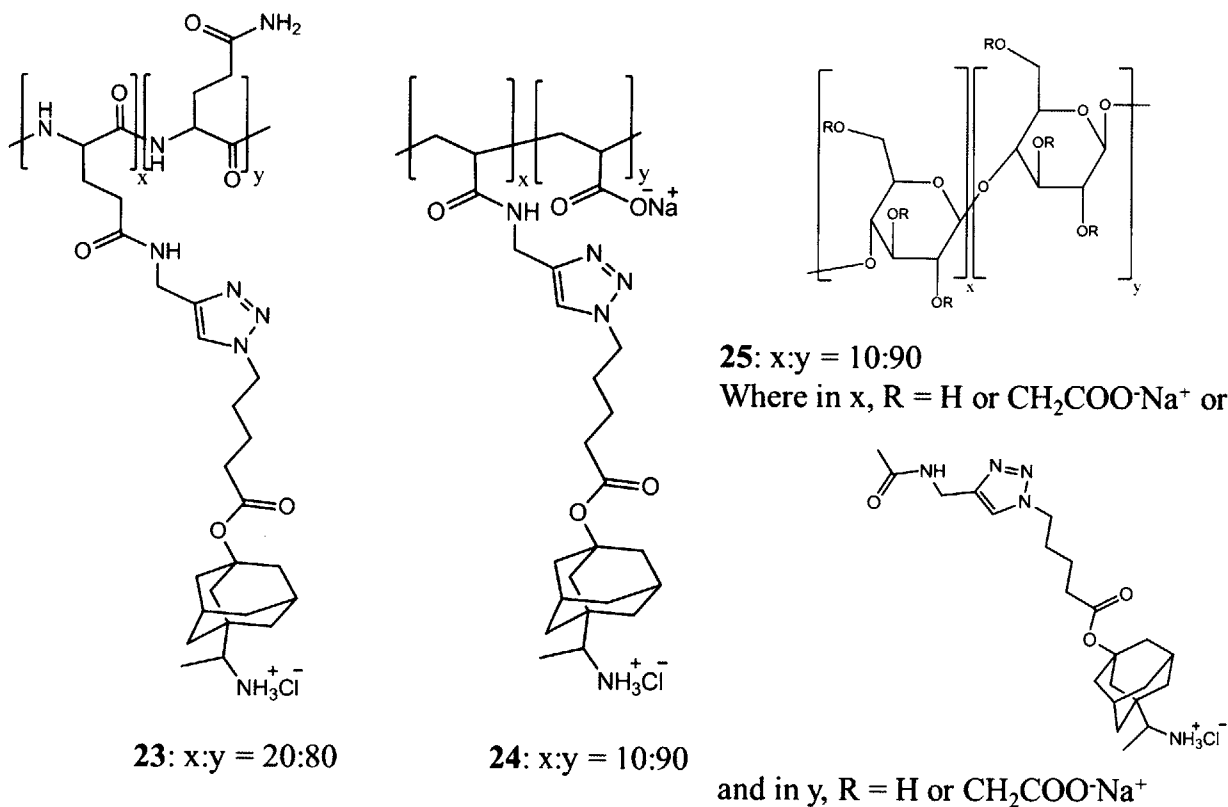


**Figure 3-6.** Chemical structures of poly-L glutamine, poly(acrylic acid Na salt), and CMC derivatized with **2**.

Polyacrylate with ~10% of its monomeric units derivatized with **2** (compound **24**, Figure 3-6) was superior to all other conjugates tested against the Wuhan strain: it overcame *all* negative effects from an OH addition to **2** with an IC<sub>50</sub> equal to that of the commercial drug itself (Table 3-2). However, against the other two influenza strains, **24** did not possess the same potency and was actually worse than many of the other polymer conjugates tested, with IC<sub>50</sub> values of 120 ± 50 μM and 280 ± 50 μM for PR8 and WSN, thus resulting in some 11-fold and 8-fold improvements, respectively, over **2** for these drug-resistant strains (Table 3-2).

Attachment of **2** to CMC at a ~20% loading (**25**, Fig. 3-6) drastically curtailed inhibition of the Wuhan strain, with an IC<sub>50</sub> of 760 ± 160 μM (Table 3-2). Similarly poor IC<sub>50</sub> values were obtained against PR8 and WSN (1,200 ± 800 μM and 780 ± 90 μM, respectively) suggesting that the inhibition afforded by these compounds might not even be caused by **2**'s action *per se* but be due to CMC's intrinsic weak antiviral activity.

In closing, in this study we have attached multiple copies of influenza M2 ion-channel inhibitors to a variety of polymers in an attempt to ameliorate, if not salvage, their ability to inhibit adamantane-resistant influenza strains. A progress toward that goal has been made in preparing **2**-polymer conjugates up to 30-fold more potent than their monomeric precursors against some drug-resistant strains.

## Acknowledgements

I am thankful to Professors Klibanov and Chen for their help in editing this chapter.

## C. Materials and Methods

### Materials

Amantadine·HCl (**1**), rimantadine·HCl (**2**), 3-amino-1-adamantanecarboxylic acid (**3**), 3-(1-aminoethyl)adamantan-1-ol·HCl (**7**), poly-L-glutamate Na salt (MW of 50-100 kDa), carboxymethylcellulose Na salt (MW of ~100 kDa) (CMC), poly(acrylic acid) (MW of ~100 kDa), and all solvents and other reagents, unless otherwise specified, were purchased from Sigma Aldrich Chemical Co. (St. Louis, MO) and used without further purification. *N*-Hydroxysulfosuccinimide (sulfo-NHS) was from Proteochem (Denver, CO), 5-azidopentanoic acid and 5-azidopentan-1-amine from Synthonix (Wake Forest, NC), and 11-azido-3,6,9-trioxaundecanoic acid from TCI America (Portland, OR).

### Syntheses

**Synthesis of 1-linker-azide (6):** Linker addition to **3** was carried out as described by Wanka *et al.*<sup>16</sup> Briefly, 300 mg (1.5 mmol) of **3** and 715 mg (6.7 mmol) of Na<sub>2</sub>CO<sub>3</sub> were suspended in a mixture of 10 mL of H<sub>2</sub>O and 5 mL of acetone, followed by stirring and placing in an ice bath. Next, Fmoc-Cl (426 mg, 1.6 mmol) in 5 mL of acetone was added over 30 min with an addition funnel. The reaction mixture was incubated at room temperature overnight and then heated to 50°C for 2 h to evaporate acetone. To purify the product, the reaction was poured over ice (35 grams) and extracted thrice with diethyl ether. The aqueous layer was then acidified to pH 5 and extracted thrice with ethyl acetate. The ethyl acetate portions were combined, washed with H<sub>2</sub>O, and dried over Na<sub>2</sub>SO<sub>4</sub> to afford an off-white powder of Fmoc-3-amino-1-adamantanecarboxylic acid (**4**) (yield= 40%). (Rf 0.47 in 10:1 CH<sub>2</sub>Cl<sub>2</sub>: MeOH). <sup>1</sup>H NMR **4** ([D<sub>8</sub>]THF) δ (400 MHz): 1.65 (2H, d, CH<sub>2</sub>-**1**), 1.72 (2H, s, CH<sub>2</sub>-**1**), 1.83 (4H, s, CH<sub>2</sub>-**1**), 1.95 (4H, s, CH<sub>2</sub>-**1**), 2.07 (H, s, CH-**1**), 2.14 (H, s, CH-**1**), 4.18 (1H, t, CH-Fmoc), 4.27 (2H, d, CH<sub>2</sub>-

Fmoc), 7.25 (2H, t, *CH*-aromatic-Fmoc), 7.3 (2H, t, *CH*-aromatic-Fmoc), 7.6 (2H, d, *CH*-aromatic-Fmoc), 7.8 (2H, d, *CH*-aromatic-Fmoc).

To synthesize **5**, **4** (220 mg, 0.53 mmol) was dissolved in 5 mL of dry THF. To that, *O*-benzotriazole-*N,N,N',N'*-tetramethyl-uronium-hexafluoro-phosphate (HBTU) (200 mg, 0.53 mmol) was added, followed by 65  $\mu$ L (0.53 mmol) of 5-azidopentan-1-amine and 68  $\mu$ L (0.5 mmol) of Hünig's base. The reaction mixture was stirred overnight and then heated to 60°C for 1 h. After cooling, 3 mL of brine was added, and the mixture was extracted with CHCl<sub>3</sub> thrice. The organic phases were combined, washed with 1 M HCl, 5% NaHCO<sub>3</sub>, H<sub>2</sub>O, and brine, and then further purified on a silica gel column with 10:1 (v/v) CH<sub>2</sub>Cl<sub>2</sub>:methanol mobile phase to afford **5**<sup>16</sup> (yield= 55%). (Rf 0.82 in 10:1 CH<sub>2</sub>Cl<sub>2</sub>: MeOH). <sup>1</sup>H NMR **5** (CDCl<sub>3</sub>)  $\delta$  (400 MHz): 1.35 (2H, m, CH<sub>2</sub>-linker), 1.47(2H, m, CH<sub>2</sub>-linker), 1.6 (4H, m, CH<sub>2</sub>-1, CH<sub>2</sub>-linker), 1.78 (4H, s, CH<sub>2</sub>-1), 1.85 (2H, d, CH<sub>2</sub>-1), 1.95 (2H, d, CH<sub>2</sub>-1), 2.05 (2H, s, CH<sub>2</sub>-1), 2.18 (2H, s, CH-1), 3.2 (2H, dd, CH<sub>2</sub>-linker), 3.24 (2H, t, CH<sub>2</sub>-linker), 4.18 (1H, t, CH-Fmoc), 4.3 (2H, d, CH<sub>2</sub>-Fmoc), 7.25 (2H, t, *CH*-aromatic-Fmoc), 7.3 (2H, t, *CH*-aromatic-Fmoc), 7.6 (2H, d, *CH*-aromatic-Fmoc), 7.7 (2H, d, *CH*-aromatic-Fmoc).

To generate the deprotected final 1-linker-azide (**6**) for attachment to poly-L-glutamate, **5** (75 mg, 0.14mmol) was dissolved in 1.2 mL of dry acetonitrile and cooled to 0°C. Diethylamine (1.2 mL) was added, and the reaction mixture was stirred for 1 h at 0°C and room temperature for 24 h. The reaction mixture was then extracted with H<sub>2</sub>O at pH 3, and the product (**6**) was recovered from the aqueous phase<sup>16</sup> (yield= 20%). (Rf 0.12 in 10:1 CH<sub>2</sub>Cl<sub>2</sub>: MeOH). <sup>1</sup>H NMR **6** (CDCl<sub>3</sub>)  $\delta$  (400 MHz): 1.27 (2H, m, CH<sub>2</sub>-linker), 1.45(2H, m, CH<sub>2</sub>-linker), 1.52 (2H, m, CH<sub>2</sub>-linker), 1.61 (2H, s, CH<sub>2</sub>-1), 1.7 (2H, d, CH<sub>2</sub>-1), 1.78 (4H, d, CH<sub>2</sub>-1), 1.83 (2H, d, CH<sub>2</sub>-1), 1.88 (2H, s, CH<sub>2</sub>-1), 3.1 (2H, t, CH<sub>2</sub>-linker), 2.25 (2H, s, CH-1), 3.25 (2H, t, CH<sub>2</sub>-linker).

**Synthesis of 2-linker-azides (11 and 12):** To obtain an organic solvent soluble free base, 3-(1-aminoethyl)adamantan-1-ol·HCl was suspended in CH<sub>2</sub>Cl<sub>2</sub> and washed with 1 M NaOH. The resultant organic layer was rotary-evaporated, and the isolated white powder of 3-(1-aminoethyl)adamantan-1-ol (**7**) was Boc-protected for subsequent chemical modification. To this end, a solution of di-*tert*-butyl dicarbonate (330 mg, 1.5 mmol) in 25 mL of CH<sub>2</sub>Cl<sub>2</sub> was added to 5 mL of CH<sub>2</sub>Cl<sub>2</sub> containing **7** (290 mg, 1.4 mmol). The reaction mixture was stirred at room temperature for 24 h after which it was extracted thrice with saturated Na<sub>2</sub>CO<sub>3</sub> and dried over Na<sub>2</sub>SO<sub>4</sub> to afford a white fluffy powder of **8**.<sup>17</sup>(yield= 95%). (Rf 0.63 in 10:1 CH<sub>2</sub>Cl<sub>2</sub>: MeOH). <sup>1</sup>H NMR **8** (CDCl<sub>3</sub>) δ (400 MHz): 0.98 (3H, d, CH<sub>3</sub>-**2**), 1.33 (2H, d, CH<sub>2</sub>-**2**), 1.39 (11H, s, Boc, CH<sub>2</sub>-**2**), 1.47 (2H, s, CH<sub>2</sub>-**2**), 1.57 (2H, d, CH<sub>2</sub>-**2**), 1.62 (2H, d, CH<sub>2</sub>-**2**), 1.75 (1H, s, CH-**2**), 2.15 (2H, s, CH<sub>2</sub>-**2**), 3.4 (1H, m, CH-**2**), 4.4 (1H, m, CH-**2**).

Next, the Boc-protected 3-(1-aminoethyl)adamantan-1-ol (**8**) was reacted with 5-azidopentanoic acid in a method similar to that of Saitoh *et al.*<sup>18</sup> Briefly, **8** (130 mg, 0.5 mmol), 5-azidopentanoic acid (130 μL, 1.0 mmol), and 4-dimethylaminopyridine (DMAP) (6 mg, 0.03mmol) were dissolved in 3 mL of chlorobenzene. To that mixture, di(2-pyridyl)thionocarbonate (DPTC) (230 mg, 1.0 mmol) was added, and the reaction mixture was refluxed for 1 h, concentrated, and purified on a silica gel column with 2:1 (v/v) hexane:ethyl acetate mobile phase to afford **9**. (yield= 55%). (Rf 0.54 in 2:1 hexane:ethyl acetate). To prepare **10**, 11-azido-3,6,9-trioxaundecanoic acid was used in place of 5-azidopentanoic acid and the reaction was purified on a silica gel column with 7:1 (v/v) CHCl<sub>3</sub>:acetone mobile phase. (yield= 65%). (Rf 0.60 in 7:1 CHCl<sub>3</sub>:acetone). <sup>1</sup>H NMR **9** (CDCl<sub>3</sub>) δ (400 MHz): 0.98 (3H, d, CH<sub>3</sub>-**2**), 1.35 (11H, s, Boc, CH<sub>2</sub>-**2**), 1.45 (2H, d, CH<sub>2</sub>-**2**), 1.57 (4H, m, CH<sub>2</sub>-linker), 1.75 (2H, m, CH<sub>2</sub>-**2**), 1.95 (3H, m, CH<sub>2</sub>-**2**, CH-**2**), 2.05 (2H, d, CH<sub>2</sub>-**2**), 2.2 (4H, m, CH<sub>2</sub>-**2**, CH<sub>2</sub>-linker), 3.22 (2H, m,

*CH*<sub>2</sub>-linker), 3.4 (1H, m, *CH*-2), 4.35 (1H, m, *CH*-2). <sup>1</sup>H NMR **10** (CDCl<sub>3</sub>) δ (400 MHz): 0.95 (3H, d, *CH*<sub>3</sub>-2), 1.35 (11H, s, *Boc*, *CH*<sub>2</sub>-2), 1.43 (2H, d, *CH*<sub>2</sub>-2), 1.54 (2H, d, *CH*<sub>2</sub>-2), 1.78 (2H, m, *CH*<sub>2</sub>-2), 1.93 (2H, d, *CH*<sub>2</sub>-2), 2.03 (2H, d, *CH*<sub>2</sub>-2), 2.09 (1H, s, *CH*-2), 2.17 (2H, s, *CH*<sub>2</sub>-2), 3.3 (2H, t, *CH*<sub>2</sub>-linker), 3.6 (11, m, *CH*<sub>2</sub>-linker, *CH*-2), 3.93 (2H, s, *CH*<sub>2</sub>-linker), 4.35 (1H, m, *CH*-2).

Deprotection of the *Boc* group was performed with 4 M HCl in dioxane, as described previously,<sup>19</sup> to yield the final 2-linker-azide conjugates (**11** and **12**). (yield= 90%). (Rf 0 in 2:1 hexane:ethyl acetate). <sup>1</sup>H NMR **11** (CDCl<sub>3</sub>) δ (400 MHz): 1.2 (3H, d, *CH*<sub>3</sub>-2), 1.5 (8H, m, *CH*<sub>2</sub>-2, *CH*<sub>2</sub>-linker), 1.65 (1H, d, *CH*-2), 1.75 (4H, s, *CH*<sub>2</sub>-2), 2.05 (2H, s, *CH*<sub>2</sub>-2), 2.15 (2H, t, *CH*<sub>2</sub>-linker), 2.2 (2H, s, *CH*<sub>2</sub>-2), 2.95 (1H, t, *CH*-2), 3.2 (2H, t, *CH*<sub>2</sub>-linker), 4.3 (1H, d, *CH*-2). <sup>1</sup>H NMR **12** (CDCl<sub>3</sub>) δ (400 MHz): 1.3 (3H, d, *CH*<sub>3</sub>-2), 1.5 (2H, d, *CH*<sub>2</sub>-2), 1.6 (2H, s, *CH*<sub>2</sub>-2), 1.72 (1H, d, *CH*-2), 1.92 (4H, m, *CH*<sub>2</sub>-2), 2.1 (2H, d, *CH*<sub>2</sub>-2), 2.25 (2H, s, *CH*<sub>2</sub>-2), 3.0 (1H, s, *CH*-2), 3.33 (2H, t, *CH*<sub>2</sub>-linker), 3.62 (11H, s, *CH*<sub>2</sub>-linker, *CH*-2), 3.95 (2H, s, *CH*<sub>2</sub>-linker).

### Polymer activation

Polymers were activated with propargylamine to incorporate a terminal alkyne for subsequent conjugation reactions with the aforementioned azide-containing inhibitors **6**, **11**, and **12**. As a representative example, poly-L-glutamate Na salt (100 mg) was dissolved in 30 mL of H<sub>2</sub>O. To that was added 300 mg of 4-(4,6-dimethoxy-1,3,5-triazin-2-yl)-4-methylmorpholinium chloride (1.1 mmol) and 7 μL (0.15 mmol) of propargylamine to afford a ~10% derivatized polymer. The reaction mixture was stirred for 5 h and purified as described previously.<sup>14,20</sup> The amount of propargyl amine was varied to tune the percent of derivatization of the polymer used. The percent of derivatization was verified by <sup>1</sup>H NMR where the integration of one propargylamine H peak was compared to that of the integration of one known polymer H peak.



For compounds **21** and **22**, poly-L-glutamate was reacted as described above with propargylamine and approximately 0.2 mol-eq. of either benzylamine or 2,2-dimethyl-1-propanamine, respectively.

To generate a poly-L-glutamine backbone for compound **23**, the purified polymer pre-derivatized to have ~20% of its monomeric units activated with propargylamine was dissolved at 10 mg/mL in 0.1 M 2-*N*-morpholinoethanesulfonate (MES) buffer containing 0.5 M NaCl, pH 6. To that mixture was added 1.2 mol-eq. of both 1-ethyl-3-(3-dimethylaminopropyl)carbodiimide and sulfo-NHS. The reaction mixture was stirred for 30 min at room temperature, after which an excess of saturated aqueous NH<sub>4</sub>OH was added. Following an overnight incubation, the product was purified for subsequent small molecule derivatization.<sup>14</sup>

### **Polymer conjugation**

Once the propargylamine-derivatized polymers were purified and quantified, they were reacted in a Cu<sup>+</sup>-catalyzed [3+2] azide-alkyne cycloaddition with the azide containing amantadine or rimantadine derivatives (**6**, **11**, and **12**) as previously described.<sup>14</sup> Percent derivatization of **1** or **2**- for each polymer-conjugate was determined by <sup>1</sup>H NMR as described above. An example <sup>1</sup>H NMR breakdown is described. <sup>1</sup>H NMR **16** (D<sub>2</sub>O) δ (600 MHz): 1.2 (3H, d, CH<sub>3</sub>-**2**), 1.5 (8H, s, CH<sub>2</sub>-**2**, CH<sub>2</sub>-linker), 2.0 (2H, m, CH<sub>2</sub>-polymer, 8H CH<sub>2</sub>-**2**, CH-**2**), 2.3 (2H, s, CH<sub>2</sub>-polymer, 4H, s, CH<sub>2</sub>-**2**, CH<sub>2</sub>-linker), 3.1 (1H, s, CH-**2**), 4.3 (1H, s, CH-polymer, 4H, d, CH<sub>2</sub>-**2**, CH<sub>2</sub>-propargylamine), 8.0 (1H, s, CH-triazole).

### **Cells, viruses, and antiviral assays**

Madin-Darby canine kidney cells (MDCK) for use in plaque reduction assays were from the American Type Culture Collection and maintained as described previously.<sup>11,21</sup> The human wild-type influenza strains A/Wuhan/359/95 (H3N2) and A/PR/8/34 (H1N1) were obtained from

the U.S. Centers for Disease Control and Prevention (Atlanta, GA) and Charles River Laboratories (North Franklin, CT), respectively. The influenza strain A/WSN/33 (H1N1) was a gift from Dr. Peter Palese of Mount Sinai School of Medicine (NY, NY). Viruses were stored in a -80°C freezer and diluted in phosphate-buffered saline (PBS) for use in assays.

Plaque reduction assays with MDCK cells were carried out to determine the half-maximal inhibitory concentration (IC<sub>50</sub>) of both monomeric and polymer-attached compounds as described before.<sup>10,11,14</sup> When analyzing polymer conjugates, the IC<sub>50</sub> values were calculated based on the concentration of the small-molecule inhibitors. In investigating the effect of the inhibitors' presence for the complete viral cycle (denoted as "In Agar"), equal concentrations of inhibitors were used for both pre-incubation with the virus and in the nutrient agar overlay.<sup>14</sup>

#### **D. References**

1. Taubenberger JK, Morens DM. 2008. The pathology of influenza virus infections. *Annu Rev Path.* 3:499-522.
2. De Clercq E. 2006. Antiviral agents active against influenza A viruses. *Nat Rev Drug Disc.* 5(12):1015-1025.
3. Lee CM, Weight AK, Haldar J, Wang L, Klibanov AM, Chen J. 2012. Polymer-attached zanamivir inhibits synergistically both early and late stages of influenza virus infection. *Proc Natl Acad Sci.* 109(50):20385-20390.
4. Bright RA, Shay DK, Shu B, Cox NJ, Klimov AI. 2006. Adamantane resistance among influenza A viruses isolated early during the 2005-2006 influenza season in the United States. *JAMA.* 295(8):891-894.

5. Das K, Aramini JM, Ma L-C, Krug RM, Arnold E. 2010. Structures of influenza A proteins and insights into antiviral drug targets. *Nat Struct Mol Biol.* 17(5):530-538.
6. Stouffer AL, Acharya R, Salom D, Levine AS, Di Costanzo L, Soto CS, Tereshko V, Nanda V, Stayrook S, DeGrado WF. 2008. Structural basis for the function and inhibition of an influenza virus proton channel. *Nature.* 451(7178):596-599.
7. Kozakov D, Chuang G-Y, Beglov D, Vajda S. 2010. Where does amantadine bind to the influenza virus M2 proton channel? *Trends Biochem Sci.* 35(9):471-475.
8. Pielak RM, Schnell JR, Chou JJ. 2009. Mechanism of drug inhibition and drug resistance of influenza A M2 channel. *Proc Natl Acad Sci.* 106(18):7379-7384.
9. Cady SD, Schmidt-Rohr K, Wang J, Soto CS, DeGrado WF, Hong M. 2010. Structure of the amantadine binding site of influenza M2 proton channels in lipid bilayers. *Nature.* 463(7281):689-692.
10. Weight AK, Haldar J, Alvarez de Cienfuegos L, Gubareva LV, Tumpey TM, Chen J, Klibanov AM. 2011. Attaching zanamivir to a polymer markedly enhances its activity against drug-resistant strains of influenza a virus. *J Pharm Sci.* 100(3):831-835.
11. Haldar J, Alvarez de Cienfuegos L, Tumpey TM, Gubareva LV, Chen J, Klibanov AM. 2010. Bifunctional polymeric inhibitors of human influenza A viruses. *Pharm Res.* 27(2):259-263.
12. Mammen M, Dahmann G, Whitesides GM. 1995. Effective inhibitors of hemagglutination by influenza-virus synthesized from polymers having active ester groups-Insight into mechanism of inhibition. *J Med Chem.* 38(21):4179-4190.

13. Mammen M, Choi S-K, Whitesides GM. 1998. Polyvalent interactions in biological systems: implications for design and use of multivalent ligands and inhibitors. *Angew Chem Int Ed.* 37(20):2754-2794.
14. Larson AM, Wang H, Cao Y, Jiang T, Chen J, M Klivanov AM. 2012. Conjugating drug candidates to polymeric chains does not necessarily enhance anti-influenza activity. *J Pharm Sci.* 101(10):3896–3905.
15. Bright RA, Medina M-j, Xu X, Perez-Oronoz G, Wallis TR, Davis XM, Povinelli L, Cox NJ, Klimov AI. 2005. Incidence of adamantane resistance among influenza A (H3N2) viruses isolated worldwide from 1994 to 2005: a cause for concern. *Lancet.* 366(9492):1175-1181.
16. Wanka L, Cabrele C, Vanejews M, Schreiner PR. 2007.  $\gamma$ -Aminoadamantanecarboxylic acids through direct C–H bond amidations. *Eur J Org Chem.* 2007(9):1474-1490.
17. Yi L, Abootorabi M, Wu YW. 2011. Semisynthesis of prenylated Rab GTPases by click ligation. *ChemBioChem.* 12(16):2413-2417.
18. Saitoh K, Shiina I, Mukaiyama T. 1998. *O,O'*-Di(2-pyridyl)Thiocarbonate as an efficient reagent for the preparation of carboxylic esters from highly hindered alcohols. *Chem Lett.* 27(7):679-680.
19. Iossifidou S, Froussio CC. 1996. Facile synthesis of 1-adamantyl esters of L- $\alpha$ -amino acids, a new class of carboxy protected derivatives. *Synthesis* (11):1355-1358.
20. Ochs CJ, Such GK, Staedler B, Caruso F. 2008. Low-fouling, biofunctionalized, and biodegradable click capsules. *Biomacromolecules.* 9(12):3389-3396.
21. Haldar J, Weight AK, Klivanov AM. 2007. Preparation, application and testing of permanent antibacterial and antiviral coatings. *Nat Protoc.* 2(10):2412-2417.

## CHAPTER 4

Decreasing herpes simplex viral infectivity in solution by surface-immobilized and suspended  
*N,N*-dodecyl,methyl-polyethylenimine

The work presented in this chapter was published in the following manuscript and is reproduced with kind permission from Springer Science and Business Media:

Larson AM, Oh HS, Knipe DM, Klibanov AM. 2013. Decreasing herpes simplex viral infectivity in solution by surface-immobilized and suspended *N,N*-dodecyl,methyl-polyethylenimine. *Pharm Res.* 30(1):25-31.

## A. Introduction

Herpes simplex viruses (HSVs) 1 and 2 are enveloped DNA viruses that can cause oral and genital lesions in humans. While typically HSV-1 causes oral lesions and HSV-2 genital ones, both are capable of infecting either region.<sup>1</sup> These communicable viruses are ubiquitous and a serious public health concern because of acute and lifelong manifestations of herpes in infected individuals.<sup>2</sup> HSV-2 is particularly prevalent, with a 16% reported frequency in people aged between 15 and 49 worldwide.<sup>3,4</sup> HSVs also have high recurrence rates of 33-90% per year in infected individuals.<sup>5</sup> Infectious viral particles are excreted from the lesions caused by HSVs and can be transmitted through such personal contact as kissing and sexual intercourse. Furthermore, individuals infected with HSV-2 have an increased risk of infection by human immunodeficiency virus.<sup>6</sup> HSV transmission can be reduced by avoiding direct contact during symptomatic outbreaks, but asymptomatic shedding of the virus is still possible resulting in transmission. Although such antiviral drugs as acyclovir reduce outbreaks and wane symptoms during them,<sup>7</sup> acyclovir-resistant HSV strains have been reported.<sup>8</sup> There is no cure or vaccine available for either HSV-1 or HSV-2; thus developing a strategy that directly prevents viral transmission is important to reduce its spread.

Certain long-chained hydrophobic polycationic polymers have been shown both *in vitro* and *in vivo* to inactivate a wide variety of microbial pathogens, including *Escherichia coli*, *Staphylococcus aureus* and *epidermides*, and *Pseudomonas aeruginosa* bacteria, *Candida albicans* yeast, and human and avian strains of enveloped influenza viruses, as well as disinfect solutions containing the non-enveloped poliovirus and rotavirus.<sup>9-21</sup> In the present work, we demonstrate that the hydrophobic polycation *N,N*-dodecyl,methyl-polyethylenimine (DMPEI)

(previously determined to be maximally antimicrobial when used as a non-covalent coating)<sup>10,12,13,20</sup> can also decrease the infectivity of HSV-1 or -2. Based on this finding, we have explored DMPEI for potential therapeutic and prophylactic uses.

## B. Results and Discussion

To ascertain whether immobilized DMPEI can reduce infectivity of aqueous solutions containing HSV-1 or HSV-2, we placed a virus-containing solution on either a DMPEI-coated or uncoated polyethylene slide and measured the change in infectivity in the solution by comparing viral titers of the resultant washings.<sup>9,16</sup> Exposure to a DMPEI-coated polyethylene slide reduced

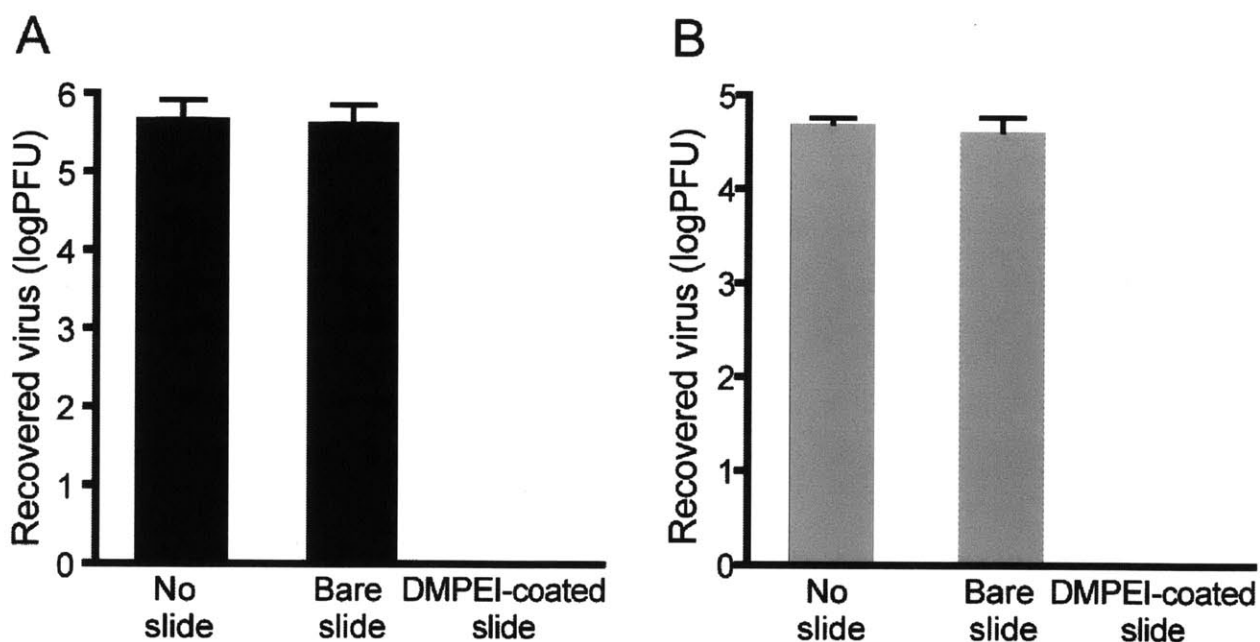


**Figure 4-1.** Reduction of viral titers of HSV-1 (A) and HSV-2 (B) incubated for 15 min at room temperature in a buffered aqueous solution (the left set of bars), in that in the presence of an uncoated polyethylene slide (the middle set of bars), and in that in the presence of a DMPEI-coated polyethylene slide (the right set of bars). In the “No slide” experiment, a virus solution was incubated in buffer only. In the “Bare slide” experiment, a virus solution was incubated between two uncoated polyethylene slides for 15 min to account for any non-specific adsorption of the virus to the slide. In the “DMPEI-coated slide” experiment, one of the two polyethylene slides was painted with the hydrophobic polycation. The limit of detection for the assay is approximately 1 PFU. The heights of the bars are mean values, and the error bars are standard deviations.

the viral titer to below the limit of detection of the plaque assay, thus yielding at least a 5-log reduction in viral titer for HSV-1 and at least a 4-log reduction for HSV-2 compared to minimal reduction for the uncoated polyethylene slide (Figure 4-1). These observations encouraged us to further explore this phenomenon and its potential applications.

Since HSVs are transmitted by direct contact with viral lesions, an antiviral formulation should ideally be available in a form that can intimately interact with infected tissues. Because DMPEI was deliberately designed as a non-leaching surface coating and it is insoluble in aqueous solution,<sup>10</sup> we explored whether its water-soluble homolog, per-methylated PEI (PMPEI), or even an underivatized PEI were capable of inactivating HSV-1 (as a soluble form of the polymer could be easily administered to a lesion). To this end, we incubated PMPEI or PEI

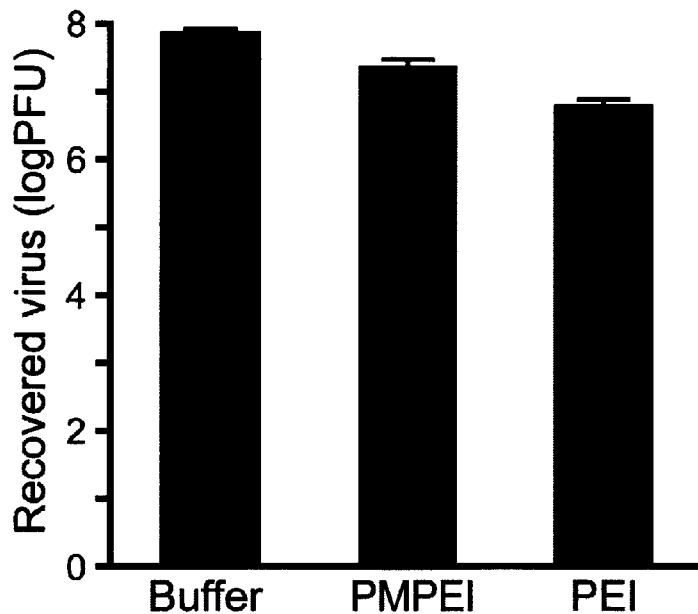


**Figure 4-2.** Reduction of viral titer of HSV-1 incubated for 30 min at room temperature in a buffered aqueous solution (the left bar), in that in the presence of PMPEI (1 mg/mL) (the middle bar), and in that in the presence of PEI (2 mg/mL) (the right bar). The heights of the bars are mean values, and the error bars are standard deviations.

with an aqueous solution containing HSV-1 and determined the consequent loss of infectivity. Not only was the polycation PMPEI incapable of lowering the HSV-1 titer by more than a single log in aqueous solution, it was less potent than the unalkylated PEI (Figure 4-2). We concluded, therefore, that the polycationic nature was not the

sole, or even the main, determinant of anti-HSV activity and substantial hydrophobicity was required as well.



We reasoned that a suspension of the hydrophobic DMPEI in aqueous buffer could circumvent the solubility issues (as well as the use of organic solvents), while still allowing a rather intimate contact with the virus and hence possibly an antiviral effect. To test this hypothesis, we prepared an aqueous suspension of DMPEI and investigated whether it was capable of inactivating HSV-1 and HSV-2. Although surface-immobilized DMPEI previously showed little toxicity to mammalian cells,<sup>21-23</sup> we found greater toxicity of DMPEI in suspension. Based on an MTS assay, we observed a 50% cell cytotoxicity (CC<sub>50</sub>) at a 120- $\mu$ g/mL polycation concentration. To determine what causes the toxicity, we subjected a 0.3-mg/mL suspension of DMPEI to filtration through a 0.45- $\mu$ m filter and compared the filtrate's toxicity in Vero cells to that of the unfiltered suspension. Since the DMPEI filtrate exhibited no visible toxicity, we concluded that toxicity must result from particles larger than approximately 0.45- $\mu$ m. Therefore, to eliminate artifacts caused by large particles during plaque assay, we modified the assay protocol: following the incubation of HSV-1 with the DMPEI suspension, we filtered the mixture through a 0.45- $\mu$ m filter, which should remove the corresponding polycation particles but not the virus (which is 0.2- $\mu$ m diameter<sup>24</sup>).

Using these conditions in a modified assay, we observed that incubating a 0.3-mg/mL DMPEI suspension with HSV-1 lowered the viral titer by more than 1.5 logs (Figure 4-3). Moreover, most of the observed antiviral activity was due to the DMPEI particles larger than 0.45  $\mu$ m because incubation with DMPEI suspension filtrate did not have a marked anti-HSV effect (Fig. 4-3). Lastly, filtering itself did not contribute to a reduction of viral titer (second bar, Fig. 4-3). The lower antiviral activity detected for the DMPEI suspension, as compared to DMPEI-coated polyethylene slides (Fig. 4-1), was likely caused by the inherent differences in surface contact between the virus and DMPEI in the two assays.

If used as a therapeutic, DMPEI would presumably be applied topically in the presence of both the virus and host cells. Therefore, we next examined a scenario where a DMPEI suspension was incubated with HSV-1 during the infection of Vero cells (Table 4-1). During this experiment, we observed a dose-dependent response for the DMPEI suspension with regard to both inhibition of HSV-1 infection and toxicity. For example, when the virus encountered a 30- $\mu$ g/mL DMPEI suspension, a 41% drop in viral titer was observed with no apparent toxicity. As the concentration of the DMPEI in the suspension was increased to 0.1, 0.3, and 0.5 mg/mL, we

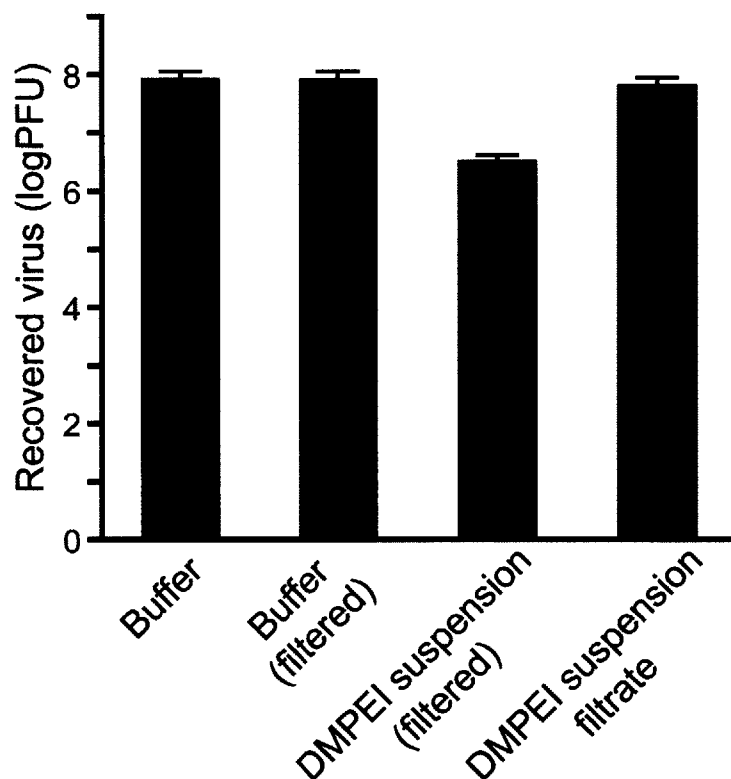


**Figure 4-3.** Reduction of viral titer of HSV-1 incubated for 30 min at room temperature in a buffered aqueous solution (the left bar), in that subsequently filtered through a 0.45- $\mu$ m filter (the middle left bar), in that containing 0.3 mg/mL of DMPEI suspension and subsequently filtered through a 0.45- $\mu$ m filter (the middle right bar), and in that of a 0.3 mg/mL DMPEI suspension filtrate (the right bar). The heights of the bars are mean values, and the error bars are standard deviations.

**Table 4-1.** Antiviral activity against HSV-1 (assessed by plaque reduction assay) and toxicity toward Vero cells (assessed visually after staining the cells) of DMPEI suspensions.

Concentration of DMPEI (mg/mL)	% reduction <sup>a</sup>	Cell viability <sup>b</sup>
0	0 ± 3	+++
0.03	41 ± 6	+++
0.1	85 ± 2	++
0.3	95 ± 8	+
0.5	100 ± 0	+

<sup>a</sup> Reduction is compared to an incubation of HSV-1 without DMPEI under otherwise the same conditions. Experiments were carried out in triplicate, with the mean and standard deviation values presented in the table. See Materials and Methods for experimental details.

<sup>b</sup> Score based on visual appearance of the cells: three pluses denote all healthy cells, two pluses denote some visible toxicity, and a single plus denotes marked visible toxicity.

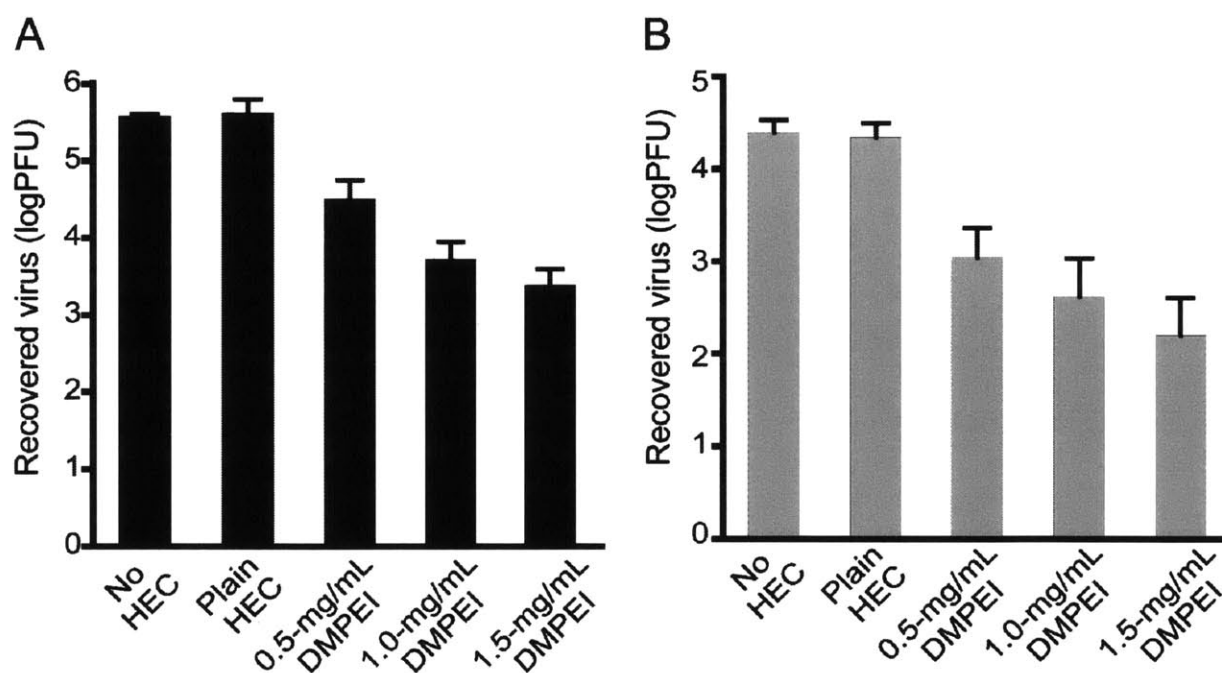


**Figure 4-4.** Reduction of viral titers of HSV-1 (A) and HSV-2 (B) incubated for 30 min at room temperature in an aqueous PBS buffer (the left set of bars), in that thickened with 1.5% HEC (the 2<sup>nd</sup> set of bars), and in that thickened with 1.5% HEC in which various concentrations of DMPEI were suspended (the 3<sup>rd</sup>, 4<sup>th</sup>, and 5<sup>th</sup> sets of bars). The heights of the bars are mean values, and the error bars are standard deviations.

observed a 85%, 95%, and 100% decrease in viral titer, respectively (Table 4-1). These marked drops in infectivity were accompanied by increasing toxicity. From these data, the half-maximal inhibitory concentration ( $IC_{50}$ ) was calculated to be 44  $\mu\text{g/mL}$ . From our previous MTS assay toxicity data, we conclude that the therapeutic index ( $CC_{50}/IC_{50}$ ) of our DMPEI suspension is  $\sim 3$ .

For a DMPEI suspension to be used as a topical therapeutic, it should be “pharmaceutically elegant”, *i.e.*, in the form of a homogeneous cream or lotion. To achieve the corresponding no-drip consistency, we thickened a DMPEI suspension by adding the common pharmaceutical excipient hydroxyethyl-cellulose (HEC).<sup>25</sup> As with the non-thickened suspensions above, we observed a dose-dependent antiviral response; for example, a 1.5-mg/mL aqueous DMPEI suspension containing 1.5% HEC elicited over a 2-log reduction in viral titer for both HSV-1 and HSV-2, while less concentrated suspensions of DMPEI resulted in a reduction in viral titers between one and two logs (Figure 4-4). Note that a control aqueous solution containing the same concentration of HEC alone had no appreciable influence on HSV viral titer (Fig. 4-4).

To explore whether DMPEI could be used in a prophylactic mode, we painted the outside surface of a male latex condom with a 50 mg/mL solution of DMPEI in butanol and, following evaporation of solvent, tested its ability to disinfect aqueous solutions of HSV-1 and HSV-2. As seen in Figure 4-5, more than a 3-log reduction in infectivity for both viruses compared to the uncoated latex condom was observed.

We also examined whether handling and extensive stretching of DMPEI-coated condoms (imitating the conditions likely to be encountered during their intended use) affected their ability to disinfect viral solutions. More than a 3-log reduction was observed with a stretched DMPEI-coated latex condom for HSV-1 and more than a 2-log reduction for HSV-2 (Fig. 4-5). The

reduced inactivation observed for the coated latex condoms, as compared to DMPEI-coated polyethylene slides (see Fig. 4-1), could be due to a lower rigidity of latex than of polyethylene resulting in less uniform coatings. In addition, stretching may produce cracks in the DMPEI coating where HSVs can remain unmolested. It was also noted that some of the DMPEI flaked off into the supplemented PBS buffer during the washing step; clearly, coating of the condoms must be optimized further.

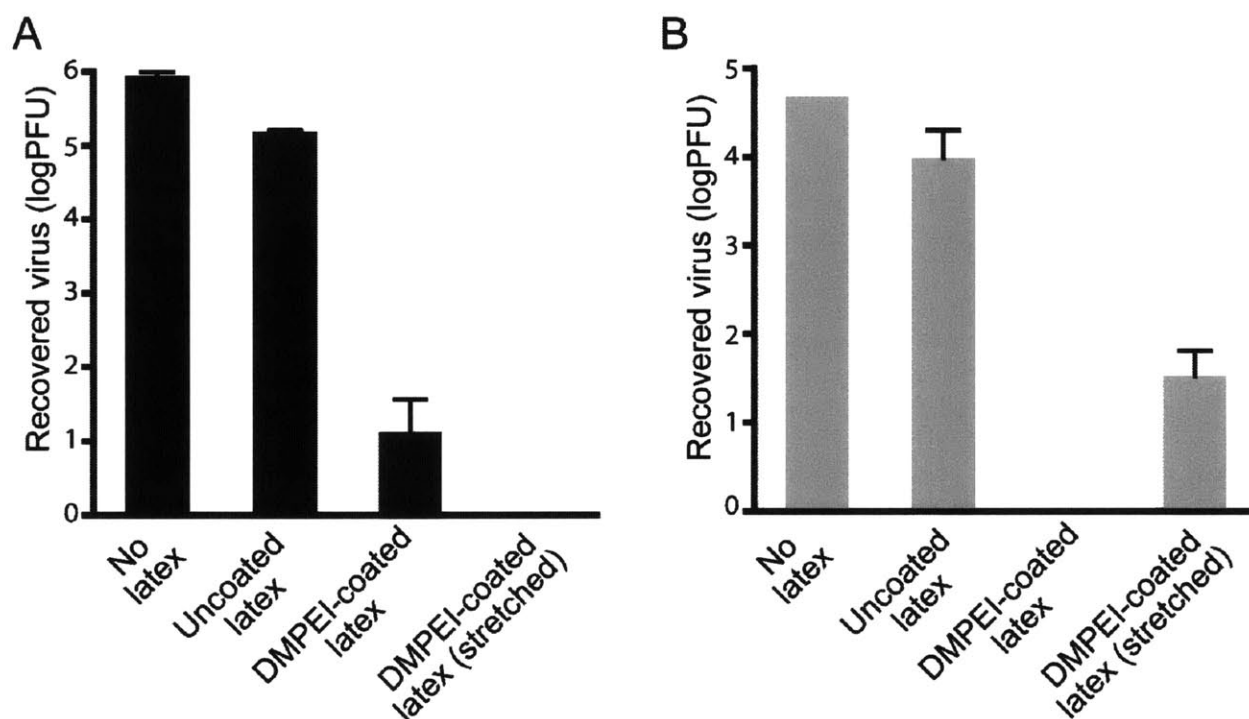


**Figure 4-5.** Reduction of viral titers of HSV-1 (A) and HSV-2 (B) incubated for 15 min at room temperature in a buffered aqueous solution (the left set of bars), in that sandwiched between an uncoated polyethylene slide and an uncoated piece of latex condom (the middle left set of bars), in that sandwiched between a DMPEI-coated latex condom and an uncoated polyethylene slide (the middle right set of bars), and in that sandwiched between a DMPEI-coated latex condom that had been stretched extensively and an uncoated polyethylene slide (the right set of bars). In the “No latex” experiment, a virus solution was incubated in buffer only. In the “Uncoated latex” experiment, a virus solution was incubated between a piece of uncoated polyethylene slide and of uncoated latex for 15 min to account for a non-specific adsorption of the virus to the slide and/or latex. In the “DMPEI-coated latex” experiment, a piece of latex was painted with the hydrophobic polycation. In the “DMPEI-coated latex (stretched)” experiment, a piece of latex was painted with the hydrophobic polycation, allowed to dry, and stretched 10-times horizontally and vertically to imitate real-life use of condoms, after which time virus solution was incubated with it. The limit of detection for the assay is approximately 1 PFU. The heights of the bars are mean values, and the error bars are standard deviations.

We have demonstrated herein that the hydrophobic polycationic material DMPEI could be employed both in a prophylactic modality (as a coating on latex condoms) and in a therapeutic modality (as a suspension) to inactivate HSVs. A drawback of the latter application is the uncovered toxicity toward mammalian cells. Although we previously observed no appreciable acute toxicity, either *in vitro*<sup>22</sup> or *in vivo*<sup>21,23</sup> for DMPEI coatings, a suspension presumably results in a more intimate contact between the cells and the hydrophobic polycation and thus greater toxicity. Future studies need to address whether the antiviral activity and toxicity are coupled and, if so, whether structural changes to the polycation can uncouple them. Once this is done, one can progress to *in vivo* studies to investigate a topical application of DMPEI in animal HSV models. As to a possible prophylactic use, both optimized noncovalent painting of, and covalent attachment of hydrophobic polycations to, latex (polyisoprene) condoms should be explored and the resultant coated condoms tested in terms of their long-term stability and safety.

### **Acknowledgements**

I am thankful to Dr. HyungSuk Oh for teaching me how to work with HSVs 1 and 2 and for his help with planning and performing experiments. I also thank him for preparing the figures that were used in this chapter. I also thank the coauthors for their help in editing the manuscript that resulted in this chapter.

### **C. Materials and Methods**

#### **Materials**

All chemicals and reagents were from Sigma-Aldrich Chemical Co. (St. Louis, MO) and used without further purification. Polyethylene sheets, from McMaster Carr (Atlanta, GA), were cut into 2.5 x 2.5-cm slides. Non-lubricated male latex condoms (Trojan<sup>®</sup>), distributed by Church

& Dwight Co. (Princeton, NJ) and obtained from a local drug store, were used in this study as the simplest type of a condom uncomplicated by possible effects of the lubricant. They were rinsed thoroughly in double-distilled (dd) H<sub>2</sub>O and cut into 3 x 4-cm rectangles for further use. The MTS assay kit (CellTiter 96<sup>®</sup> AQueous Non-Radioactive Cell Proliferation Assay) was purchased from Promega (Madison, WI). Dulbecco's Modified Eagle Medium (DMEM) was from Cellgro (Manassas, VA) and supplemented with 5% fetal bovine serum (FBS), 5% bovine calf serum (BCS), 1% penicillin, 1% streptomycin, 4.5 g/L glucose, and 2 mM L-glutamine for cell culture. Human immunoglobulin (IgG) (cat# NDC 0944-2700-02) was from Baxter (Deerfield, IL) and used to supplement DMEM in the plaque assay. Giemsa cell stain utilized in plaque assays was from Sigma-Aldrich.

### **Syntheses of polycations**

DMPEI was synthesized from linear 217-kDa polyethylenimine (PEI) as previously described.<sup>15</sup> The NMR structure is in Appendix C and is consistent with the literature. Permethylated PEI (PMPEI) was synthesized similarly to a reported procedure.<sup>26</sup> Briefly, 1 g of 750-kDa branched PEI was dissolved in 15 mL of anhydrous methanol, and an excess (17.2 mL) of iodomethane was added to the solution at room temperature. The mixture was refluxed at 65 °C for 2 h, followed by cooling to room temperature, addition of 928 mg of NaOH, and heating for an additional 12 h. The solvent was then removed by rotary evaporation, and the resultant solid was dissolved in ddH<sub>2</sub>O and dialyzed against it four times, followed by lyophilization to obtain solid PMPEI. The structure of PMPEI was verified by elemental analysis (C, 24.7%; H, 5.58%; N, 9.14%) and NMR (<sup>1</sup>H NMR (D<sub>2</sub>O)  $\delta$  (400 MHz) for PMPEI: 2.8-4.6 (CH<sub>2</sub>, m, CH<sub>3</sub>, s)). The NMR structure can be found in Appendix C.

### **Preparation of slides and coated condoms**

Coated slides were prepared by painting one side of a 2.5 x 2.5-cm polyethylene slide with a 50 mg/mL solution of DMPEI in chloroform, followed by solvent evaporation; this painting was performed in quadruplicate.<sup>15</sup> Coated condoms were prepared similarly, except that DMPEI was dissolved in butanol.<sup>22</sup>

### **Cells and viruses**

HSV-1 KOS strain and HSV-2 186syn<sup>+</sup>-1 strain were originally obtained from Priscilla A. Schaffer.<sup>27,28</sup> The viruses were diluted with an aqueous buffer (phosphate-buffered saline (PBS) supplemented with 1% BCS, 0.01% glucose). Vero cells were from the American Type Culture Collection (#CCL-81, Manassas, VA) and maintained in supplemented cell culture DMEM (described above) at 37 °C in a 5% CO<sub>2</sub> atmosphere. They were grown to confluent monolayers in 6-well plates or T25 flasks for use in plaque assays.

### **Antiviral assay for DMPEI-coated polyethylene slides**

To determine the antiviral effect of DMPEI against HSV-1 and HSV-2, a DMPEI-coated polyethylene slide was placed in a polystyrene Petri dish (6.0 x 1.5-cm), and a 10- $\mu$ L droplet of either HSV-1 ( $(4.4 \pm 3.9) \times 10^5$  plaque forming units (PFU)) or HSV-2 ( $(5.0 \pm 0.69) \times 10^4$  PFU) was added to the middle of the coated region. The droplet was sandwiched with a plain polyethylene slide to increase surface contact of the virus with the coated slide. After 15 min at room temperature, the slides were separated and washed thoroughly with 0.99 mL of the supplemented PBS buffer. The washings were collected, serially diluted, and analyzed in the plaque assay as described below. The infectious viral titer from the above experiments was compared to those of a control with two uncoated slides and a control with the virus never in contact with slides to determine the relative reduction in viral titer upon incubation with DMPEI-coated slides.<sup>9,12,15</sup>



## **Plaque assay**

Ten-fold serial dilutions of the washings from the antiviral assays were tested in the plaque assay to calculate infectious viral titers. Specifically, cell growth medium was removed from confluent monolayers of Vero cells in a 6-well plate and replaced with 0.5 mL of diluted virus in each well. The plate was gently shaken for 1 h at 37 °C to initiate infection, after which the virus solutions were removed and replaced with 2.5 mL of DMEM supplemented with 1% BCS and 0.16% human IgG (for HSV-2, DMEM with 1% BCS and 0.32% human IgG was used). The cells were incubated for 2 days at 37 °C and 3 days at 34 °C for HSV-1 and HSV-2, respectively, then fixed with ice-cold methanol for 8-10 min and stained with Giemsa dye. Plaques were counted to determine the viral titer of the solutions.

## **Antiviral assay with PEI and PMPEI**

HSV-1 (10 µL containing  $(7.8 \pm 0.40) \times 10^7$  PFU) was incubated with 0.99 mL of either branched 750-kDa PEI (2 mg/mL) or PMPEI (1 mg/mL) in the supplemented PBS buffer for 30 min on a rotating arm. Serial dilutions of the resultant mixtures were tested with the plaque assay and compared to HSV-1 incubated with the supplemented PBS buffer alone to determine the antiviral effect of the polycations.

## **Preparation of DMPEI suspensions**

DMPEI was dissolved in dimethylsulfoxide at 10 mg/mL and added to 3 volumes of ddH<sub>2</sub>O with vigorous stirring. The resultant mixture was lyophilized and resuspended in ddH<sub>2</sub>O with vigorous stirring and sonication until the suspension was devoid of visible chunks. The stock DMPEI suspension was diluted in PBS for further use.

A DMPEI suspension thickened with hydroxyethyl-cellulose (HEC) was prepared by making a 1.5% solution of HEC in 2.5 mL of PBS containing the desired concentration of

DMPEI. The mixture was heated gently and stirred until the HEC dissolved and the solution thickened.

### **MTS assay**

A 3 mg/mL DMPEI suspension in PBS was 10-fold serially diluted, followed by incubation of 100  $\mu$ L thereof for 1 h with confluent monolayers of Vero cells seeded in a 96-well plate. After 1 h, the serial dilutions of DMPEI suspension were removed, and the cells were washed twice with PBS and replenished with 100  $\mu$ L of fresh DMEM. The MTS assay was carried out according to the manufacturer's instructions.

### **Antiviral assays with DMPEI suspensions**

To quantify the antiviral effect of a DMPEI suspension, 10  $\mu$ L of a HSV-1 solution ( $(8.7 \pm 2.8) \times 10^7$  PFU) was incubated with 0.99 mL of a DMPEI suspension (0.3 mg/mL) for 30 min on a rotating arm. Thereafter, the virus and suspension mixture was filtered with a 0.45- $\mu$ m cut-off filter (Pall Life Sciences), and the filtrate was 10-fold serially diluted and used in a plaque assay to determine the reduction in viral titer. Controls in which HSV-1 was incubated either in the supplemented PBS buffer and not filtered, or in the supplemented PBS buffer and subsequently filtered, or with a 0.3 mg/mL DMPEI suspension solution filtrate were performed in parallel.

The antiviral effect of a DMPEI suspension present during infection was determined by incubating different concentrations of the suspension (or just the supplemented PBS buffer as a control) with HSV-1 during infection of a confluent Vero cell monolayer in a T25 flask. Specifically, 0.5 mL of a DMPEI suspension (or the supplemented PBS buffer) and 0.5 mL containing  $210 \pm 10$  PFU of HSV-1 were mixed in a T25 flask and gently agitated for 1 h at 37  $^{\circ}$ C. Then the virus and DMPEI suspension mixture was removed and replaced with 5 mL of

DMEM containing 1% BCS and 0.16% human IgG. The T25 flasks were incubated, fixed, and stained as described above to determine the viral titer with and without the DMPEI suspension treatment.

For antiviral assays with various concentrations of DMPEI suspensions containing 1.5% HEC, 25  $\mu\text{L}$  of either HSV-1 ( $(3.8 \pm 0.20) \times 10^5$  PFU) or HSV-2 ( $(2.5 \pm 0.90) \times 10^4$  PFU) was added to 2.5 mL of HEC-thickened DMPEI suspensions in 20-mL scintillation vials containing 1-cm long magnetic stir bars (to aid in mixing). Vials were placed on a rotating arm for 30 min, after which time 0.5 mL of the solution was carefully withdrawn by a pipette and diluted for the subsequent plaque assay. Controls containing 2.5 mL of plain PBS, as well as a 1.5% HEC solution in the absence of DMPEI, were also carried out.

#### **Antiviral assay for DMPEI-coated condoms**

To assess the antiviral activity of the coated latex condoms, the above-described procedure for polyethylene slides was followed except that a piece of coated condom replaced the coated slide. In addition, to better mimic the intended real-life use of a condom, we also tested a piece of coated condom that had been stretched both horizontally and vertically ten times after painting (denoted as a stretched latex condom) to determine the effect of stretching and handling on antiviral activity. After a 15-min incubation with HSV-1 ( $(8.8 \pm 0.80) \times 10^5$  PFU) or HSV-2 ( $(4.8 \pm 0.1) \times 10^4$  PFU), the plain slide was separated from the condom piece, and both were submerged in a 50-mL falcon tube containing 10 mL of the supplemented PBS buffer. This 10-mL washing was serially diluted and tested in the plaque assay. The same experiment was performed with a piece of uncoated latex condom and also without one as controls.

## D. References

1. Looker KJ, Garnett GP. 2005. A systematic review of the epidemiology and interaction of herpes simplex virus types 1 and 2. *Sex Transm Infect.* 81(2):103-107.
2. Rao P, Hong Thanh P, Kulkarni A, Yang Y, Liu X, Knipe DM, Cresswell P, Yuan W. 2011. Herpes simplex virus 1 glycoprotein B and US3 collaborate to inhibit CD1d antigen presentation and NKT cell function. *J Virol.* 85(16):8093-8104.
3. Centers for Disease Control and Prevention. 2010. Seroprevalence of herpes simplex virus type 2 among persons aged 14-49 years--United States, 2005-2008. *Morb Mortal Week Rep.* 59(15):456-459.
4. Looker KJ, Gamett GP, Schmid GP. 2008. An estimate of the global prevalence and incidence of herpes simplex virus type 2 infection. *Bull World Health Org.* 86(10):805-812.
5. Roizman B, Knipe DM, Whitley RJ. 2007. Herpes simplex viruses; In: *Fields' Virology*. Eds. Knipe DM, Howley PM. 5th ed. Philadelphia: Wolters Kluwer Health/ Lippincott Williams & Wilkins.
6. Freeman EE, Weiss HA, Glynn JR, Cross PL, Whitworth JA, Hayes RJ. 2006. Herpes simplex virus 2 infection increases HIV acquisition in men and women: systematic review and meta-analysis of longitudinal studies. *AIDS.* 20(1):73-83.
7. O'Brien JJ, Campolirichards DM. 1989. Acyclovir- an updated review of its antiviral activity, pharmacokinetic properties and therapeutic efficacy. *Drugs.* 37(3):233-309.
8. Piret J, Boivin G. 2011. Resistance of herpes simplex viruses to nucleoside analogues: mechanisms, prevalence, and management. *Antimicrob Agents and Chemother.* 55(2):459-472.

9. Haldar J, An D, Alvarez de Cienfuegos L, Chen J, Klivanov AM. 2006. Polymeric coatings that inactivate both influenza virus and pathogenic bacteria. *Proc Natl Acad Sci.* 103(47):17667-17671.
10. Klivanov AM. 2007. Permanently microbicidal materials coatings. *J Mat Chem.* 17(24):2479-2482.
11. Lin J, Qiu SY, Lewis K, Klivanov AM. 2003. Mechanism of bactericidal and fungicidal activities of textiles covalently modified with alkylated polyethylenimine. *Biotechnol Bioeng.* 83(2):168-172.
12. Larson AM, Hsu BB, Rautaray D, Haldar J, Chen J, Klivanov AM. 2011. Hydrophobic polycationic coatings disinfect poliovirus and rotavirus solutions. *Biotechnol Bioeng.* 108(3):720-723.
13. Haldar J, Chen J, Tumpey TM, Gubareva LV, Klivanov AM. 2008. Hydrophobic polycationic coatings inactivate wild-type and zanamivir- and/or oseltamivir-resistant human and avian influenza viruses. *Biotechnol Lett.* 30(3):475-479.
14. Haldar J, Weight AK, Klivanov AM. 2007. Preparation, application and testing of permanent antibacterial and antiviral coatings. *Nat Protoc.* 2(10):2412-2417.
15. Hsu BB, Ouyang J, Wong SY, Hammond PT, Klivanov AM. 2011. On structural damage incurred by bacteria upon exposure to hydrophobic polycationic coatings. *Biotechnol Lett.* 33(2):411-416.
16. Hsu BB, Wong SY, Hammond PT, Chen J, Klivanov AM. 2011. Mechanism of inactivation of influenza viruses by immobilized hydrophobic polycations. *Proc Natl Acad Sci.* 108(1):61-66.

17. Lin J, Murthy SK, Olsen BD, Gleason KK, Klibanov AM. 2003. Making thin polymeric materials, including fabrics, microbicidal and also water-repellent. *Biotechnol Lett.* 25(19):1661-1665.
18. Lin J, Qiu SY, Lewis K, Klibanov AM. 2002. Bactericidal properties of flat surfaces and nanoparticles derivatized with alkylated polyethylenimines. *Biotechnol Prog.* 18(5):1082-1086.
19. Milovic NM, Wang J, Lewis K, Klibanov AM. 2005. Immobilized *N*-alkylated polyethylenimine avidly kills bacteria by rupturing cell membranes with no resistance developed. *Biotechnol Bioeng.* 90(6):715-722.
20. Park D, Wang J, Klibanov AM. 2006. One-step, painting-like coating procedures to make surfaces highly and permanently bactericidal. *Biotechnol Prog.* 22(2):584-589.
21. Behlau I, Mukherjee K, Todani A, Tisdale AS, Cade F, Wang L, Leonard EM, Zakka FR, Gilmore MS, Jakobiec FA, Dohlman CH, Klibanov AM. 2011. Biocompatibility and biofilm inhibition of *N,N*-hexyl,methyl-polyethylenimine bonded to Boston Keratoprosthesis materials. *Biomaterials.* 32(34):8783-8796.
22. Mukherjee K, Rivera JJ, Klibanov AM. 2008. Practical aspects of hydrophobic polycationic bactericidal "paints". *Appl Biochem Biotechnol.* 151(1):61-70.
23. Schaer TP, Stewart S, Hsu BB, Klibanov AM. 2012. Hydrophobic polycationic coatings that inhibit biofilms and support bone healing during infection. *Biomaterials.* 33(5):1245-1254.
24. Grunewald K, Desai P, Winkler DC, Heymann JB, Belnap DM, Baumeister W, Steven AC. 2003. Three-dimensional structure of herpes simplex virus from cryo-electron tomography. *Science.* 302(5649):1396-1398.

25. Nel AM, Smythe SC, Habibi S, Kaptur PE, Romano JW. 2010. Pharmacokinetics of 2 dapivirine vaginal microbicide gels and their safety vs. hydroxyethyl cellulose-based universal placebo gel. *JAIDS*. 55(2):161-169.
26. Thomas M, Klibanov AM. 2002. Enhancing polyethylenimine's delivery of plasmid DNA into mammalian cells. *Proc Natl Acad Sci*. 99(23):14640-14645.
27. Schaffer P, Vonka V, Lewis R, Benyeshm M. 1970. Temperature-sensitive mutants of herpes simplex virus. *Virology*. 42(4):1144-&.
28. Spang AE, Godowski PJ, Knipe DM. 1983. Characterization of herpes-simplex virus-2 temperature-sensitive mutants whose lesions map in or near the coding sequences for the major DNA-binding protein. *J Virol*. 45(1):332-342.

## CHAPTER 5

### Hydrophobic polycationic coatings disinfect poliovirus and rotavirus solutions

The work presented in this chapter was published in the following manuscripts reproduced with kind permission from Wiley Periodicals, Inc (Copyright © 2010) and from Springer Science and Business Media:

Larson AM, Hsu BB, Rautaray D, Haldar J, Chen J, Klibanov AM. 2011. Hydrophobic polycationic coatings disinfect poliovirus and rotavirus solutions. *Biotechnol Bioeng.* 108(3):720-3.

Park D, Larson AM, Klibanov AM, Wang Y. 2013. Antiviral and antibacterial polyurethanes of various modalities. *Appl Biochem Biotechnol.* 169(4):1134-46.



## A. Introduction

More than half a century after the groundbreaking poliovirus vaccine was developed, the virus remains a public health threat in many African and South Asian countries.<sup>1</sup> Poliovirus, like other enteric waterborne viruses, is mainly transmitted through contaminated drinking sources in areas of poor sanitation. Once infected, a person can develop poliomyelitis, a debilitating disease causing muscle atrophy and paralysis.<sup>2</sup> Rotavirus, another waterborne human pathogen, also poses a danger in the developing world. It is the chief cause of gastroenteritis and diarrhea in children, causing some 600,000 infant deaths worldwide annually.<sup>3</sup> Therefore, stopping transmission of these viruses from potable water supplies would reduce the spread of disease.

Certain hydrophobic polycations, such as some polyethylenimines (PEIs), have been found to confer antimicrobial properties to materials' surfaces.<sup>4</sup> For example, *N,N*-hexyl,methyl-PEI (HMPEI) covalently attached, and *N,N*-dodecyl,methyl-PEI (DMPEI) deposited, onto glass have been shown to kill human pathogenic bacteria *S. aureus* and *E. coli*, as well as to inactivate multiple influenza virus strains, including drug-resistant ones.<sup>5-7</sup> The lipid membranes of bacteria or the envelopes of viruses are damaged by the hydrophobic polycationic chains, thus causing death or inactivation of the bacterium or virus, respectively.<sup>4</sup> Since the foregoing mechanism applies only to viruses containing a lipid envelope, it has been unknown heretofore whether immobilized hydrophobic polycations also can disinfect *non-enveloped*, protein-coated viruses, such as the aforementioned poliovirus and rotavirus.<sup>2</sup> The present study sheds light on this question.

## B. Results and Discussion

To explore the activity of hydrophobic polycationic coatings against poliovirus, a 10- $\mu$ L droplet of viral solution was sandwiched between a polyethylene slide painted with linear DMPEI and an otherwise identical bare (untreated) slide. After a 30-min incubation at room temperature, the slides were separated and washed to recover the viral particles. The washings were 2-fold serially diluted, and 200- $\mu$ L of each dilution was used to infect monolayers of HeLa cells in a plaque assay. Following the initial infection period, the viral dilutions were aspirated

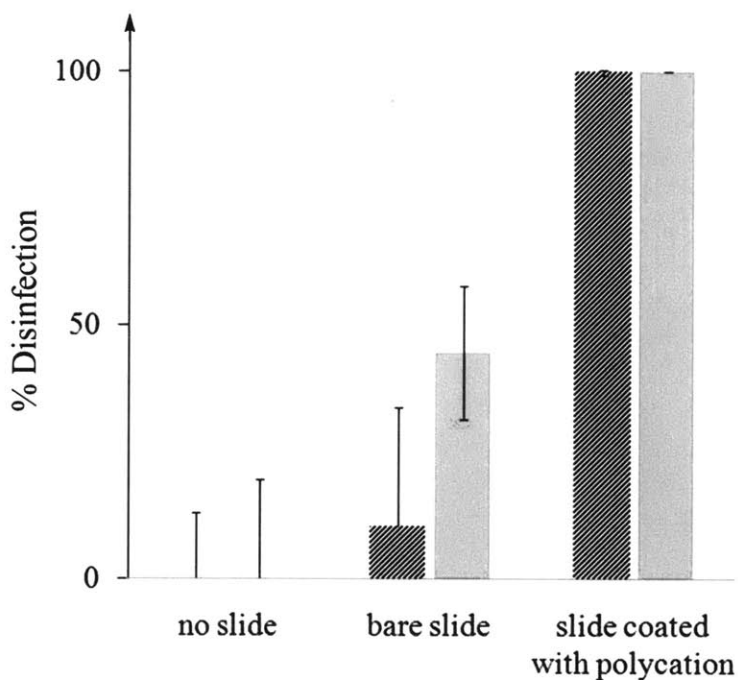


**Figure 5-1.** The disinfection of poliovirus solutions by polyethylene slides painted with DMPEI and glass slides covalently derivatized with HMPEI. In each set of two bars, the left one corresponds to polyethylene slides, whereas the right one to glass slides. “No slide” refers to a 30-min incubation at room temperature of poliovirus in aqueous solution and serves as a benchmark for 0% disinfection. “Bare slide” shows poliovirus incubated between two untreated polyethylene slides or two underivatized glass slides. “Slide coated with polycation” refers to coatings with DMPEI and HMPEI and shows approximately 100% disinfection in the case of incubation with a painted polyethylene slide and 100% disinfection in the case of incubation with a covalently modified glass slide. Each experiment was carried out at least in triplicate. For other conditions, see Materials and Methods.

off the cells and replaced with a nutrient-rich agar solution. Following a 60-h incubation at 37°C to promote the formation of plaques the cells were fixed with formaldehyde, stained with crystal violet dye after the agar overlay was removed, and allowed to dry overnight for plaques to be counted.

Essentially no poliovirus plaques could be detected after such an incubation in contact with a slide painted with DMPEI, as compared to a 100% infectivity recovery from a control in which viruses not in contact with any slides were incubated for 30 min under the same conditions (control #1)(Figure 5-1). To ascertain whether contact with an uncoated polyethylene surface plays a role in the reduction of viral titer observed, an additional control (#2) was carried out in which both slides sandwiching the viruses were bare. No significant decrease in the viral titer was observed for this condition, indicating that the surface-deposited hydrophobic polycations are responsible for disinfecting poliovirus from solution (Fig. 5-1).

Covalent attachment of hydrophobic polycations to surfaces provides a more robust coating than merely physical deposition by painting. Therefore, to test the generality of the foregoing findings, in addition to painted polyethylene slides, glass slides were covalently modified with branched HMPEI and tested against poliovirus in the same fashion. Washings from the derivatized glass slides that contacted poliovirus produced no plaques (Fig. 5-1), indicating high disinfecting potency. In the case of control #2 (bare slides), there was approximately a 2-fold reduction in recovered infectious viral particles, probably due to a nonspecific adsorption of the virus to the glass surface.

Separately, we found that the covalently coated glass slides that had been used to disinfect polioviruses could be fully regenerated and successfully re-used after a UV irradiation and ultrasonication in methanol.

To shed light on whether the immobilized hydrophobic polycations remove poliovirus from solution by adsorbing it or, alternatively, damage the virus to make it non-infective, we tested the viability of the virus in the presence of the common quaternary ammonium detergent dodecyltrimethylammonium chloride (DDTMAC). Incubating poliovirus for 30 min at room temperature in plain PBS or in the presence of 0.095 M DDTMAC yielded indistinguishable infectivities,  $(1.5 \pm 0.37) \times 10^4$  PFU/mL and  $(1.9 \pm 0.23) \times 10^4$  PFU/mL, respectively. The dissolved detergent structurally mimicking our hydrophobic polycations present at a concentration far above DDTMAC's critical micelle concentration (CMC) value of 22 mM<sup>8</sup> failed to adversely affect poliovirus under the same conditions at which immobilized DMPEI and HMPEI completely disinfected solutions containing it (Fig. 5-1). This observation suggested that the poliovirus in solution might in fact not be inactivated, but merely adsorbed to the slide.

**Table 5-1.** The recovery of poliovirus by washing uncoated and DMPEI-coated polyethylene slides with the detergents cetyltrimethylammonium chloride (CTAC) and Tween 80.<sup>a</sup>

Treatment	Viral titer, PFU/mL
Control virus solution	$(1.9 \pm 0.7) \times 10^5$
Plain slide, CTAC wash	$(1.8 \pm 0.4) \times 10^5$
Plain slide, Tween 80 wash	$(1.6 \pm 0.7) \times 10^5$
Coated slide, CTAC wash	$(0.13 \pm 0.1) \times 10^5$
Coated slide, Tween 80 wash	$(0.6 \pm 0.1) \times 10^5$

<sup>a</sup>Plain or coated slides were incubated with poliovirus and washed with a detergent.

To further explore this adherence vs. inactivation mechanism, we performed a slide assay where following incubation with the virus, we washed the plain or DMPEI-coated slide sets with

one of two detergents: the cationic cetyltrimethylammonium chloride (CTAC) or the non-ionic Tween 80, in an attempt to disrupt any adsorption of the virus to the slides and recover either infectious or inactivated polioviruses that reversibly adhered to the surfaces. Indeed, analysis of the washings for both detergents revealed the recovery of some of the infectivity lost from the original solution (Table 5-1) for both bare and DMPEI coated slides, pointing to the adsorption, not inactivation, mechanism.

Next, we sought to investigate how our hydrophobic polycationic coatings acted against another non-enveloped virus, rotavirus. Rotavirus was incubated between a polyethylene slide

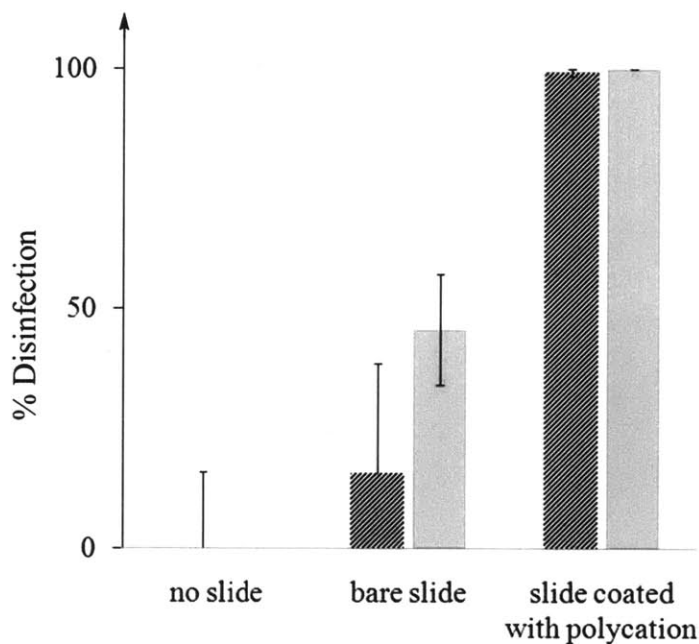


**Figure 5-2.** The time course of disinfection of rotavirus solutions by polyethylene painted with. In each set of two bars, the left one corresponds to a 15-min incubation, whereas the right one a to 30-min incubation between slides. “No slide” depicts a 30-min incubation at room temperature of rotavirus in aqueous solution, and serves as a benchmark for 0% disinfection (control #1). “Bare slide” shows rotavirus incubated between two untreated polyethylene slides (control #2). For treated conditions, after 15 min, nearly 100% reduction in infectious particles recovered is shown. After 30 min, no infectious viral particles could be recovered. Each experiment was carried out at least in duplicate. For other conditions, see Materials and Methods.

coated with linear DMPEI and its bare counterpart. After a 15-min incubation between the slides, only a single infectious virion could be recovered even from the most concentrated washings (as compared to approximately 100 plaques in control # 1 of the same concentration), and no plaques were observed after a 30-min incubation (Figure 5-2). In contrast, in the bare sandwiched slide incubation (control # 2), only a minimal reduction compared to no slide contact was detected which grew with time (Fig. 5-2), pointing to sensitivity of the employed strain of rotavirus to contact with surfaces.

The findings reported herein demonstrate for the first time that hydrophobic polycationic coatings can disinfect not only solutions containing enveloped viruses but also their protein-coated, non-enveloped counterparts, namely poliovirus and rotavirus.

### **Acknowledgements**

I am thankful to Jayanta Halder for teaching me the rotavirus plaque assay, Bryan Hsu for synthesizing DMPEI and slide preparation, and all the coauthors of the two manuscripts that resulted in this chapter.

## **C. Materials and Methods**

### **Chemicals**

Branched PEI (750 kDa), dodecyltrimethylammonium chloride (DDTMAC), and all organic solvents and reagents for synthesis were from Sigma-Aldrich Chemical Co. (St. Louis, MO). Linear PEI (217 kDa) was synthesized as described by Thomas et al.<sup>9</sup> Glass slides were from VWR International (West Chester, PA) and polyethylene sheets from McMaster-Carr (Elmhurst, IL); both were cut into 2.5 x 2.5 cm squares. Linear *N,N*-dodecylmethyl-PEI (DMPEI) was synthesized as described by Halder et al.<sup>10</sup> Branched immobilized *N,N*-

hexyl,methyl-PEI (HMPEI) was synthesized as described by Lin et al.<sup>11</sup> after derivatizing plain glass slides with 3-aminopropyltriethoxysilane.<sup>12</sup>

### **Cells and Viruses**

HeLa cells and MA-104 cells (CCL-2 and CRL-2378.1, respectively) were obtained from ATCC (Manassas, VA). Cells were grown at 37°C in a humidified-air atmosphere (5% CO<sub>2</sub>/95% air) in Eagle's minimum essential medium (EMEM, ATCC # 30-2003) supplemented with 10% heat-inactivated fetal bovine serum (FBS), 100 units/mL penicillin G, and 100 µg/mL streptomycin. Poliovirus strain Chat and rotavirus strain Wa were also obtained from ATCC (VR-1562 and VR-2018, respectively). The viruses were stored at -80°C and diluted 20-fold and 2,000-fold in incomplete media for assays with polyethylene and glass slides, respectively.

### **Slide preparation**

Polyethylene slides were painted with a 50 mg/mL solution of DMPEI in CHCl<sub>3</sub> in triplicate to maximize the slide's coverage.<sup>10</sup> Glass slides covalently derivatized with branched HMPEI were thoroughly washed with distilled water prior to use.<sup>11</sup>

### **Antiviral assays**

A covalently modified glass slide or painted polyethylene slide was placed treated side up in a polystyrene Petri dish (6.0 x 1.5 cm), and 10 µL of a virus solution in incomplete EMEM [(2.2 ± 0.9) × 10<sup>4</sup> PFU of poliovirus in a coated polyethylene slide assay, (1.0 ± 0.5) × 10<sup>3</sup> PFU of poliovirus in a covalently modified slide assay, and (5.1 ± 0.8) × 10<sup>3</sup> PFU of rotavirus in a coated polyethylene slide assay] was placed in the center of the slide. The droplet was sandwiched by a bare slide of the same material as the first. In the case of poliovirus challenged

by a coated polyethylene slide, a 1-lb weight was placed on top of the sandwiched slides to ensure complete spreading of the 10  $\mu$ L droplet. After a 30-min incubation at room temperature, the sandwiched slides were separated with tweezers and the sides contacting virus were washed thoroughly with 990  $\mu$ L of incomplete EMEM.<sup>7,10</sup> Washings were used to assay for infectious viral particles recovered post-incubation with slide surfaces. For poliovirus plaque assays, the washings were 2-fold serially diluted six times. In the case of rotavirus, 500  $\mu$ L of the undiluted washings were treated with 500  $\mu$ L of a 10  $\mu$ g/mL solution of porcine trypsin (Sigma Aldrich) at 37°C for 1 h. Trypsin-treated washings were subsequently 2-fold serially diluted five times and used in the plaque assay.

In the case of DDTMAC, poliovirus was incubated in 10  $\mu$ L of a solution of 0.095 M detergent for 30 min. After the incubation, virus and detergent were diluted in 990  $\mu$ L of EMEM and subsequently diluted further for the plaque assay.

### **Poliovirus plaque assay**

Monolayers of HeLa cells in six-well plates were washed twice with 12 mL of PBS and infected with 200  $\mu$ L of the 2-fold serially diluted washings in each well. After 1 h of infection at room temperature, virus solutions were aspirated from the cells and replaced by 3 mL of nutrient-rich agar (incomplete EMEM supplemented with 2% heat-inactivated FBS, 100 units/mL penicillin G, 100  $\mu$ g/mL streptomycin, and 0.45% Seakem LE Agarose from Lonza (Walkersville, MD)). Plates were then placed in a 37°C incubator with a humidified-air atmosphere (5% CO<sub>2</sub> /95% air). Sixty hours post-infection, cells were fixed with 17.5% formaldehyde in distilled H<sub>2</sub>O for at least 20 min and then stained with 0.5% crystal violet dye



for 1 min. Plates were washed with distilled H<sub>2</sub>O to remove excess dye, and plaques were counted the next day.<sup>13,14</sup>

#### **Antiviral assay of DMPEI-coated slides incubated with poliovirus and followed by washing with detergent solutions**

Polyethylene slides coated with DMPEI were tested for antiviral activities as outlined above for poliovirus, except that in the washing step the viruses were washed off the slide with 990 µl of 0.1% cetyltrimethylammonium chloride (CTAC) in PBS or 0.05% Tween 80 in 0.5 M NaCl solution. In controls, solutions of viruses were incubated between two plain polyethylene slides and washed with detergent solutions.

#### **Rotavirus plaque assay**

The rotavirus plaque assay was performed in a similar fashion to poliovirus with minor deviations. Monolayers of MA-104 cells were washed twice with 12 mL of incomplete EMEM lacking phenol red dye supplied by Quality Biological (Gaithersburg, MD) supplemented with 4 mM L-glutamine, 100 units/mL penicillin G, and 100 µg/mL streptomycin. Cells were infected with 200 µL of the 2-fold serially diluted washings in each well for 1 h at 37°C. After infection, virus solutions were aspirated, and 4 mL of nutrient-rich agar was placed on top of cells (incomplete EMEM supplemented with 0.01% DEAE-dextran, 100 units/mL penicillin G, 100 µg/mL streptomycin, 0.5 µg/mL porcine trypsin, and 0.6% agar (purified agar, L28; Oxoid Co., Hampshire, U.K.)). Three to four days post-infection, cells were fixed and stained with crystal violet dye as described above.<sup>15</sup>

## D. References

1. Minor PD. 2004. Polio eradication, cessation of vaccination and re-emergence of disease. *Nat Rev Microbiol.* 2(6):473-482.
2. Bosch A. 2010. Human enteric viruses in the water environment: a minireview. *Int Microbiol.* 1(3):191-196.
3. Parashar UD, Gibson CJ, Bresee JS, Glass RI. 2006. Rotavirus and severe childhood diarrhea. *Emerging Infect Dis.* 12(2):304-306.
4. Klibanov AM. 2007. Permanently microbicidal materials coatings. *J Mat Chem.* 17(24):2479-2482.
5. Haldar J, An D, Alvarez de Cienfuegos L, Chen J, Klibanov AM. 2006. Polymeric coatings that inactivate both influenza virus and pathogenic bacteria. *Proc Natl Acad Sci.* 103(47):17667-17671.
6. Haldar J, Weight AK, Klibanov AM. 2007. Preparation, application and testing of permanent antibacterial and antiviral coatings. *Nat Protoc.* 2(10):2412-2417.
7. Haldar J, Chen J, Tumpey TM, Gubareva LV, Klibanov AM. 2008. Hydrophobic polycationic coatings inactivate wild-type and zanamivir- and/or oseltamivir-resistant human and avian influenza viruses. *Biotechnol Lett.* 30(3):475-479.
8. Mehta S, Bhasin K, Chauhan R, Dham S. 2005. Effect of temperature on critical micelle concentration and thermodynamic behavior of dodecyldimethylammonium bromide and dodecyltrimethylammonium chloride in aqueous media. *Colloids Surf A* (255):153-157.
9. Thomas M, Klibanov AM. 2002. Enhancing polyethylenimine's delivery of plasmid DNA into mammalian cells. *Proc Natl Acad Sci.* 99(23):14640-14645.

10. Haldar J, An DQ, Alvarez de Cienfuegos L, Chen JZ, Klibanov AM. 2006. Polymeric coatings that inactivate both influenza virus and pathogenic bacteria. *Proc Natl Acad Sci.* 103(47):17667-17671.
11. Lin J, Qiu SY, Lewis K, Klibanov AM. 2002. Bactericidal properties of flat surfaces and nanoparticles derivatized with alkylated polyethylenimines. *Biotechnol Prog.* 18(5):1082-1086.
12. Tiller JC, Lee SB, Lewis K, Klibanov AM. 2002. Polymer surfaces derivatized with poly(vinyl-N-hexylpyridinium) kill airborne and waterborne bacteria. *Biotechnol Bioeng.* 79(4):465-471.
13. Boone E, Albrecht P. 1983. Conventional and enhanced plaque neutralization assay for polio antibody. *J Virol Methods.* 6(4):193-202.
14. Nuanualsuwan S, Cliver DO. 2002. Pretreatment to avoid positive RT-PCR results with inactivated viruses. *J Virol Methods.* 104(2):217-225.
15. Arnold M, Patton JT, McDonald SM. 2009. Culturing, storage, and quantification of rotaviruses. *Curr Protoc Microbiol.* 15C:1-24.

## CHAPTER 6

Biocidal packaging for pharmaceuticals, foods, and other perishables

This chapter will be published as the following review article:

Larson AM and Klivanov AM. 2013. Biocidal packaging for pharmaceuticals, foods, and other perishables. *Annu Rev Chem Biomol Eng.* 4:171–186.

## **A. Introduction**

Perishable goods, such as pharmaceuticals and foods, must be packaged in a way that protects their integrity over significant periods of time. This is no easy task. For example, according to the Centers for Disease Control and Prevention, in the United States alone, some 48 million illnesses and 3,000 deaths are caused annually by bacterially-contaminated foods.<sup>1</sup> Furthermore, microbial contamination of pharmaceuticals accounts for millions of dollars of extra costs to the industry by necessitating product recalls and disruptions in manufacturing; contaminated pharmaceuticals also may result in unsafe products being unwittingly administered to the general public.<sup>2</sup> In addition, medical devices (e.g., catheters and prefilled syringes) are liable to microbial contamination and colonization. Likewise, leather garments and other goods (e.g., gloves, shoes, purses, and briefcases) may become moldy and potentially unusable when exposed to high temperatures and humidity prevalent in many parts of the world. In an effort to curb the public health hardships and financial losses stemming from biologically-tainted perishable goods, scientists have embarked on extensive research to develop packaging methods that prevent, or at least reduce, microbial contamination and growth.

Historically, product packaging has been intended to function as a passive physical barrier, aiming to create a blockade between the product itself and contaminants external to the product, including dust, grime, and microorganisms. However, over recent decades increasing emphasis has been placed on active packaging that also directly and beneficially affects the interior environment of the product. Active packaging not only provides a mechanical barrier to external contaminants but also can control moisture levels, oxygen content, and other properties of the interior of the package.<sup>3-5</sup> In particular, many approaches to improve active packaging have focused on generating an inhospitable environment for microorganisms to grow and

multiply inside the package.<sup>6</sup> In this review, we deal with this latter type of active packaging by discussing mechanisms of both established and emerging antimicrobial strategies employed for that purpose. These methods can be incorporated into packaging for goods that need a sterile environment and/or resistance to the growth of microorganisms (such as bacteria and fungi).

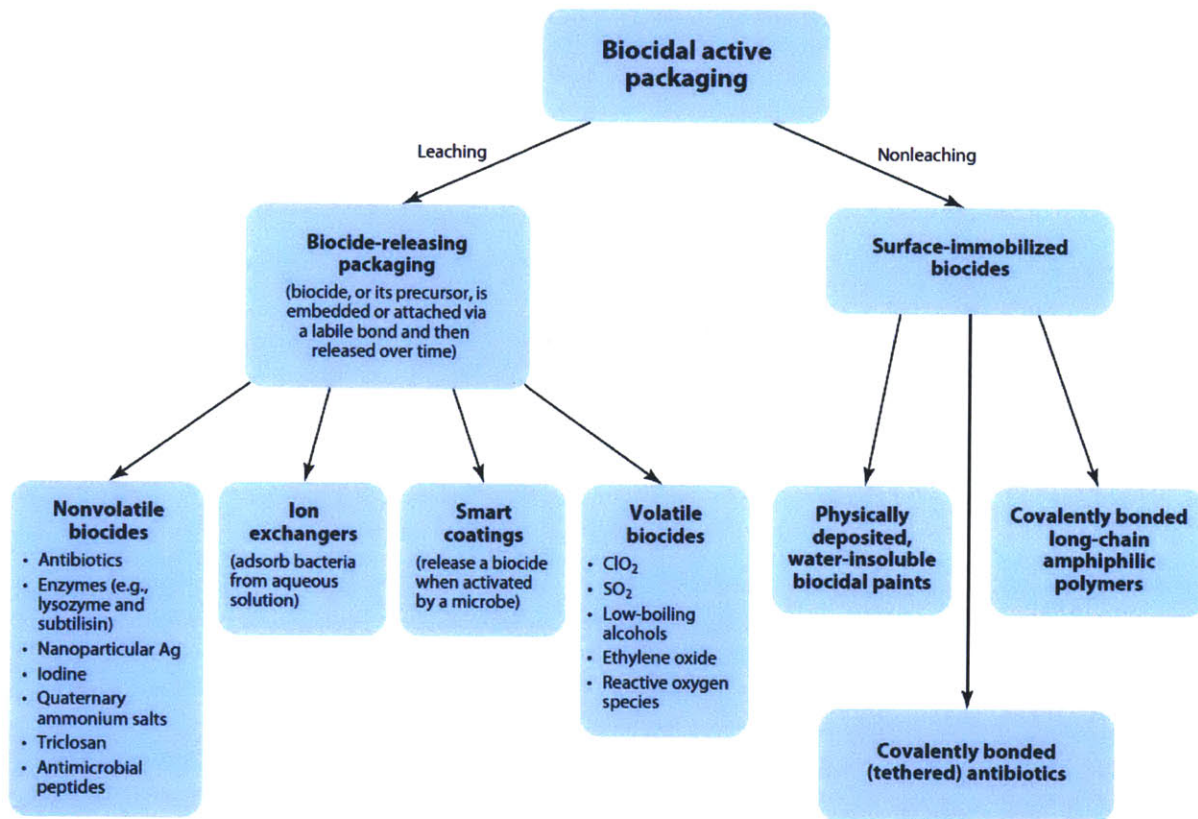


**Figure 6-1.** Schematic depiction of various forms of biocidal active packaging.

Although the biocidal materials discussed herein all hinder microbial growth, they achieve this objective by a variety of diverse means that fall into one of two general categories. The first approach involves gradually releasing (leaching) a biocide into the environment of the packaged good from the packaging material. The second involves affixing nonleaching biocidal material coatings to, or incorporating them into, materials used for packaging. Within each of

these categories, several specific antimicrobial approaches, schematically depicted in Figure 6-1, have been explored. The goal of this review is not to provide comprehensive coverage of all of these approaches but rather to critically discuss and illustrate the mechanisms of the most common and/or promising ones.

## **B. Active Biocide Releasing Packaging**

In this group of methods, a biocide (or its precursor) is embedded within, or attached via a labile bond to, a packaging material in a way that allows for its release over time. The gradual liberation of biocides from active packaging can generate a high biocide concentration in the interior of the package, thereby killing microorganisms therein. It also allows for deep penetration of the biocide into the contents of the package, which can result in a large area of microbial inhibition. The biocides used can range from simple gases that possess broad antimicrobial properties to structurally complex antibiotics that act on specific subtypes of bacteria.<sup>2,7</sup> In this section, we discuss the use of both volatile and nonvolatile biocides that can be impregnated into a packaging material for subsequent release, as well as the use of ion-exchange resins to adsorb bacteria from aqueous solutions. Lastly, we describe the use of futuristic, smart biocidal coatings capable of emitting a biocide only when needed (i.e., when triggered by the presence of a microbe). It should be noted at the outset that, despite their undeniable efficacy, biocide-leaching materials suffer from inherent drawbacks, including the release of toxic materials, the potential for generating resistant strains of microbes in the presence of sublethal concentrations of biocides, and the eventual exhaustion of the biocide's supply.<sup>8,9</sup>

## **Volatile Biocides**

Volatile biocides (i.e., those present predominantly in the gaseous phase under ambient conditions) have been used for various applications, including sterilization of medical equipment and disinfection of drinking water and foodstuffs.<sup>2,7</sup> Examples include sulfur dioxide (SO<sub>2</sub>), reportedly used as early as 800 BC for sterilization,<sup>2</sup> and more modern chemicals such as chlorine dioxide (ClO<sub>2</sub>), ethylene oxide, low-boiling alcohols, ozone (O<sub>3</sub>), and singlet oxygen species.

Gaseous disinfectants like SO<sub>2</sub> and ClO<sub>2</sub> generally work by dissolving in aqueous solution and generating reactive species therein that damage bacterial (and sometimes fungal) cellular components.<sup>2,7,10</sup> Ethylene oxide, which has been used as a method of choice for medical device sterilization since the 1950s, is a broad-spectrum alkylating agent that is particularly reactive toward –SH and other protein-reactive groups in microbes that it encounters.<sup>11,12</sup> However, unlike SO<sub>2</sub> and ClO<sub>2</sub>, ethylene oxide is mutagenic, which makes it a less attractive option for many applications.<sup>7</sup>

Another sterilization method utilizes aqueous solutions of low-boiling alcohols, such as ethanol and isopropanol. These alcohols are thought to denature proteins and disaggregate lipids of an offending microbe, as well as to dehydrate microbial cells. Although they are potent and wide-spectrum disinfectants against bacteria, fungi, and even some viruses,<sup>2,7</sup> volatile alcohols are not sporicidal<sup>7</sup> and also possess distinct tastes, which makes them incompatible with the sterilization of many foods.

Certain compounds, although not biocidal themselves, can generate potent biocide singlet oxygen when exposed to visible light in the presence of molecular O<sub>2</sub>.<sup>13</sup> In this process, the quantum of light interacts with a photosensitizing molecule and excites it to its singlet state.



Through a series of subsequent fast chemical transformations, this energy is transferred to a ground-state oxygen molecule in the vicinity of the photosensitizing molecule, which can generate a variety of reactive oxygen species (ROS), including superoxide radicals, hydroxyl radicals, or singlet oxygen; all of these ROS possess biocidal activity.<sup>13</sup> Their reach is limited, however; for example, singlet oxygen is very short-lived and thus can travel up to only 0.1  $\mu\text{m}$  in solution and 1 mm in air.<sup>14</sup> Nevertheless, the most effective photosensitizing molecules have been shown to be active against bacteria, fungi, and some viruses.<sup>13,15,16</sup> Their sterilizing potential can be harnessed for application in packaging either by incorporating them into material coatings<sup>14</sup> or by employing them as small molecules leached into solution.<sup>17</sup> For example, Luksiene et al.<sup>17</sup> demonstrated that incubation of 5-aminolevulinic acid, the biosynthetic precursor to the photosensitizing porphyrin ring structure, with the foodborne bacterium *Bacillus cereus* resulted in the synthesis of biocidal agents capable of producing singlet  $\text{O}_2$  that was active against both planktonic and surface-adhered bacteria after illumination with a 400-nm light. In an attempt to develop a surface coating that could generate singlet oxygen for biocidal action, Landgrebe et al.<sup>14</sup> generated a polymer scaffold decorated with compounds containing metal ligands that are photosensitizers and proposed that this material could be deposited on surfaces that have access to sunlight and oxygen for bactericidal, fungicidal, and virucidal action. Although the use of singlet oxygen and other ROS for disinfection is attractive, because their generation is catalytic and relies only on external light and atmospheric oxygen, their application is unsuitable for light-sensitive goods or for those that require anaerobic environments.

## Nonvolatile Biocides

Nonvolatile biocides make up the majority of disinfectants in commercial use today. They can be imbedded into materials that leach the chemical on tunable timescales or added to products to kill or inhibit the growth of offending microbes.

Even such simple elemental entities as Ag and I<sub>2</sub> in aqueous solution exhibit high antimicrobial activity against bacteria, fungi, and some enveloped viruses.<sup>7,18-20</sup> Silver's antimicrobial properties have been utilized for centuries and were perhaps unknowingly harnessed in the time of Alexander the Great (335 BC) who, along with his senior officers, was known to drink water from silver flasks, consequently avoiding contraction of infectious diseases during his travel.<sup>21,22</sup> Notably, the use of nanoparticulate Ag or silver salts as disinfectants is common in a variety of products, including foods, clothing, and medical devices.<sup>9,19,23</sup> In these applications, Ag can be incorporated into the packaging material for release into the surroundings.<sup>9</sup> Although nanoparticulate Ag is used, its antimicrobial action actually results from the Ag<sup>+</sup> cations generated therefrom under aerobic conditions.<sup>24</sup> Silver ions can react with thiol and imidazole groups of microbial enzymes, thereby inhibiting them; other, yet-to-be-discovered biocidal mechanisms appear to exist as well.<sup>7,18,23</sup> A representative example of the utilization of Ag in a product for antimicrobial activity is the Swach<sup>®</sup> nanotech water purifier system manufactured by TATA Chemicals in India. This system incorporates Ag nanoparticles into rice husk ash, which is used to filter contaminated water; it kills bacteria through the action of the released Ag<sup>+</sup> and also absorbs chemical pollutants on the charcoal-like ash.<sup>25</sup> Many other examples of devices employing silver for antimicrobial activity also have been reported.<sup>23,24,26</sup>

The increase of Ag-containing products for commercial use has been accompanied by a growing concern from a toxicological standpoint about the safety and tolerability of high

concentrations of free  $\text{Ag}^+$  ions.<sup>25,26</sup> Moreover, bacterial resistance to Ag has been observed in the form of both efflux pumps removing the metal from bacteria and such silver-binding proteins as SilE (small periplasmic Ag-binding protein) to quench the activity of the  $\text{Ag}^+$  ions.<sup>21,27</sup>

Like Ag,  $\text{I}_2$  in aqueous solution exhibits broad-spectrum biocidal activity.<sup>7</sup> Although its method of action is far from elucidated, iodine-containing species apparently iodinate and damage proteins, polynucleotides, and fatty acids of the microbes that they encounter.<sup>7</sup> In one example of a second-generation iodine formulation, a complex of povidone (polyvinylpyrrolidone) with  $\text{I}_2$  in solution acts as a vehicle to deliver the biocide to its microbial targets. This complex is used widely because it is less caustic than aqueous  $\text{I}_2$  solutions and the polyvinylpyrrolidone carrier is thought to interact with microbes' outer membranes.<sup>7,28</sup>

Quaternary ammonium compounds (QACs) are known to inactivate bacteria, fungi, and enveloped viruses.<sup>29-31</sup> Their amphiphilic structure comprises a polar quaternary amine head group and a hydrophobic tail (e.g., a long alkyl chain). Although there are many variations in the minutiae of their structures, the length of the alkyl chain in the most potent QACs is generally 12 to 16 carbons.<sup>29</sup> QACs are thought to target the cytoplasmic membrane of bacteria and the plasma membrane of fungi, thereby disrupting the organization and integrity of their membranes;<sup>7</sup> this mechanism also might explain their activity against enveloped viruses, such as influenza and herpes simplex viruses.<sup>30,31</sup>

The high efficacy of modern commercial antibiotics and antifungals makes them obvious candidates for utilization in active packaging. For example, the controlled release of the antibiotic gentamicin<sup>32</sup> and the antifungal amphotericin B<sup>33</sup> from polymeric matrices impregnated with them has been described. For the former, a bolus release over two to four hours was achieved from a hydrolytically degradable, polyelectrolyte multilayered film; the leached

antibiotic was capable of inhibiting the growth of *Staphylococcus aureus* in the vicinity of film-coated substrates.<sup>32</sup> The release of amphotericin B from a dextran-based hydrogel was tuned to take place for over 50 days for potential use as a coating in urethral catheters (which have known susceptibility to fungal infections). The amphotericin-impregnated hydrogel, referred to as amphogel, was capable of killing *Candida albicans* within two hours of contact.<sup>33</sup> Both of these approaches could be translated readily into packaging materials for preserving perishables with susceptibility to bacterial or fungal infections. Additionally, more broadly acting antimicrobials like triclosan could be incorporated into similar packaging systems to generate sterile interior environments.<sup>34</sup>

Amphiphilic peptides such as magainin, excreted from the skin of the African frog *Xenopus laevis*,<sup>35</sup> and others;<sup>36,37</sup> bacteriocins, like nisin from *Lactococcus lactis*,<sup>38,39</sup> enzymes, like lysozyme from biological secretions,<sup>38,40</sup> and biopolymers, like chitosan from crustaceans and arthropods<sup>38,41,42</sup> have been demonstrated to be biocidal. Thus, they too have the potential to be incorporated into packaging to protect products from microbial contamination and damage. In one reported example, a water-soluble chitosan-arginine derivative was tested for its ability to kill *Escherichia coli* added to the liquid that surrounds chicken in packaging (referred to as chicken juice), which is commonly colonized by pathogenic bacteria and implicated in food poisoning. The chitosan-arginine effectively reduced the *E. coli* load of the chicken juice by over 6 logs (i.e., at least  $10^6$  times) after 20 hours; it also killed microbes endogenous to the chicken juice.<sup>41</sup> Presumably such a biocide can also be incorporated into a polymeric packaging to be released over time, thus reducing the overall quantity required to be effective.

## **Ion-Exchange Methods**

Anion exchange, in which negatively charged ions electrostatically bound to a solid cationic surface are exchanged for different anions from solution, has been proposed as a method of capturing bacteria from aqueous media.<sup>43-45</sup> Because bacteria are negatively charged around physiological pH, owing to the presence of the phosphate head groups on the phospholipids in their outer membranes, they can be subjected to a variant of anion-exchange chromatography as a method to remove them from solution.<sup>43</sup> Researchers also have creatively combined the anion-exchange method with a leachable biocide component for applications in water purification by physically adsorbing poorly soluble Ag salts into the pores of macroreticular anion-exchange resins.<sup>44</sup> Once bacteria come into contact with the polymeric resin, they electrostatically bind to them; then, the Ag<sup>+</sup> ions inactivate these captured microbes. This approach resulted in a near sterilization of aqueous solutions containing the pathogenic bacteria *E. coli*, *Pseudomonas aeruginosa*, and *Streptococcus faecalis*.<sup>44</sup> The main limitation of (an)ion-exchange antimicrobial methods is that they are generally applicable only to aqueous solutions that lack significant salt concentrations that would interfere with the intended ion exchange.

### **‘Smart Coatings’ that Release Biocides When Needed**

Smart coatings are those designed to selectively release their antimicrobial payload when activated by a specific external stimulus. For the application in packaging, the payload is any of the aforementioned biocides, and the external stimulus is an offending microbial pathogen.<sup>46</sup> In principle, these coatings are advantageous over conventional leaching methods outlined above because the biocide is not released continuously into the environment but rather, at least in theory, only when needed.<sup>47</sup>

Li et al.<sup>47</sup> developed a biocidal formation utilizing both the conventional leaching and smart coating technologies. ClO<sub>2</sub> and the metallic biocide ZnCl<sub>2</sub><sup>48</sup> were incorporated into a polyoxyethylene-polyoxypropylene matrix in a water-in-oil-in-water double emulsion.<sup>47</sup> The resultant polymeric material released the gaseous ClO<sub>2</sub> biocide constantly over a 28-day period, and the ClO<sub>2</sub> released was capable of inhibiting the growth of *S. aureus* up to 3 mm away from the source. When an aqueous droplet containing the bacteria came in immediate contact with the polymer, the water dissolved the outer portion of the polymeric matrix, causing not only an extra burst of ClO<sub>2</sub> but also a direct exposure to the ZnCl<sub>2</sub>, which led to bacterial inactivation. The breakdown of the polymeric material as a result of contact with a pathogen-containing medium illustrates the smart-release concept.<sup>47</sup> However, droplets containing no pathogen could also presumably dissolve the polymeric material for release, which thus points to the need for pathogen-specific methods of polymer breakdown.

Another example of this concept involves a fabricated polymeric material called Surfacine<sup>®</sup>. It incorporates the water-insoluble silver salt AgI embedded in modified poly(hexamethylene biguanide), which itself is a potent biocide and fungicide.<sup>11,49,50</sup> Once a microbe comes into contact with a surface coated with this polymeric formulation, the pathogen's membrane dissolves in the biguanide network, and the Ag<sup>+</sup> ions dissociate from the iodide and preferentially bind to their targets in the immobilized bacteria.<sup>46,51,52</sup> The polymeric antimicrobial material is active against both Gram-positive and Gram-negative bacteria, including the notorious methicillin-resistant *S. aureus* (MRSA) and vancomycin-resistant *Enterococci* (VRE), as well as fungi. Because the Ag is present as an insoluble salt, it is released only when an offending bacterium contacts the surface and its membrane is disrupted by the

polymer,<sup>11</sup> which thus allows for washing of the material without leaching Ag<sup>+</sup> ions from the polymer into solution.

### **C. Active Packaging Materials that do *not* release a biocide (i.e., disinfection on contact)**

As an alternative to releasing biocides, packaging materials can be subjected to chemical modifications to incorporate nonleaching, surface-immobilized biocides. They can also be coated with water-insoluble biocidal paints that can kill microbes on contact. Advantages of such nonleaching approaches include avoiding release of toxic agents and eliminating the issue of exhausting the biocide emitted from the coating.<sup>8,53</sup> However, because the biocidal material in this scenario is incorporated onto the surface of the packaging material, its activity is restricted to that region; consequently, such coatings cannot reach the interior contents of the package as far as leached biocides can. As a result, this method is successful in killing only pathogens that come in immediate contact with the surface of the packaged goods. Although the coated surface can become covered with the microbial carcasses, as well as dust and grime, any such activity-disabling buildup often can be washed away to regenerate biocidal activity and allow repeated use.<sup>54</sup>

### **Antibiotics and Biocidal Enzymes Covalently Attached to Materials' Surfaces**

Antibiotics and antibacterial enzymes can be tethered to surfaces to potentially render said surfaces biocidal, biostatic (i.e., inhibiting microbial growth), or antifouling. This approach has been explored for the antibiotics vancomycin,<sup>55</sup> triclosan,<sup>56</sup> penicillin,<sup>57,58</sup> ampicillin,<sup>59</sup> and amoxicillin,<sup>60</sup> just to name a few, as well as for such biocidal enzymes as the glycoside hydrolase lysozyme<sup>61</sup> and the protease subtilisin.<sup>62,63</sup> Because the covalently-attached agent is sequestered

to the packaging and cannot traverse deeply across the microbial membrane, it must target molecules on the exterior of the pathogen.

Urban and coworkers<sup>57-60,64</sup> elegantly explored the attachment of  $\beta$ -lactam antibiotics to polymeric surfaces by utilizing microwave plasma reactions in the presence of maleic anhydride to generate functionalized surfaces that are reactive with antibiotics (Figure 6-2). In one

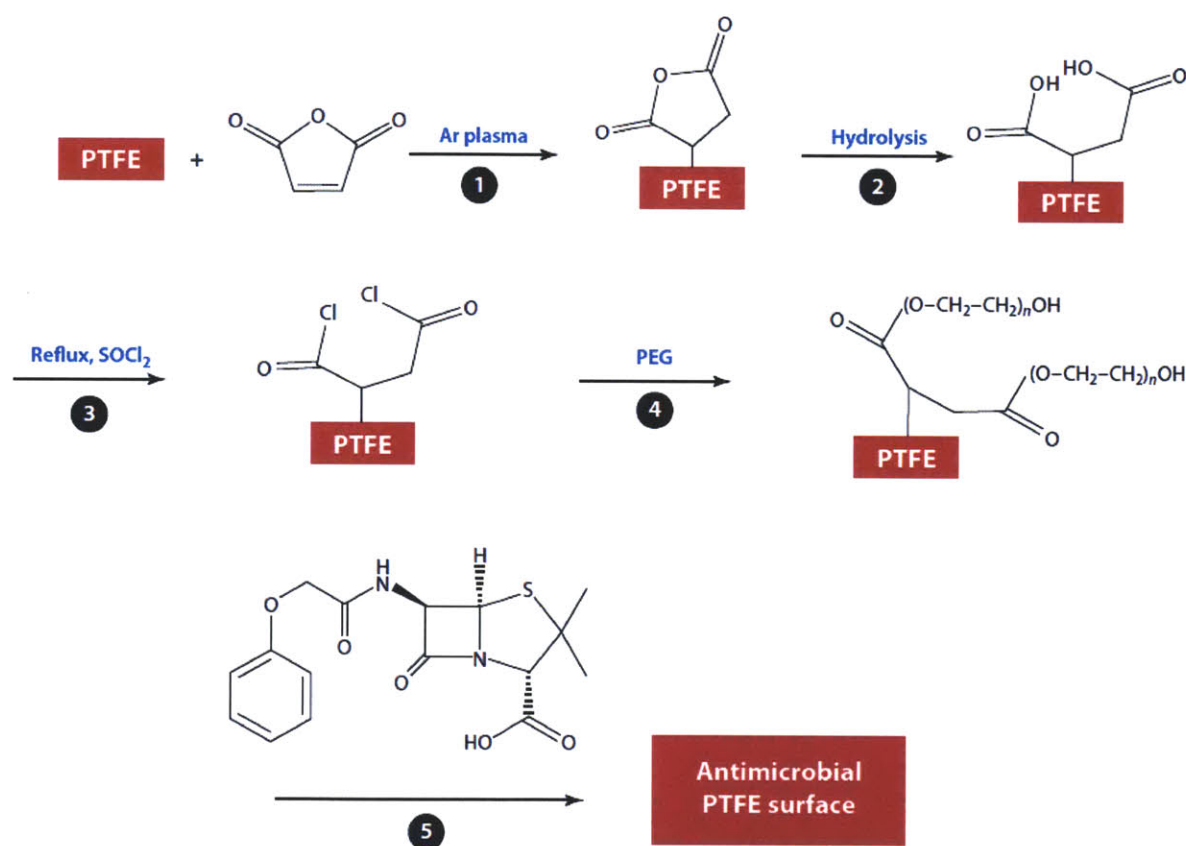


**Figure 6-2.** Schematic representation of the derivatization of polytetrafluoroethylene (PTFE) with the antibiotic ampicillin (ref 57). ① A functionalizable surface is generated by reaction between the PTFE and maleic anhydride in Ar plasma. ② The immobilized maleic anhydride is hydrolyzed for subsequent ③ activation and ④ derivatization with HO-PEG-OH. ⑤ Lastly, the immobilized linker PEG-OH reacts with the carboxylic acid of ampicillin in a Steglich esterification to generate the ampicillin-decorated surface. Figure courtesy of Professor M.W. Urban.



example, penicillin-derivatized surfaces were incubated with *S. aureus*, whose subsequent growth was assessed as a function of time. The antibiotic-coated surfaces were found to retard the growth of the bacteria in solution by almost 80%, as compared with the uncoated substrates. These studies also uncovered the necessity of a long linker, like a poly(ethylene glycol) moiety, between the functionalized surface and the antibiotic to ensure that the latter reaches its target and inhibits growth and proliferation of the microorganisms.<sup>57</sup> The proposed biocidal mechanism involves interaction between the tethered  $\beta$ -lactam antibiotics and the transpeptidase enzymes in the cell walls of the bacteria adhered to the coated surfaces. This interaction inhibits cell wall biosynthesis and thus exerts a bacteriostatic action that halts any subsequent bacterial proliferation, which is analogous to how leached  $\beta$ -lactam antibiotics work.<sup>59,64</sup>

Veluchamy et al.<sup>62</sup> investigated the relatively nonspecific protease subtilisin covalently attached to polycaprolactam (nylon 6) for applications in food packaging. When the immobilized enzyme was challenged with various strains of bacteria and fungi in liquid media, its antimicrobial efficacy outperformed that of the bare polymer up to five-fold. The subtilisin-coated nylon was also assessed for its real-life potential as a biocidal food packaging material. In this test, fresh ham steaks deliberately inoculated with *S. aureus* or *E. coli* were wrapped in a piece of either plain nylon or that derivatized with subtilisin. The enzyme-coated polymer, but not its underivatized predecessor, reduced the bacterial load of the food by 2 log units for *S. aureus* and 3 log units for *E. coli* after a six-day incubation at 4°C, thereby validating the potential of this material for use in food packaging.<sup>62</sup>

### **Long, Moderately Hydrophobic Polycations Covalently Attached to Surfaces**

The outer cellular membranes of bacteria and fungi are hydrophobic, as are lipid envelopes of some viruses, and also possess a net negative charge. It was, therefore, reasoned<sup>65-74</sup>

that certain surface-attached, long-chained hydrophobic polycations (e.g., those mimicking QACs) should be able to interact with these membranes, at least in a manner similar to that of conventional water-soluble QACs, to disrupt the membrane's molecular order, and to kill the microbe.<sup>8,75</sup>

For example, we investigated the structure-activity relationship of these polymeric QAC biocides attached to various materials. In initial studies,<sup>73</sup> glass slides were covalently derivatized with poly(4-vinylpyridine) (PVP), which was then *N*-alkylated with bromohexane to generate a moderately hydrophobic polycationic surface. The slides were subsequently sprayed with solutions of the representative human pathogens *E. coli*, *S. aureus* and *epidermidis*, and *P. aeruginosa* to mimic how a cough or a sneeze would spread germs. The droplets were allowed to dry, and a nutrient agar overlay was put on top of the slides, thereby allowing bacteria that were still viable to multiply and form colonies. When assayed for colony formation 24 hours later, between 94% and 99% of the initial bacteria were killed upon exposure to the *N*-alkyl-PVP-coated surfaces for all bacterial species tested, whereas the plain surfaces exhibited no appreciable antibacterial activity.<sup>73</sup> Importantly, the *N*-hexyl-PVP-coated surface did not leach the polycations;<sup>8</sup> it was also active against a mutant strain of *S. aureus* expressing multidrug resistance pumps, which confer resistance to monomeric QACs. These and other findings reveal that despite immobilized *N*-hexyl-PVP's chemical similarities to low-molecular-weight QACs and possibly a similar membrane-disrupting mechanism, it is not susceptible to the same bacterial resistance pathway.<sup>75,76</sup>

The structure-activity relationship studies, involving a range of different alkyl moieties, revealed that to be antimicrobially competent the immobilized *N*-alkyl-PVPs had to be hydrophobic, but not excessively so.<sup>72</sup> For example, the glass surfaces derivatized with the

relatively hydrophilic *N*-methyl-PVP and *N*-ethyl-PVP were impotent in this regard, probably owing to their low affinity for cellular membranes. Likewise, the very hydrophobic *N*-hexadecyl-PVP was not antimicrobial, presumably because of strong interactions between its polymeric chains that resulted in a “cooked-spaghetti”-like mass. A significant positive charge proved important, too: The surface-attached, underivatized PVP was essentially nonbiocidal.

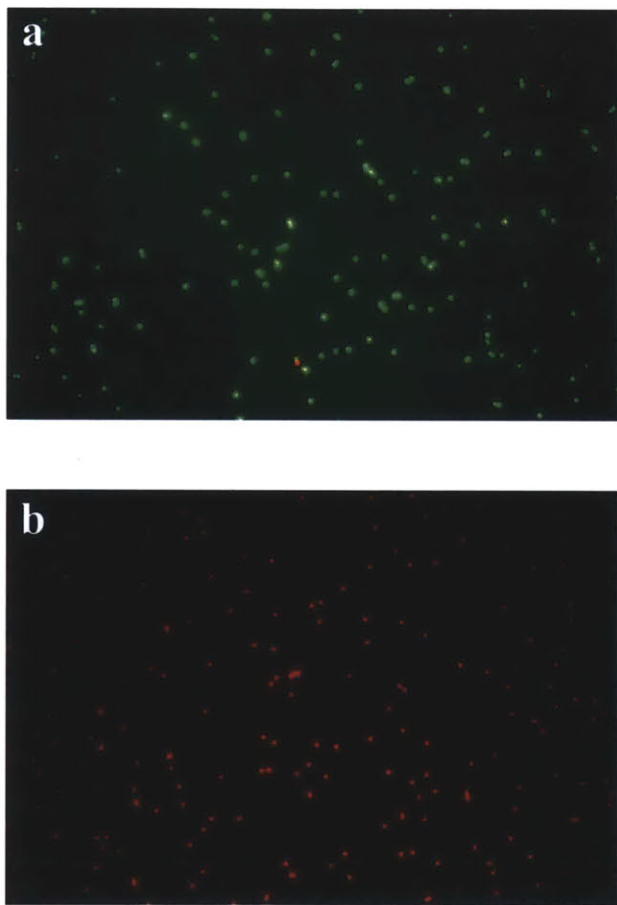


**Figure 6-3.** Live-dead analysis of *Staphylococcus aureus* cells after a two-hour exposure to the surface of (a) an underivatized amino-glass slide and (b) of that covalently derivatized with HMPEI; live (green) and dead (red) bacterial cells shown. Similar results were obtained with *Escherichia coli*. See Reference 76 for further details. Figure courtesy of Professor Kim Lewis.

That immobilized *N*-hexyl-PVP, or even the PVP polymeric platform itself, is by no means unique as a biocide was demonstrated by potent bactericidal and fungicidal activities of surface-attached hydrophobic polycations, which were prepared by quaternizing the common commercial polymer polyethylenimine (PEI) covalently attached to a variety of substrates, including glass, cotton, polyester, wool, and nylon, as well as iron nanoparticles.<sup>71,74,77,78</sup> Similarly to PVP, *N*-hexylation of the glass-attached PEI resulted in a substantial bactericidal efficiency against both Gram-positive and Gram-negative bacteria and the pathogenic yeast *C. albicans*.<sup>71,74,79</sup> Once the remaining unreacted amines on the *N*-hexyl-PEI were further

derivatized with iodomethane to generate a still higher degree of quaternization, the resultant *N,N*-hexyl,methyl-PEI (HMPEI) was even more antibacterial.<sup>74</sup> In contrast, either negatively charged, zwitterionic, or uncharged immobilized PEI derivatives were not bactericidal, which reinforces the importance of the polycationic species.<sup>74</sup> It was also found that only high-molecular-weight, surface-attached polycations were antibacterial.<sup>71</sup>

The mechanism of this bactericidal phenomenon has been studied using various techniques, including fluorescent live/dead cell assays (Figure 6-3).<sup>71,75,76</sup> The data obtained point to severe damage to the outer bacterial cell membrane, which resulted in the loss of integrity, on exposure to immobilized HMPEI. It is noteworthy that neither *S. aureus* nor *E. coli* was able to develop any resistance to the surface-attached polycations over at least a dozen successive generations.<sup>71</sup> Because of the great variety of materials that can be derivatized and the wide spectrum of the resultant biocidal action, these surfaces could be employed in biocidal packaging, especially because the coated materials were found to be nontoxic both in vitro and in vivo.<sup>54,78,80</sup>

In addition to the aforementioned hydrophobic polycations, Degrado and coworkers have also investigated amphiphilic peptides<sup>36</sup> and copolymers<sup>81</sup> covalently bonded to surfaces for antimicrobial properties. Likewise, Haynie et al.<sup>82</sup> attached magainin and structurally similar peptides to polyamide water-insoluble resins and assessed their activity against various strains of waterborne bacteria and yeasts. The resultant nonleaching conjugates were effective in reducing the solution loads of *S. aureus* and *E. coli* by approximately 5 logs and *C. albicans* by 3 logs.

### **Water-Insoluble Biocidal Paints Physically Deposited onto Surfaces**

Although covalent attachment of hydrophobic polycations is a reliable and permanent method to render materials antimicrobial, it is potentially costly and entails multistep, surface-

specific chemistries that cannot be performed readily by untrained personnel. Therefore, for some uses there is a merit in more facile, albeit less robust, antimicrobial coatings; in terms of the ease of application, common paints represent an attractive role model.<sup>83</sup>

We found that when HMPEI, which was previously employed for covalent attachment, was instead dissolved in an organic solvent, painted onto glass slides, and exposed to aqueous solution, the polycation leached.<sup>83</sup> To prevent this from happening (i.e., to make the paint

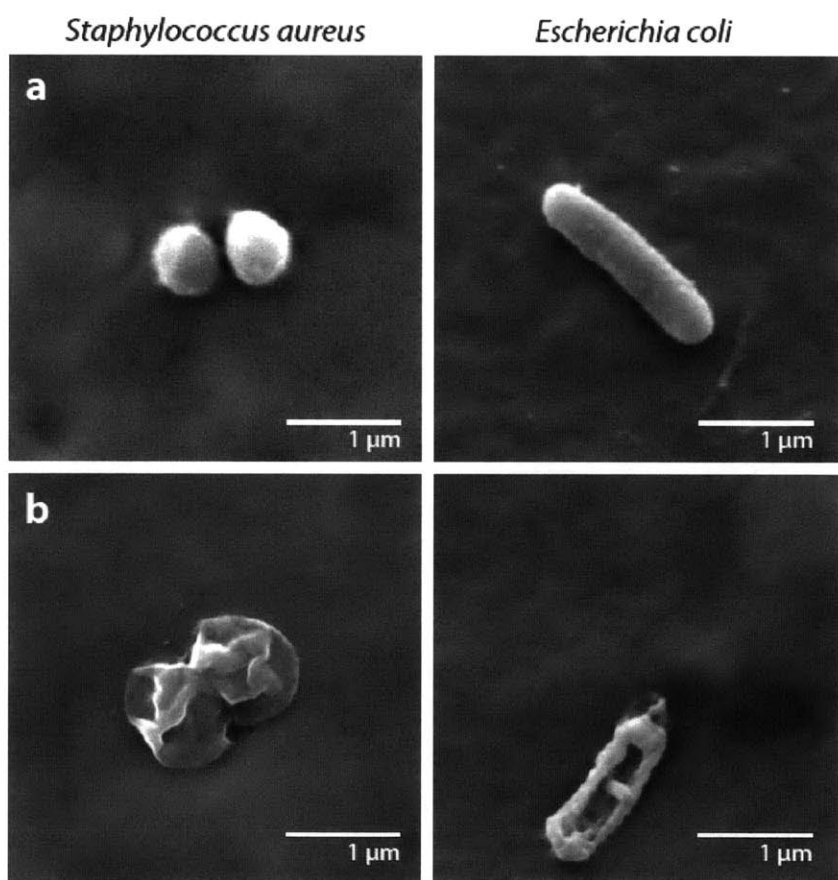


**Figure 6-4.** Scanning electron microscopy images of *Staphylococcus aureus* and *Escherichia coli* cells after interaction with either (a) plain, uncoated silicon wafers or (b) DMPEI-coated ones. Obvious severe damage to their structural integrity is observed for the bacteria incubated with the biocidal coating (ref 84). Figure courtesy of Bryan Hsu.

permanent, like a regular oil paint), we made the polycation more hydrophobic by replacing the C<sub>6</sub> groups with C<sub>12</sub> ones during the synthesis. Indeed, the resultant *N,N*-dodecyl,methyl-PEI (DMPEI) physically deposited onto surfaces exhibited no detectable leaching into aqueous solution and yet, in contrast to the untreated surfaces, still possessed excellent activity against both *S. aureus* and *E. coli* in our airborne assay.<sup>83</sup> Live/dead and

scanning electron microscopy imaging revealed that DMPEI-coated surfaces killed bacteria by imparting severe damage to their membranes (Figure 6-4). Consistent with this conclusion, when in contact with painted surfaces, *E. coli* released a disproportionately large amount of periplasmic proteins vis-à-vis plasma proteins into solution, which again points to a disruption of the outer membrane of the bacteria.<sup>84</sup> As in the case of covalently immobilized HMPEI, the antimicrobial activity of surfaces painted with DMPEI could be gradually poisoned by dead bacterial carcasses blocking the surface, but antimicrobial activity could be rejuvenated by washing.<sup>54</sup>

It is also worth noting that DMPEI was active against both wild-type and drug-resistant strains of influenza viruses<sup>85,86</sup> by disrupting their lipid envelopes and resulting in visibly damaged viral particles (Figure 6-5).<sup>30</sup>

Mechanistic investigation of this phenomenon revealed that the damaged virus sticks to the painted surface and becomes disrupted, and its RNA leaks out, as is schematically illustrated

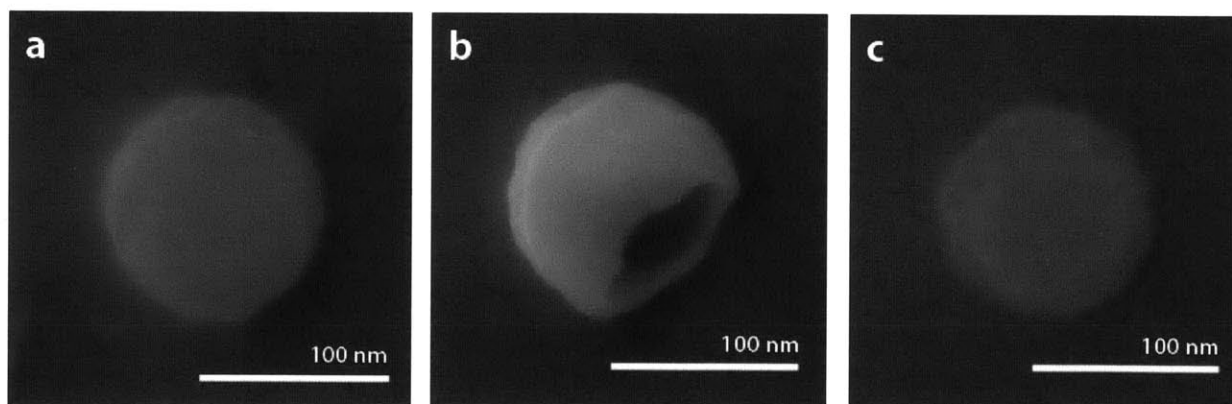


**Figure 6-5.** Scanning electron microscopy images of influenza viral particles after a 30-min interaction with either (a) plain, uncoated silicon wafers or (b,c) DMPEI-coated ones (ref. 30). The majority of the viral particles from the coated condition have severe lipid envelope damage (b), whereas others do not (c). Figure courtesy of Bryan Hsu.

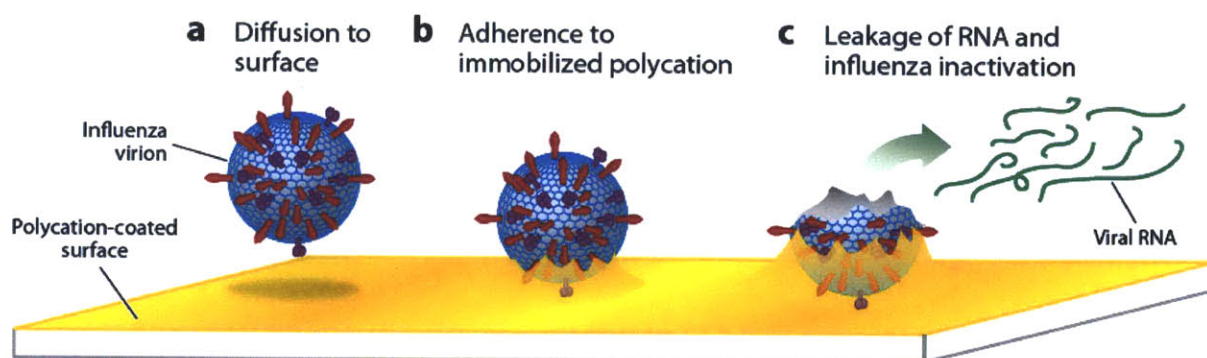


**Figure 6-6.** Schematic mechanism of inactivation of influenza virus by DMPEI-coated surfaces (ref 30). (a) An influenza viral particle diffuses from solution to interact with the polycation coated surface. (b) The viral particle becomes strongly adhered to the surface. Substantial damage to the virion occurs from this interaction, resulting in (c) leakage of the viral RNA into solution and inactivation of the virus. Figure courtesy of Bryan Hsu.

in Figure 6-6. Interestingly, painted DMPEI can not only inactivate human and avian influenza viruses but also disinfect solutions containing other enveloped viruses, such as herpes simplex viruses 1 and 2<sup>87</sup> as well as the nonenveloped rotavirus and poliovirus.<sup>88</sup>

As an alternative to painting, DMPEI can be incorporated as a cationic component into submicrometer-thick, layer-by-layer (LBL) films along with polyacrylate or other polyanions. Wong et al.<sup>89,90</sup> found that these LBL films not only are bactericidal against *S. aureus* and *E. coli* but also possess antifouling properties against serum proteins. This latter property, if general may be particularly valuable for packaging applications owing to its potential to prevent protein adsorption to coated surfaces and consequent poisoning of their antimicrobial properties.

Many other polymers have been proposed recently that can be made into antimicrobial paints themselves or can be incorporated into regular paints to render them antimicrobial.<sup>91-96</sup> One example is an aniline copolymer, which exhibits biocidal activity, as well as insolubility, not only in water but also in almost all common solvents (thus eliminating even the possibility of

leaching).<sup>92</sup> Separately, antibacterial polynorborene derivatives were reported that could be incorporated into paints or lacquers to be deposited on surfaces requiring sterility.<sup>91</sup>

### **Concluding Remarks**

The reduction of microbial load in perishable goods not only yields safer products but also can extend their shelf life by protecting them from decay.<sup>26</sup> Herein we outline a range of approaches to generate sterile environments or to halt the growth of bacteria and/or fungi that can be applied to commercial packaging for such products. These approaches can be used individually or in combination; although none of them is perfect, they illustrate the breadth of the science involved and provide a rich menu of methodologies to select from, depending on the specific features of the intended application.

### **Acknowledgments**

I am thankful to Professors Marek Urban and Kim Lewis, and Bryan Hsu for figures, Alan Stonebreaker for figure edits, and Professor Klivanov for his collaboration and edits on this chapter.

### **D. References**

1. Scallan E, Griffin PM, Angulo FJ, Tauxe RV, Hoekstra RM. 2011. Foodborne illness acquired in the United States-unspecified agents. *Emerg Infect Dis.* 17(1):16-22.
2. Jimenez L. 2004. Microorganisms in food packaging in the environment and their relevance to pharmaceutical processes. In: *Microbial contamination control in the pharmaceutical industry* ed., Jimenez L. New York: Marcel Dekker.



3. Mathiowitz E, Jacob JS, Jong YS, Hekal TM, Spano W, Guemonprez R, Klibanov AM, Langer R. 2001. Novel desiccants based on designed polymeric blends. *J Appl Polym Sci.* 80(3):317-327.
4. Hekal IM. 2001. Monolithic polymer composition having a releasing material. US Patent No. 6,316,520.
5. Smolander M, Chaudhry Q. 2010. Nanotechnologies in food. In: *Nanotechnologies in food*, ed. Chaudhry Q, Castle L, Watkins R. Cambridge, UK: RSC Publishing.
6. Balasubramanian A, Rosenberg LE, Yam K, Chikindas ML. 2009. Antimicrobial packaging: potential vs. reality—a review. *J Appl Packag Res.* 3:193-221.
7. McDonnell G, Russell AD 1999. Antiseptics and disinfectants: Activity, action, and resistance. *Clin Microbiol Rev.* 12(1):147-179.
8. Klibanov AM. 2007. Permanently microbicidal materials coatings. *J Mat Chem.* 17(24):2479-2482.
9. Manorama SV, Basak P, Singh S. 2012. Antimicrobial polymer composites. In: *Nanocomposite Particles for Bio-Applications: Materials and Bio-Interfaces*. ed. Daniel-de-Silva AL, Trinadade T. Boca Raton, Fla: Pan Stanford Publishing.
10. Rahn O, Conn JE. 1944. Effect of increase in acidity on antiseptic efficiency. *Ind Eng Chem.* 36:185-187.
11. Rutala WA, Weber DJ. 2001. New disinfection and sterilization methods. *Emerg Infect Dis.* 7(2):348-353.
12. Sheely LL, Volpitto PP. 1966. An inexpensive and satisfactory method for gas sterilization of anesthetic equipment. *Anesthesiology.* 27(1):95-96.

13. Hamblin MR, Hasan T. 2004. Photodynamic therapy: a new antimicrobial approach to infectious disease? *Photochem Photobiol Sci.* 3(5):436-450.
14. Landgrebe KD, Hastings DJ, Smith TP, Cuny GD, Sengupta A, Mudalige CD, Brandys FA. 2002. Limiting the presence of microorganisms using polymer-bound metal-containing compositions. US Patent No. 6,432,396.
15. Lazzaro A, Corominas M, Martí C, Flors C, Izquierdo LR, Grillo TA, Luis JG, Nonell S. 2004. Light-and singlet oxygen-mediated antifungal activity of phenylphenalenone phytoalexins. *Photochem Photobiol Sci.* 3(7):706-710.
16. Hudson J, Lopez-Bazzocchi I, Towers G. 1991. Antiviral activities of hypericin. *Antivir Res.* 15(2):101-112.
17. Luksiene Z, Buchovec I, Paskeviciute E. 2009. Inactivation of food pathogen *Bacillus cereus* by photosensitization *in vitro* and on the surface of packaging material. *J Appl Microbiol.* 107(6):2037-2046.
18. Jung WK, Koo HC, Kim KW, Shin S, Kim SH, Park YH. 2008. Antibacterial activity and mechanism of action of the silver ion in *Staphylococcus aureus* and *Escherichia coli*. *Appl Environ Microbiol.* 74(7):2171-2178.
19. Lara HH, Garza-Trevino EN, Ixtapan-Turrent L, Singh DK. 2011. Silver nanoparticles are broad-spectrum bactericidal and virucidal compounds. *J Nanobiotechnol.* 9:30.
20. Murphy J, Hickey J, Duan Y. 1998. Iodine-based microbial decontamination system. US Patent No. 5,772,971.
21. Silver S, Phung LT, Silver G. 2006. Silver as biocides in burn and wound dressings and bacterial resistance to silver compounds. *J Ind Microbiol Biotechnol* 33(7):627-634.

22. Black V, Njewel G. 2010. Search for the next “silver bullet”: a review of literature. *J Ark Acad Sci.* 64:50.
23. Morones JR, Elechiguerra JL, Camacho A, Holt K, Kouri JB, Ramirez JT, Yacaman MJ. 2005. The bactericidal effect of silver nanoparticles. *Nanotechnology.* 16(10):2346-2353.
24. Xiu ZM, Zhang QB, Puppala H, Colvin VL, Alvarez PJJ. 2012. Negligible particle-specific antibacterial activity of silver nanoparticles. *Nano Letters.* 12:4271-75.
25. Subramanian V, Woodson T, Cozzens S. 2012. Nanotechnology in India: inferring links between emerging technologies and development. In: *Making it to the forefront: nanotechnology-- a developing country perspective.* ed. Aydogan-Duda N. New York; Springer.
26. Appendini P, Hotchkiss JH. 2002. Review of antimicrobial food packaging. *Innov Food Sci Emerg Technol.* 3(2):113-126.
27. Gupta A, Silver S. 1998. Molecular genetics - silver as a biocide: will resistance become a problem? *Nat Biotechnol.* 16(10):888-888.
28. Zamora JL. 1986. Chemical and microbiologic characteristics and toxicity of povidone-iodine solutions. *Am J Surg.* 151(3):400-406.
29. Schaeufele PJ. 1984. Advances in quaternary ammonium biocides. *J Am Oil Chem Soc.* 61(2):387-389.
30. Hsu BB, Wong SY, Hammond PT, Chen J, Klivanov AM. 2011. Mechanism of inactivation of influenza viruses by immobilized hydrophobic polycations. *Proc Natl Acad Sci.* 108(1):61-66.
31. Weber DJ, Barbee SL, Sobsey MD, Rutala WA. 1999. The effect of blood on the antiviral activity of sodium hypochlorite, a phenolic, and a quaternary ammonium compound. *Infect Contr Hosp Epidemiol.* 20(12):821-827.

32. Wong SY, Moskowitz JS, Veselinovic J, Rosario RA, Timachova K, Blaisse MR, Fuller RC, Klibanov AM, Hammond PT. 2010. Dual functional polyelectrolyte multilayer coatings for implants: permanent microbicidal base with controlled release of therapeutic agents. *J Am Chem Soc.* 132(50):17840-17848.
33. Zumbuehl A, Ferreira L, Kuhn D, Astashkina A, Long L, Yeo Y, Iaconis T, Ghannoum M, Fink GR, Langer R, Kohane DS. 2007. Antifungal hydrogels. *Proc Natl Acad Sci.* 104(32):12994-12998.
34. Liauw CM, Taylor RL, Maryan C, Kato R, Wilkinson AN, Cheerarot O. 2011. Organomontmorillonite as a controlled release reservoir for triclosan in silicone elastomer: a flow micro-calorimetry and leaching study. *Macromol Symp.* 301(1):96-103.
35. Ludtke SJ, He K, Heller WT, Harroun TA, Yang L, Huang HW. 1996. Membrane pores induced by magainin. *Biochemistry.* 35(43):13723-13728.
36. Degrado WF, Tew GN, Klein ML, Liu D, Yuan J. 2004. Facially amphiphilic polymers as anti-infective agents. US Patent No. 20,040,185,257.
37. Degrado WF, Hamuro Y, Liu D. 2004. Design, preparation, and properties of antibacterial  $\beta$ -peptides. US Patent No. 6,677,431.
38. Tiwari BK, Valdramidis VP, O'Donnell CP, Muthukumarappan K, Bourke P, Cullen P. 2009. Application of natural antimicrobials for food preservation. *J Agric Food Chem.* 57(14):5987-6000.
39. Jin T, Zhang H. 2008. Biodegradable polylactic acid polymer with nisin for use in antimicrobial food packaging. *J Food Sci.* 73(3):M127-M134.

40. Buonocore G, Nobile M, Panizza A, Bove S, Battaglia G, Nicolais L. 2003. Modeling the lysozyme release kinetics from antimicrobial films intended for food packaging applications. *J Food Sci.* 68(4):1365-1370.
41. Lahmer RA, Williams AP, Townsend S, Baker S, Jones DL. 2012. Antibacterial action of chitosan-arginine against *Escherichia coli* O157 in chicken juice. *Food Contr.* 26(1):206-211.
42. Chung YC, Yeh JY, Tsai CF. 2011. Antibacterial characteristics and activity of water-soluble chitosan derivatives prepared by the Maillard reaction. *Molecules.* 16(10):8504-8514.
43. Stacy L. Daniels LLK. 1967. The separation of bacteria by adsorption onto ion exchange resins. *Bioeng Food Proc.* 62:142-148.
44. Costin RC. 1978. Microbiocidal macroreticular ion exchange resins, their method of preparation and use. US Patent No. 4,076,622.
45. Gartner WJ. 1983. Bacteriocidal resins and disinfection of water therewith. US Patent No. 4,420,590.
46. Subramanyam S, Yurkovetsiky A, Hale D, Sawan SP. 2000. A chemically intelligent antimicrobial coating for urologic devices. *J Endourol.* 14(1):43-48.
47. Li Y, Leung WK, Yeung KL, Lau PS, Kwan JKC. 2009. A multilevel antimicrobial coating based on polymer-encapsulated ClO<sub>2</sub>. *Langmuir.* 25(23):13472-13480.
48. Aarestrup FM, Hasman H. 2004. Susceptibility of different bacterial species isolated from food animals to copper sulphate, zinc chloride and antimicrobial substances used for disinfection. *Vet Microbiol.* 100(1):83-89.
49. Allen MJ, White GF, Morby AP. 2006. The response of *Escherichia coli* to exposure to the biocide polyhexamethylene biguanide. *Microbiology.* 152:989-1000.

50. Messick CR, Pendland SL, Moshirfar M, Fiscella RG, Losnedahl KJ, Schriever CA, Schreckenberger PC. 1999. *In-vitro* activity of polyhexamethylene biguanide (PHMB) against fungal isolates associated with infective keratitis. *J Antimicrob Chemother.* 44(2):297-298.
51. Sawan SP, Subramanyam S, Yurkovetskiy A. 2000. Contact-killing antimicrobial devices. US Patent No. 6,126,931.
52. Sawan SP, Subramanyam S, Yurkovetskiy A. 2001. Contact-killing non-leaching antimicrobial materials. US Patent No. 6,264,936.
53. Kenawy ER, Worley SD, Broughton R. 2007. The chemistry and applications of antimicrobial polymers: A state-of-the-art review. *Biomacromolecules.* 8(5):1359-1384.
54. Mukherjee K, Rivera JJ, Klibanov AM. 2008. Practical aspects of hydrophobic polycationic bactericidal "paints". *Appl Biochem Biotechnol.* 151(1):61-70.
55. Gu HW, Ho PL, Tong E, Wang L, Xu B. 2003. Presenting vancomycin on nanoparticles to enhance antimicrobial activities. *Nano Lett.* 3(9):1261-1263.
56. Kugel AJ, Ebert SM, Stafslie SJ, Hevus I, Kohut A, Voronov A, Chisholm BJ. 2012. Synthesis and characterization of novel antimicrobial polymers containing pendent triclosan moieties. *React Funct Polym.* 72(1):69-76.
57. Aumsuwan N, Heinhorst S, Urban MW. 2007. Antibacterial surfaces on expanded polytetrafluoroethylene; penicillin attachment. *Biomacromolecules.* 8(2):713-718.
58. Aumsuwan N, Heinhorst S, Urban MW. 2007. The effectiveness of antibiotic activity of penicillin attached to expanded poly(tetrafluoroethylene) (ePTFE) surfaces: A quantitative assessment. *Biomacromolecules.* 8(11):3525-3530.

59. Aumsuwan N, Danyus RC, Heinhorst S, Urban MW. 2008. Attachment of ampicillin to expanded poly(tetrafluoroethylene): Surface reactions leading to inhibition of microbial growth. *Biomacromolecules*. 9(7):1712-1718.
60. Bae WS, Urban MW. 2006. Creating patterned poly(dimethylsiloxane) surfaces with amoxicillin and poly(ethylene glycol). *Langmuir*. 22(24):10277-10283.
61. Han J. 2003. Antimicrobial food packaging. In: *Novel Food Packaging Techniques*, ed. R Ahvenainen. Boca Raton, FL: CRC Press
62. Veluchamy P, Sivakumar PM, Doble M. 2011. Immobilization of subtilisin on polycaprolactam for antimicrobial food packaging applications. *J Agric Food Chem*. 59(20):10869–10878.
63. Tiller JC 2011. Antimicrobial Surfaces. *Adv Polym Sci Bioact Surf*. 240:193-217.
64. Urban MW, Aumsuwan N. 2010. Method of attaching drug compounds to non-reactive polymer surfaces. US Patent No. 7,854,941.
65. Schroeder JD, Scales CJ. 2011. Method of preserving food using antimicrobial packaging. US Patent No. 7,981,408.
66. Schroeder JD, Scales CJ. 2005. Method of preserving food using antimicrobial packaging. US Patent No. 20,050,271,780.
67. Chuang VT. 2009. Antimicrobial compositions and methods of making the same. US Patent No. 20,090,081,152.
68. Mahmoud H. 2009. Anti-microbial polyurethane dispersion, method for the manufacture thereof, application method, and articles provided with an anti-microbial coating. WO Patent No. 138,221.

69. Dhende VP, Samanta S, Jones DM, Hardin IR, Locklin J. 2011. One-step photochemical synthesis of permanent, nonleaching, ultrathin antimicrobial coatings for textiles and plastics. *ACS Appl Mater Interfaces*. 3(8):2830–2837.
70. Lin J, Tiller JC, Lee SB, Lewis K, Klivanov AM. 2002. Insights into bactericidal action of surface-attached poly(vinyl-N-hexylpyridinium) chains. *Biotechnol Lett*. 24(10):801-805.
71. Lin J, Qiu SY, Lewis K, Klivanov AM. 2003. Mechanism of bactericidal and fungicidal activities of textiles covalently modified with alkylated polyethylenimine. *Biotechnol Bioeng*. 83(2):168-172.
72. Tiller JC, Liao CJ, Lewis K, Klivanov AM. 2001. Designing surfaces that kill bacteria on contact. *PNAS*. 98(11):5981-5985.
73. Tiller JC, Lee SB, Lewis K, Klivanov AM. 2002. Polymer surfaces derivatized with poly(vinyl-N-hexylpyridinium) kill airborne and waterborne bacteria. *Biotechnol Bioeng*. 79(4):465-471.
74. Lin J, Qiu SY, Lewis K, Klivanov AM. 2002. Bactericidal properties of flat surfaces and nanoparticles derivatized with alkylated polyethylenimines. *Biotechnol Prog*. 18(5):1082-1086.
75. Lewis K, Klivanov AM. 2005. Surpassing nature: rational design of sterile-surface materials. *Trends Biotechnol*. 23(7):343-348.
76. Milovic NM, Wang J, Lewis K, Klivanov AM. 2005. Immobilized N-alkylated polyethylenimine avidly kills bacteria by rupturing cell membranes with no resistance developed. *Biotechnol Bioeng*. 90(6):715-722.
77. Hsu BB, Klivanov AM. 2011. Light-activated covalent coating of cotton with bactericidal hydrophobic polycations. *Biomacromolecules*. 12(1):6-9.

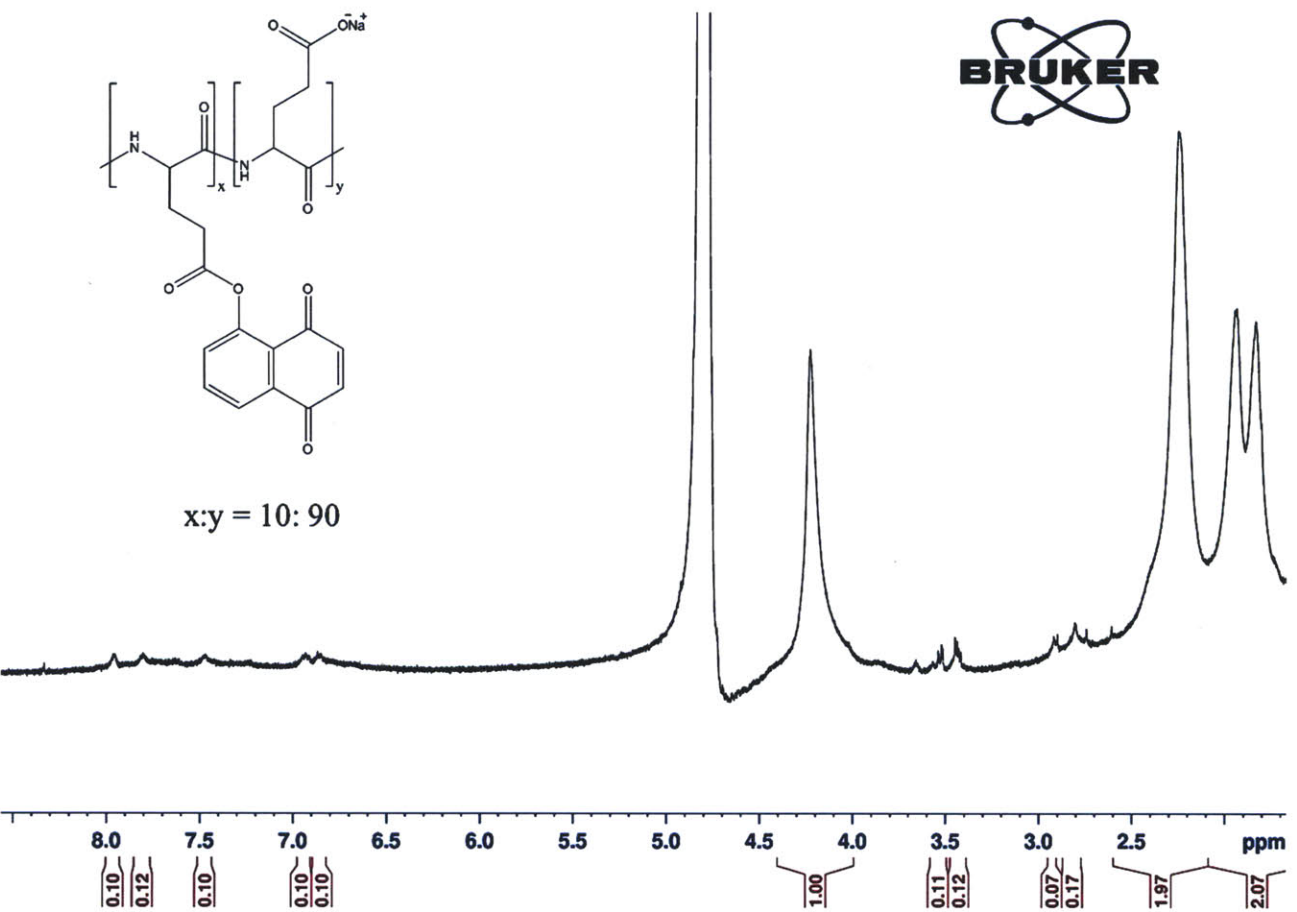


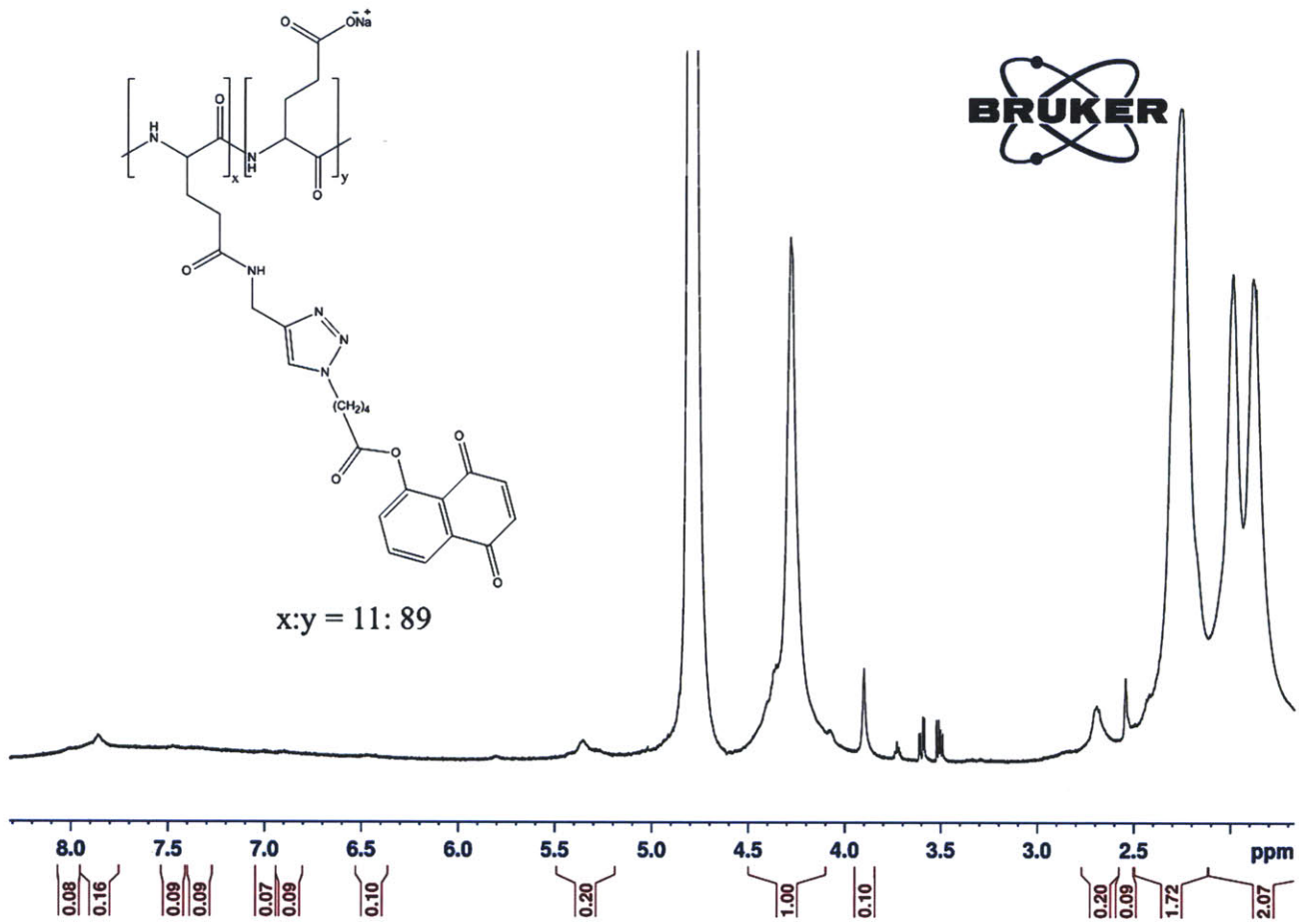
78. Schaer TP, Stewart S, Hsu BB, Klibanov AM. 2012. Hydrophobic polycationic coatings that inhibit biofilms and support bone healing during infection. *Biomaterials*. 33(5):1245-1254.
79. Lin J, Murthy SK, Olsen BD, Gleason KK, Klibanov AM 2003. Making thin polymeric materials, including fabrics, microbicidal and also water-repellent. *Biotechnol Lett*. 25(19):1661-1665.
80. Behlau I, Mukherjee K, Todani A, Tisdale AS, Cade F, Wang L, Leonard EM, Zakka FR, Gilmore MS, Jakobiec FA, Dohlman CH, Klibanov AM. 2011. Biocompatibility and biofilm inhibition of N,N-hexyl,methyl-polyethylenimine bonded to Boston Keratoprosthesis materials. *Biomaterials*. 32(34):8783-8796.
81. Kuroda K, Degrado WF. 2006. Antimicrobial copolymers and uses thereof. US Patent No. 20,060,024,264.
82. Haynie SL, Crum GA, Doele BA. 1995. Antimicrobial activities of amphiphilic peptides covalently bonded to a water-insoluble resin. *Antimicrob Agents Chemother*. 39(2):301-307.
83. Park D, Wang J, Klibanov AM. 2006. One-step, painting-like coating procedures to make surfaces highly and permanently bactericidal. *Biotechnol Prog*. 22(2):584-589.
84. Hsu BB, Ouyang J, Wong SY, Hammond PT, Klibanov AM. 2011. On structural damage incurred by bacteria upon exposure to hydrophobic polycationic coatings. *Biotechnol Lett*. 33(2):411-416.
85. Haldar J, Chen J, Tumpey TM, Gubareva LV, Klibanov AM. 2008. Hydrophobic polycationic coatings inactivate wild-type and zanamivir- and/or oseltamivir-resistant human and avian influenza viruses. *Biotechnol Lett*. 30(3):475-479.
86. Haldar J, Weight AK, Klibanov AM. 2007. Preparation, application and testing of permanent antibacterial and antiviral coatings. *Nat Protoc*. 2(10):2412-2417.

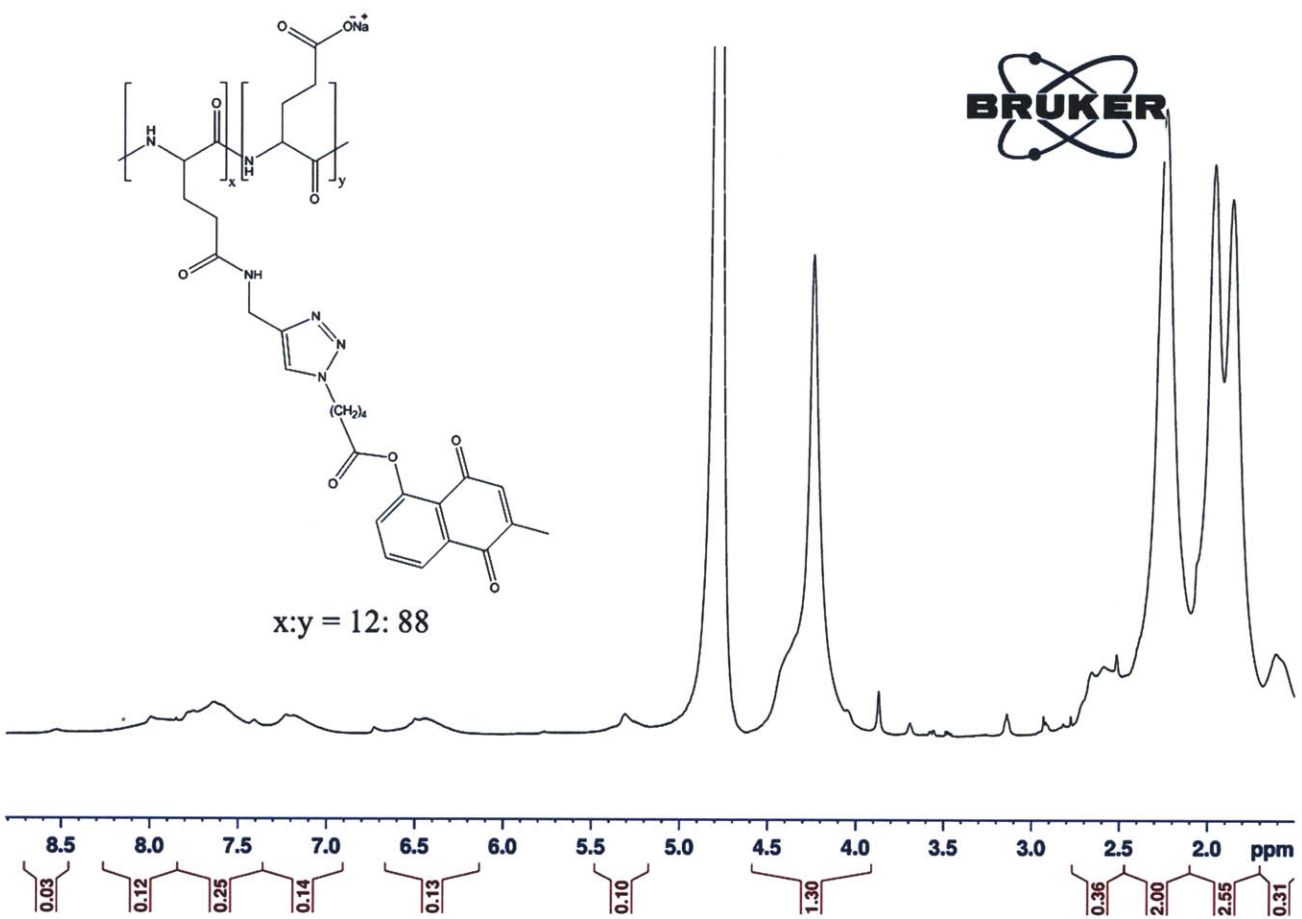
87. Larson AM, Oh H, Knipe DM, Klivanov AM. 2012. Decreasing herpes simplex viral infectivity in solution by surface-immobilized and suspended *N,N*-dodecyl,methyl-polyethylenimine. *Pharm Res.* 30:25-31.
88. Larson AM, Hsu BB, Rautaray D, Haldar J, Chen J, Klivanov AM. 2011. Hydrophobic polycationic coatings disinfect poliovirus and rotavirus solutions. *Biotechnol Bioeng.* 108(3):720-723.
89. Wong SY, Li Q, Veselinovic J, Kim BS, Klivanov AM, Hammond PT. 2010. Bactericidal and virucidal ultrathin films assembled layer by layer from polycationic *N*-alkylated polyethylenimines and polyanions. *Biomaterials.* 31(14):4079-4087.
90. Wong SY, Han L, Timachova K, Veselinovic J, Hyder MN, Ortiz C, Klivanov AM, Hammond PT. 2012. Drastically Lowered Protein Adsorption on Microbicidal Hydrophobic/Hydrophilic Polyelectrolyte Multilayers. *Biomacromolecules.* 13(3):719-726.
91. Tew GN, Ilker F, Coughlin BE. 2007. Amphiphilic polynorbornene derivatives and methods of using the same. EP Patent No 1,793,838.
92. Gizdavic-Nikolaidis M. 2009. Bioactive aniline copolymers. WO Patent No. WO/2009/041,837.
93. Schönemyr L, Holmberg K, Persson D. 2007. Antimicrobial and antiviral product. EP Patent No. 1,830,639.
94. Krishnan V. 2009. Antimicrobial and antistatic polymers and methods of using such polymers on various substrates. US Patent No. 7,491,753.
95. Scott RW, Brehm-stecher BF. 2009. Combination of synthetic antimicrobial polymers and sesquiterpenoid compounds. US Patent No. 20,090,081,153.

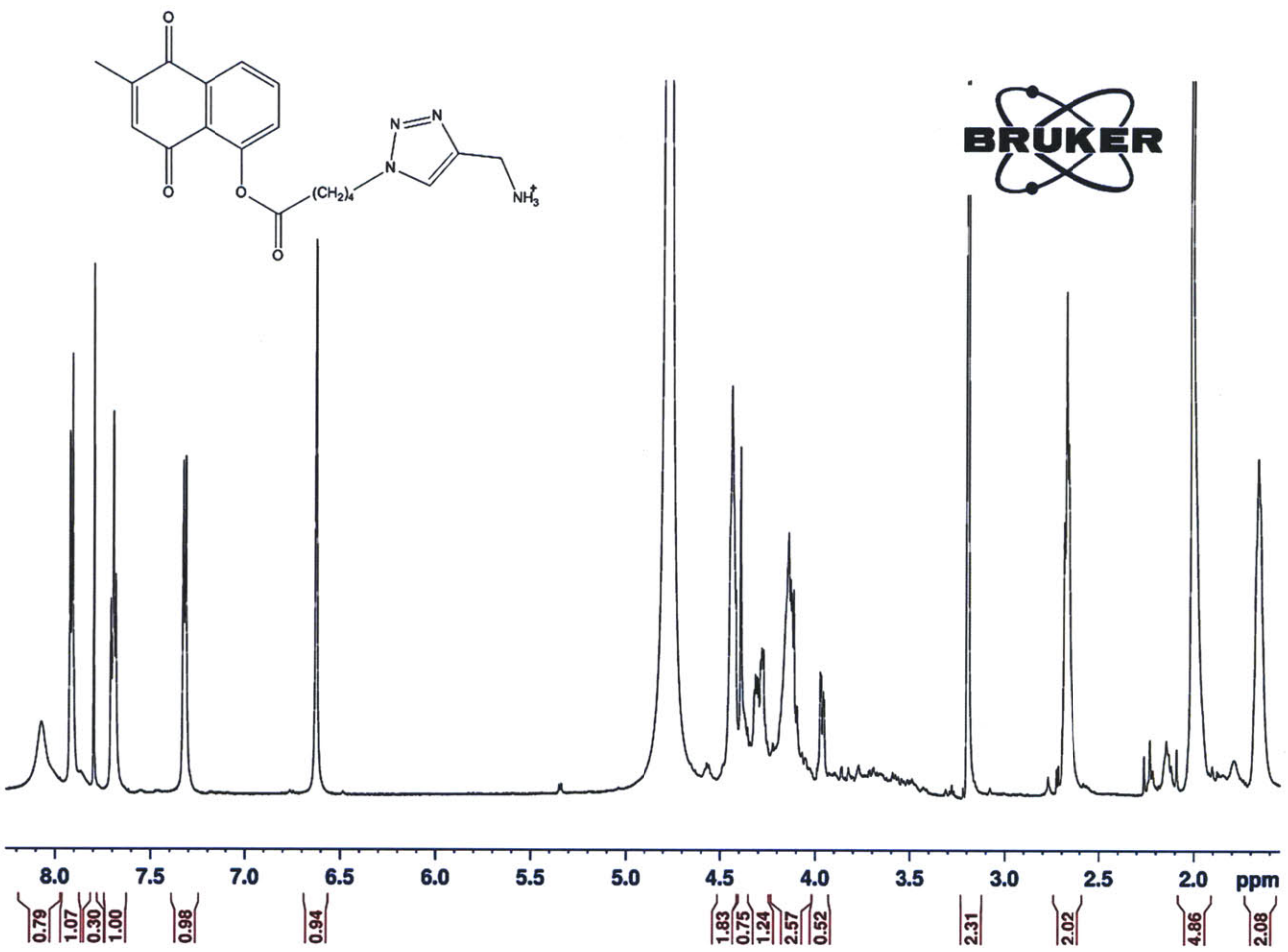
96. Hunter RL, Emanuele MR, Carpenter RH. 1996. Method for inhibiting microbial binding to surfaces. US Patent No. 5,494,660.

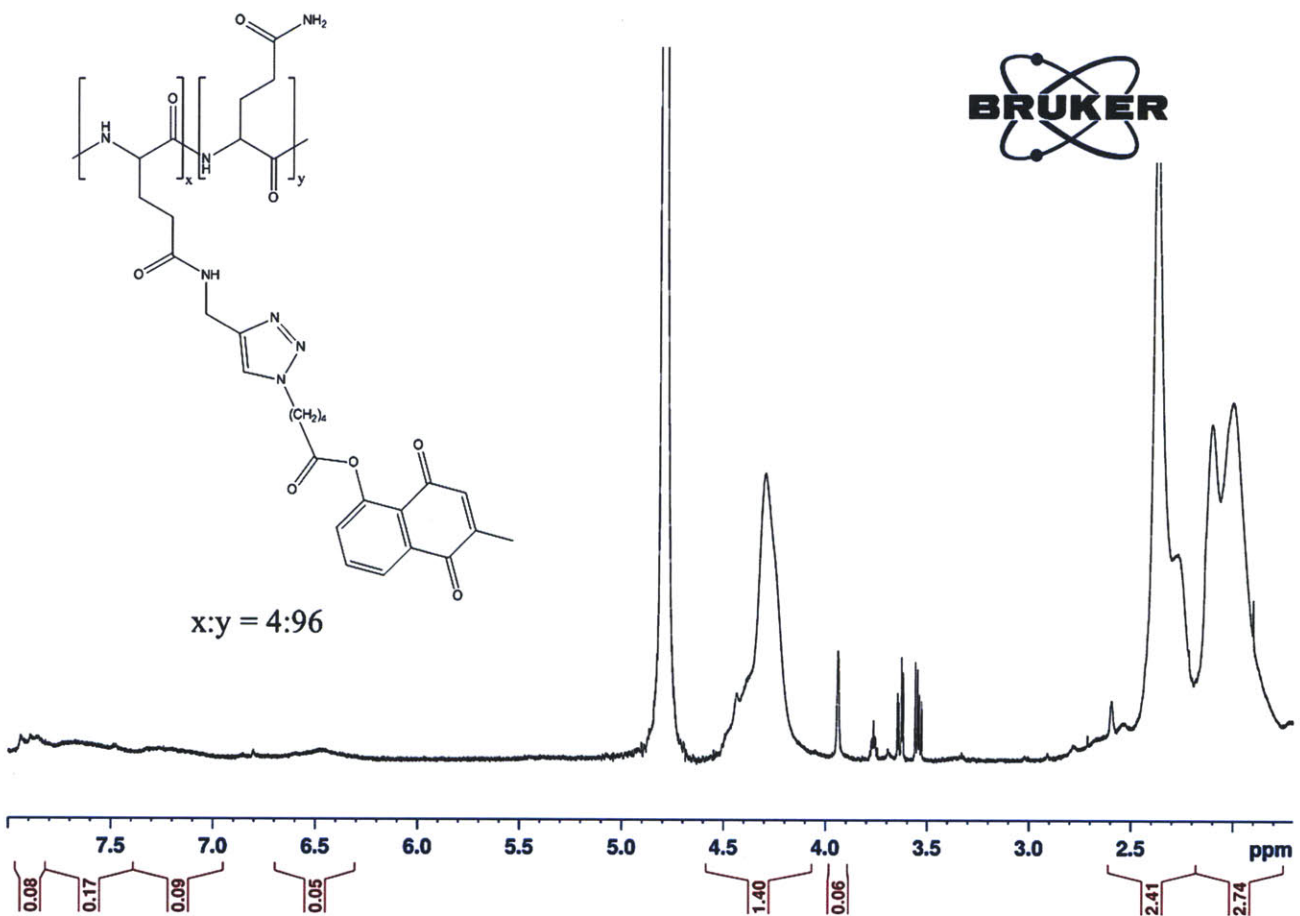
**Appendix A:** Selected NMR structures from Chapter 2  
(Unlabeled peaks are thought to be residual solvent or benign contaminants.)  
Poly-L-glutamate Na salt derivatized with 5-hydroxynaphthalene-1,4-dione (Chapter 2-2a)





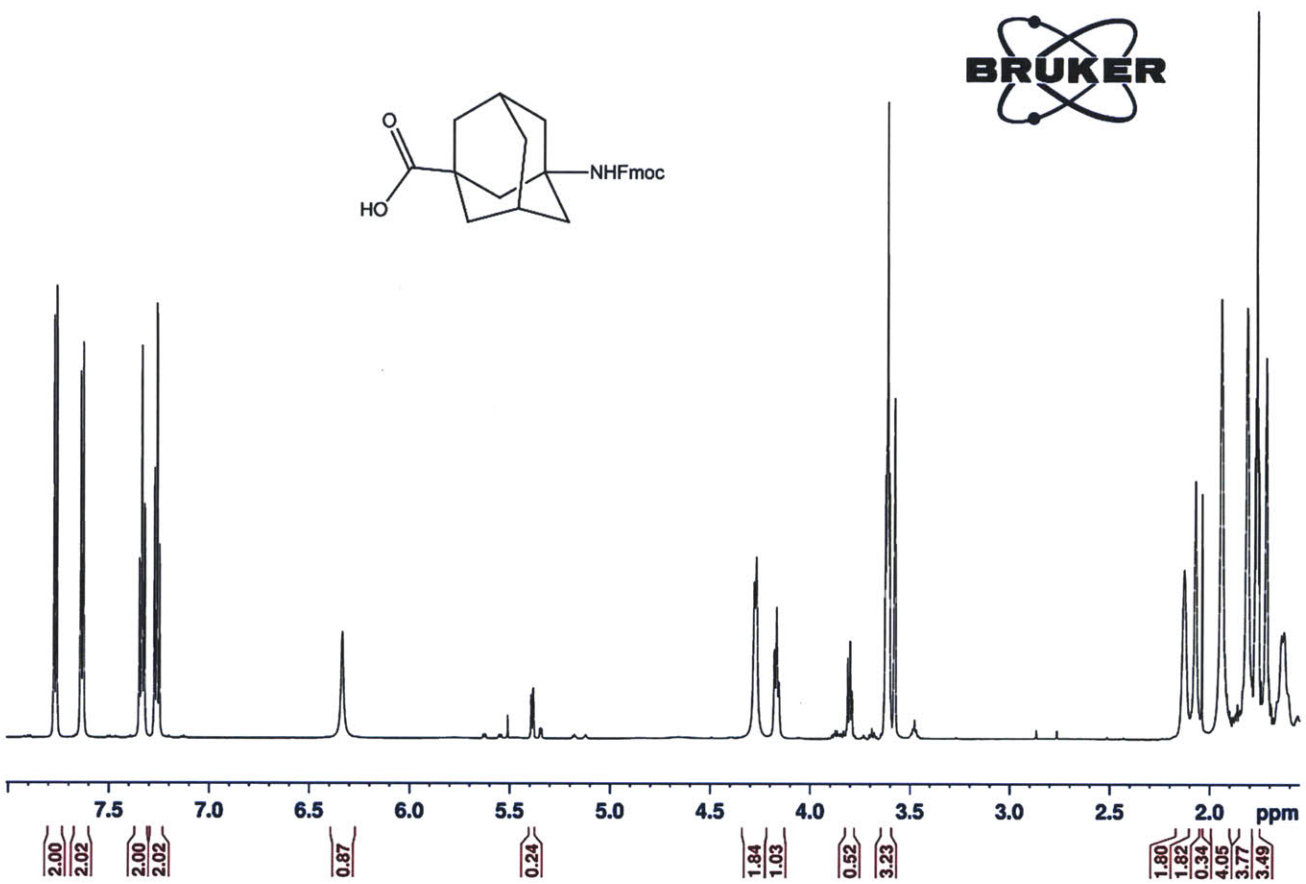


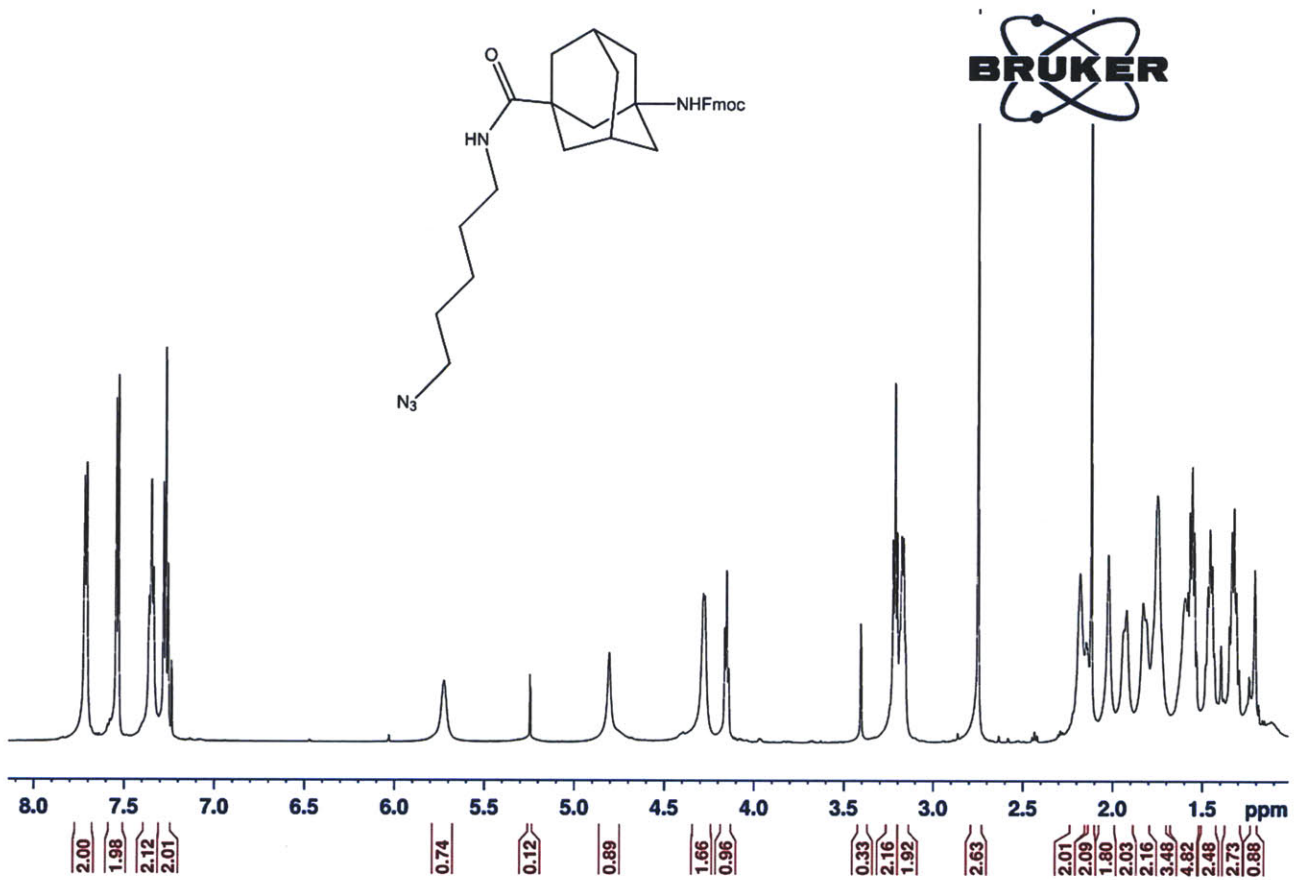


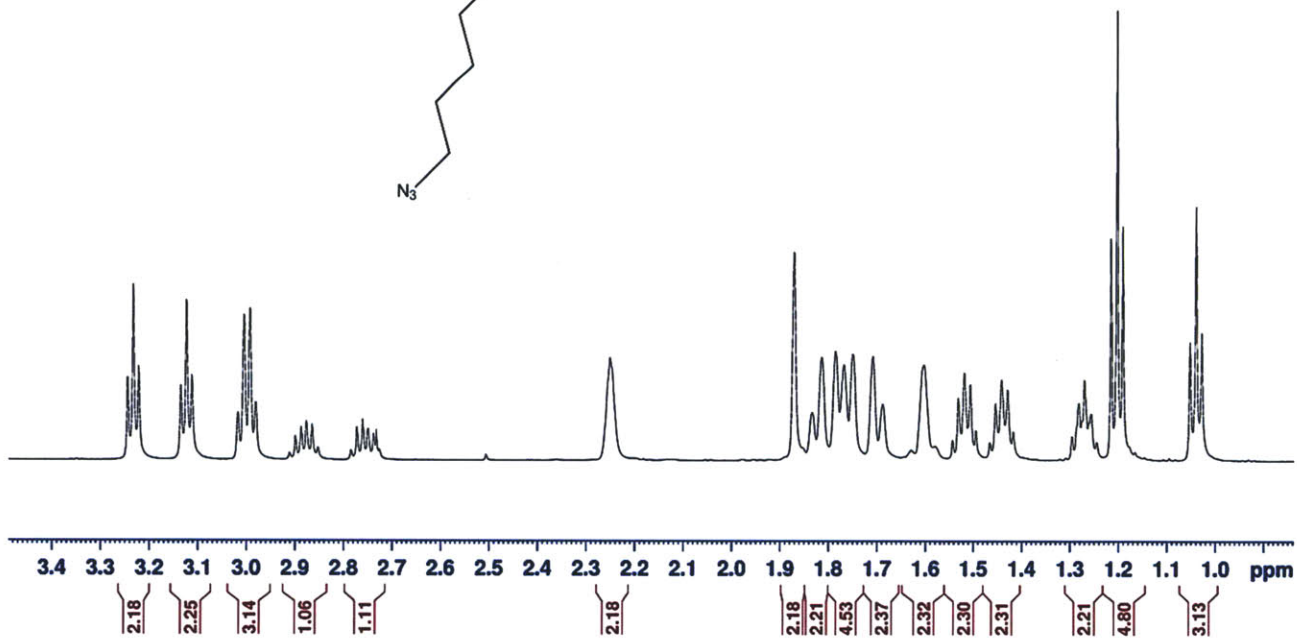
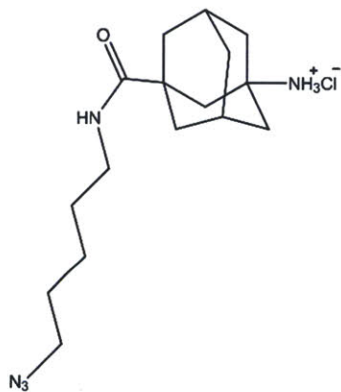


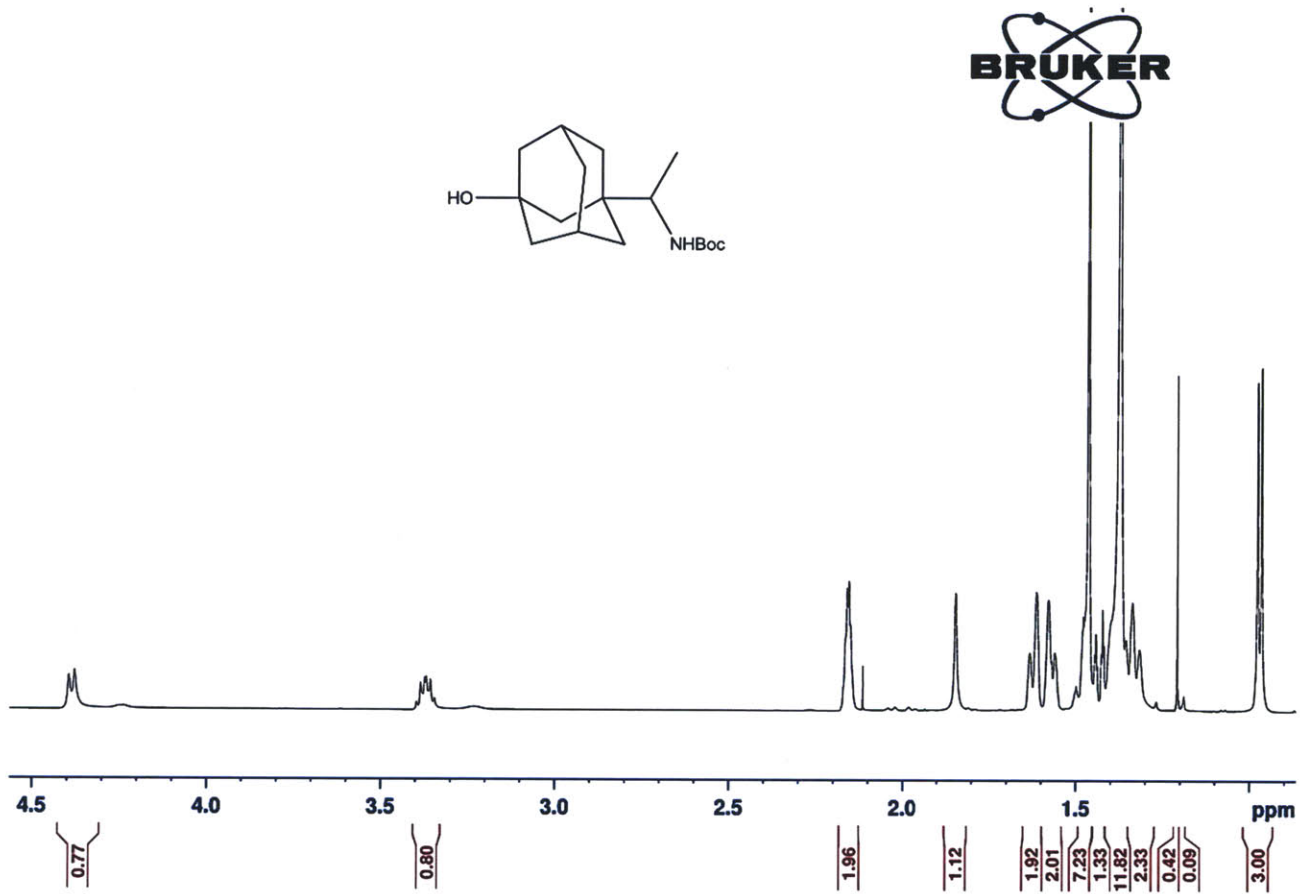


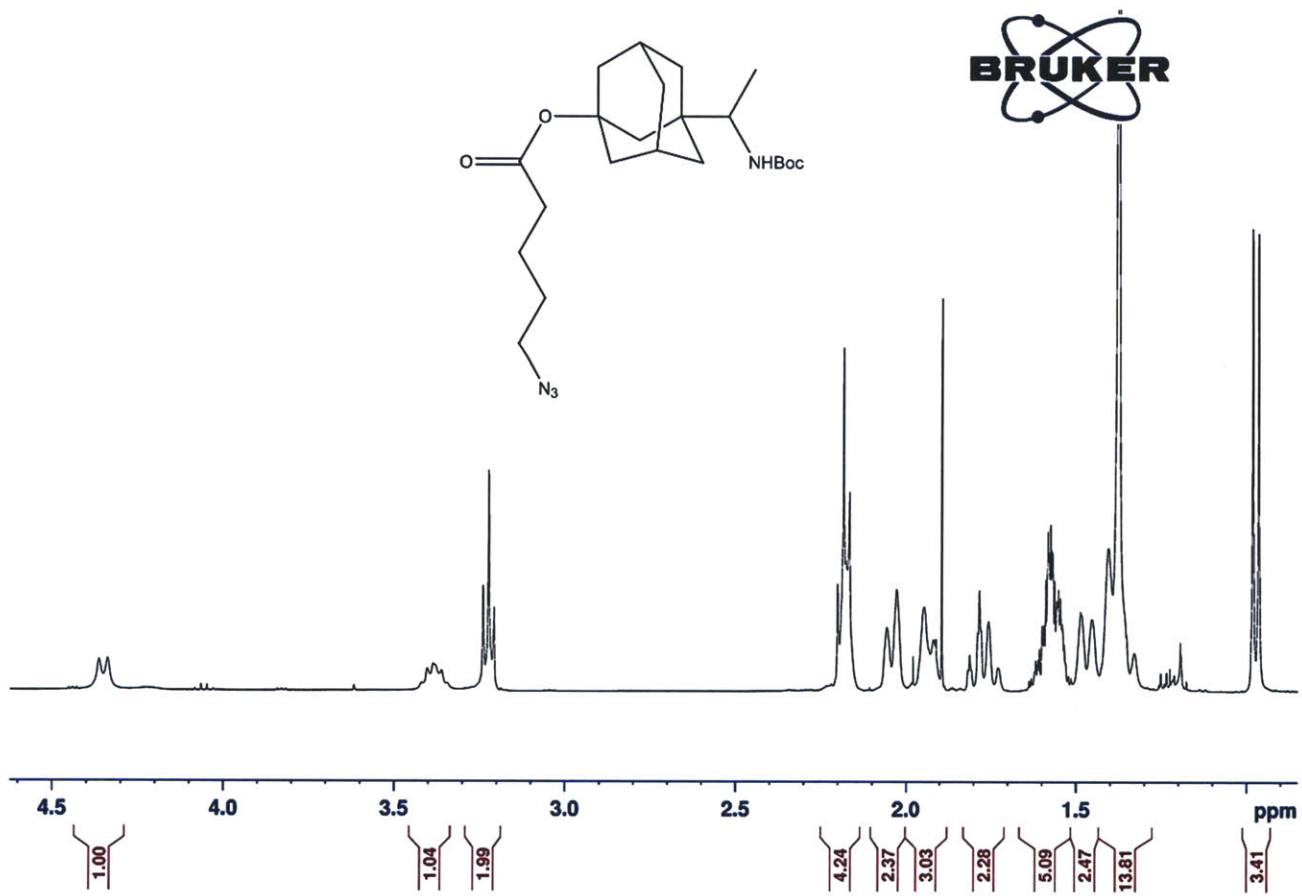
**Appendix B:** Selected NMR structures from Chapter 3  
(Unlabeled peaks are thought to be residual solvent or benign contaminants.)  
*N*-Fmoc-amantadine-COOH (Chapter 3-4)

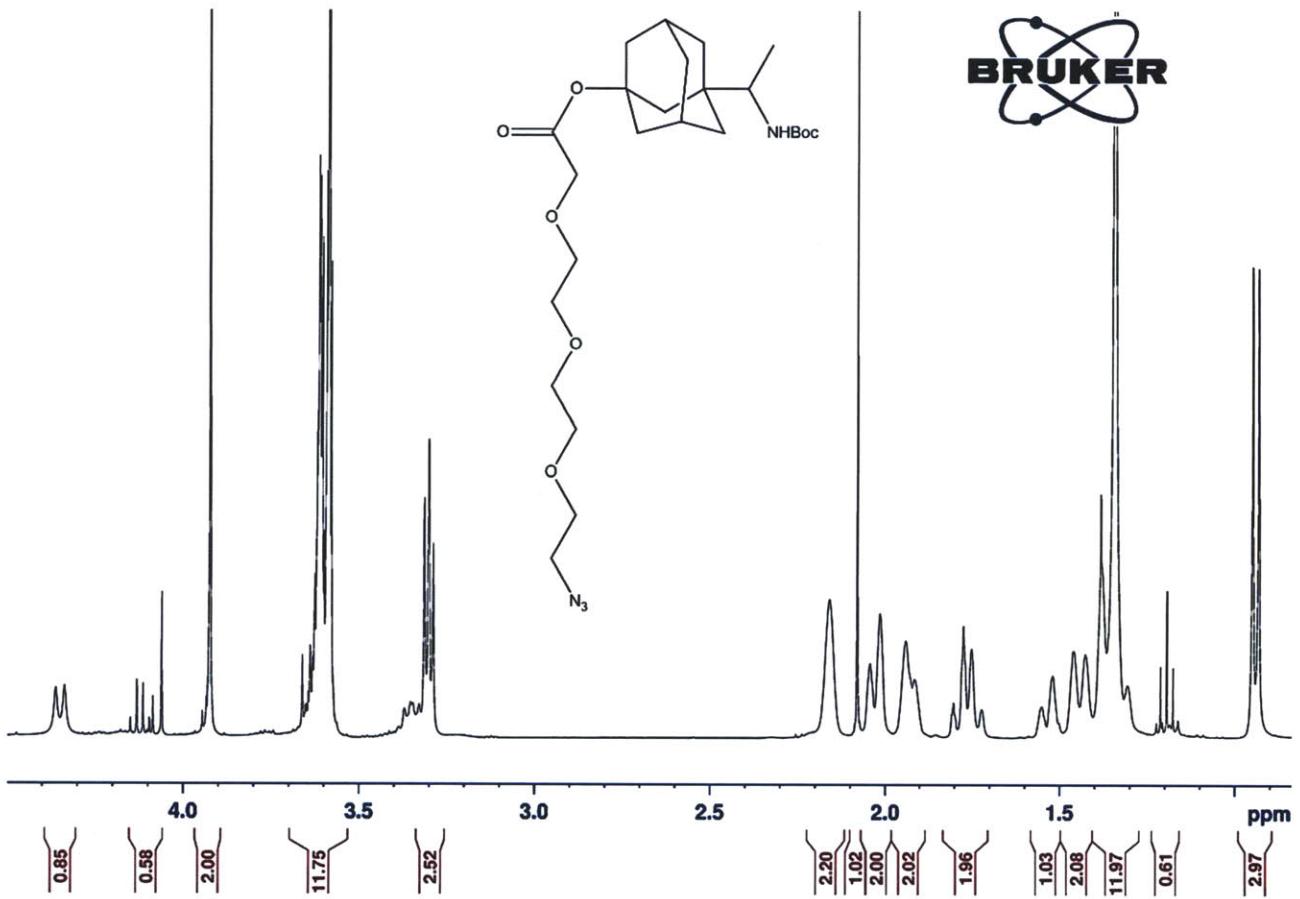


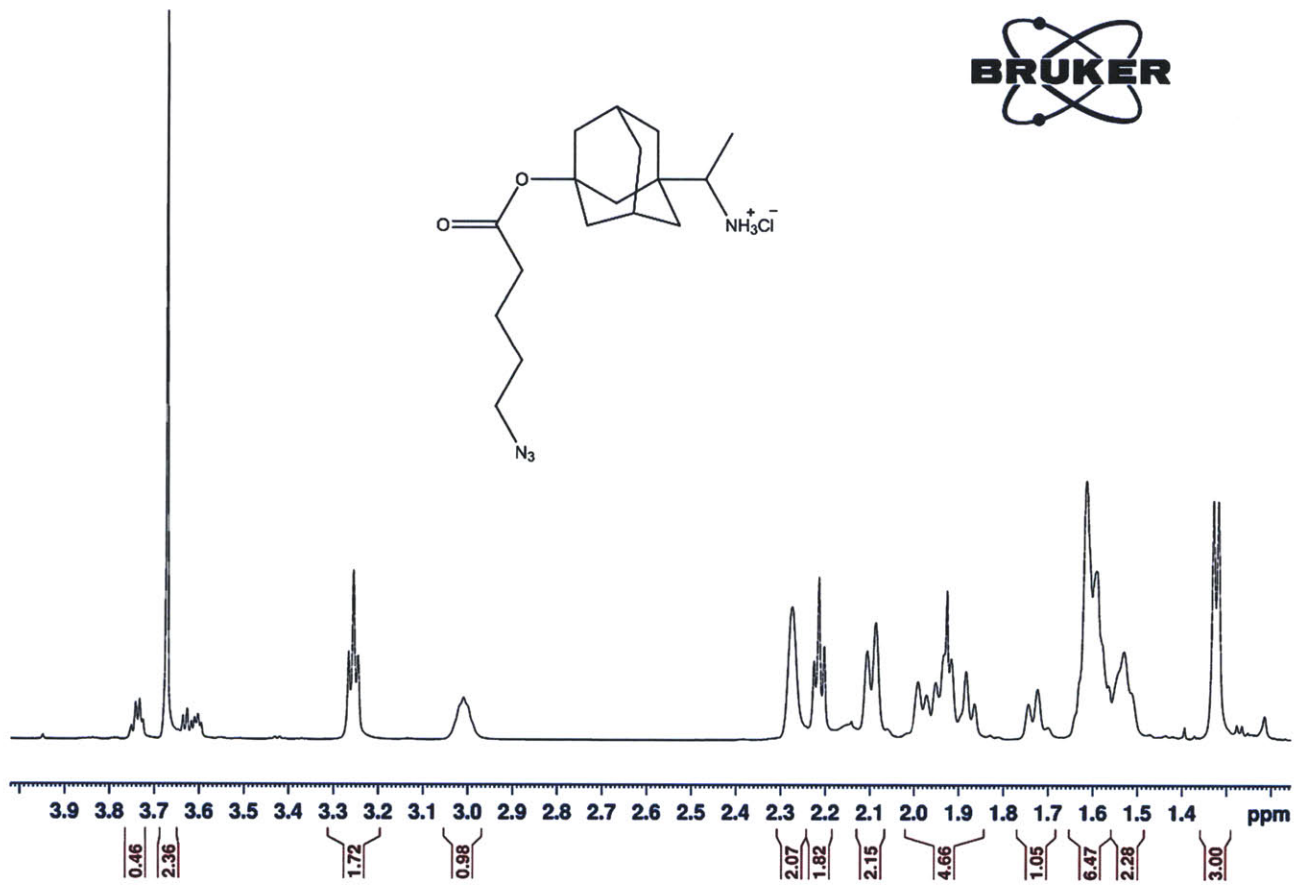
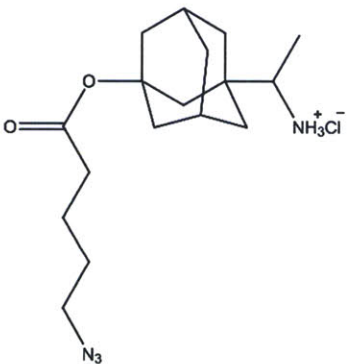


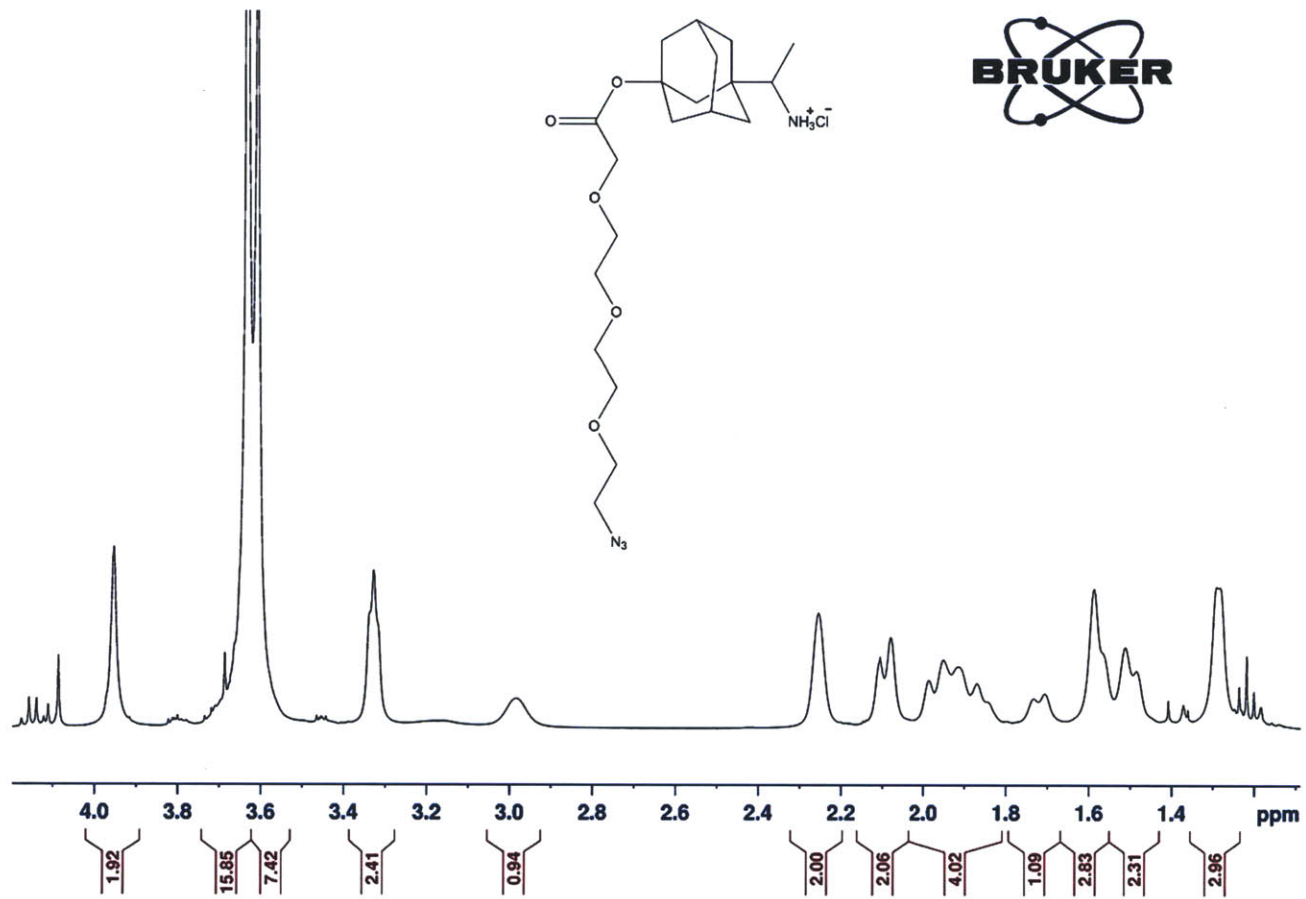




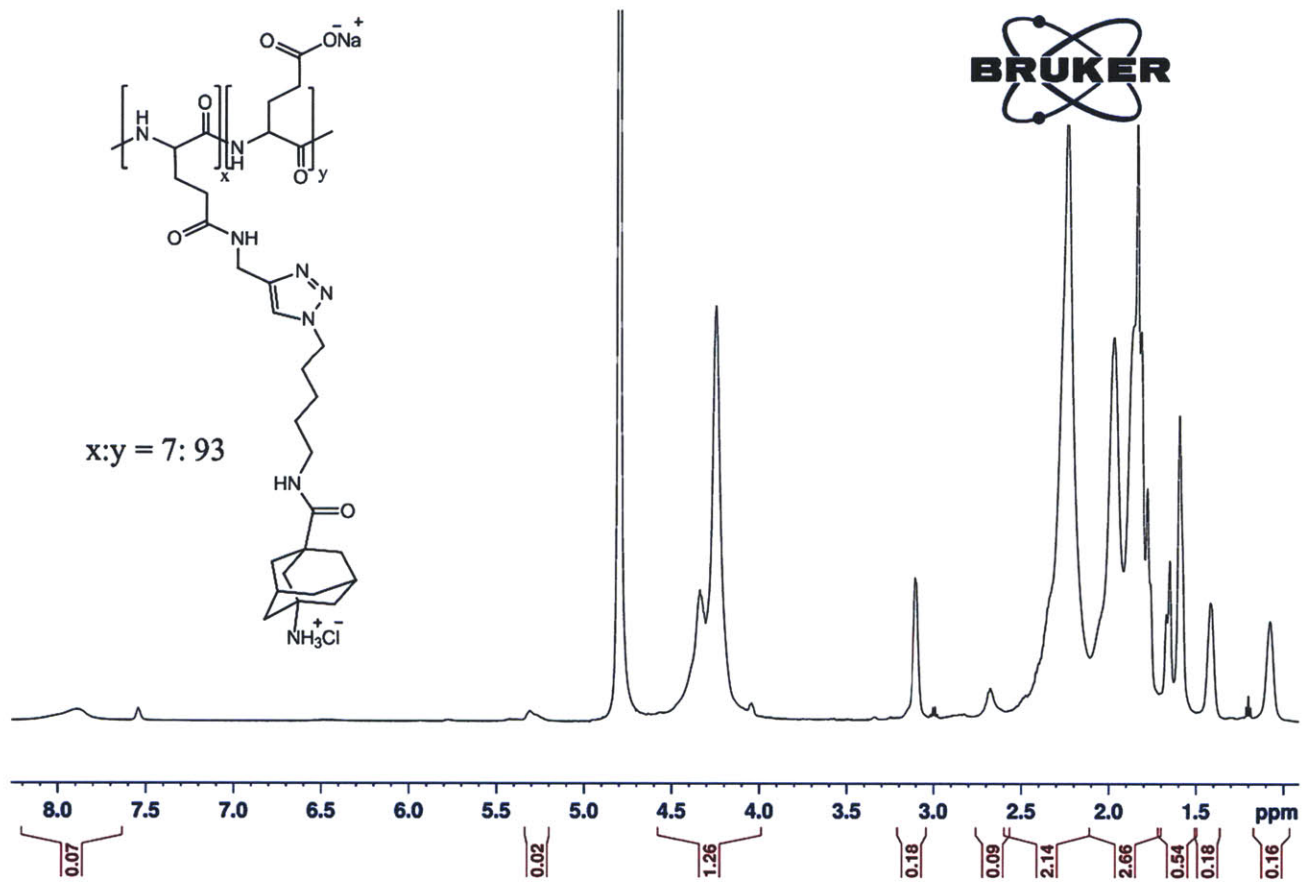


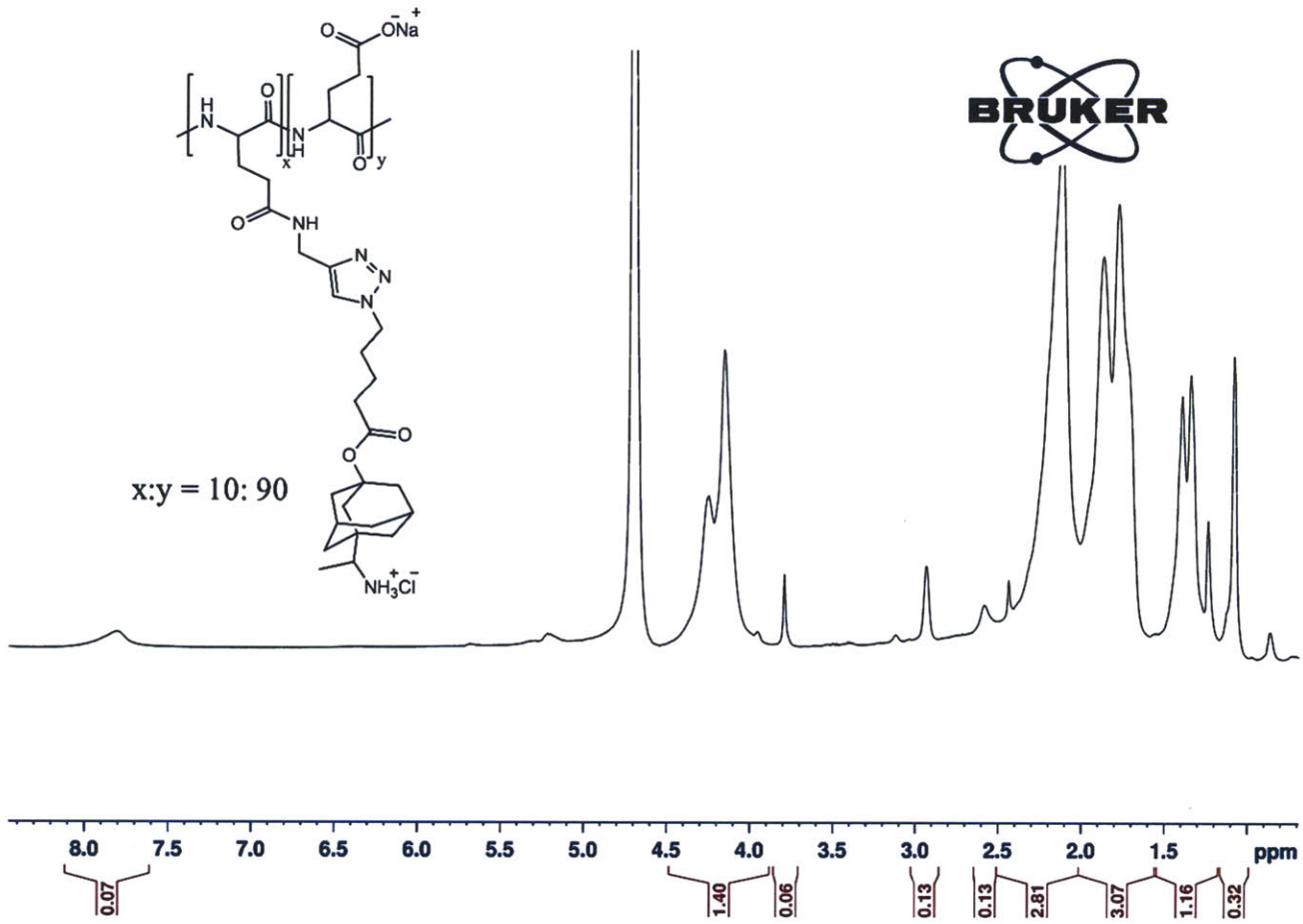


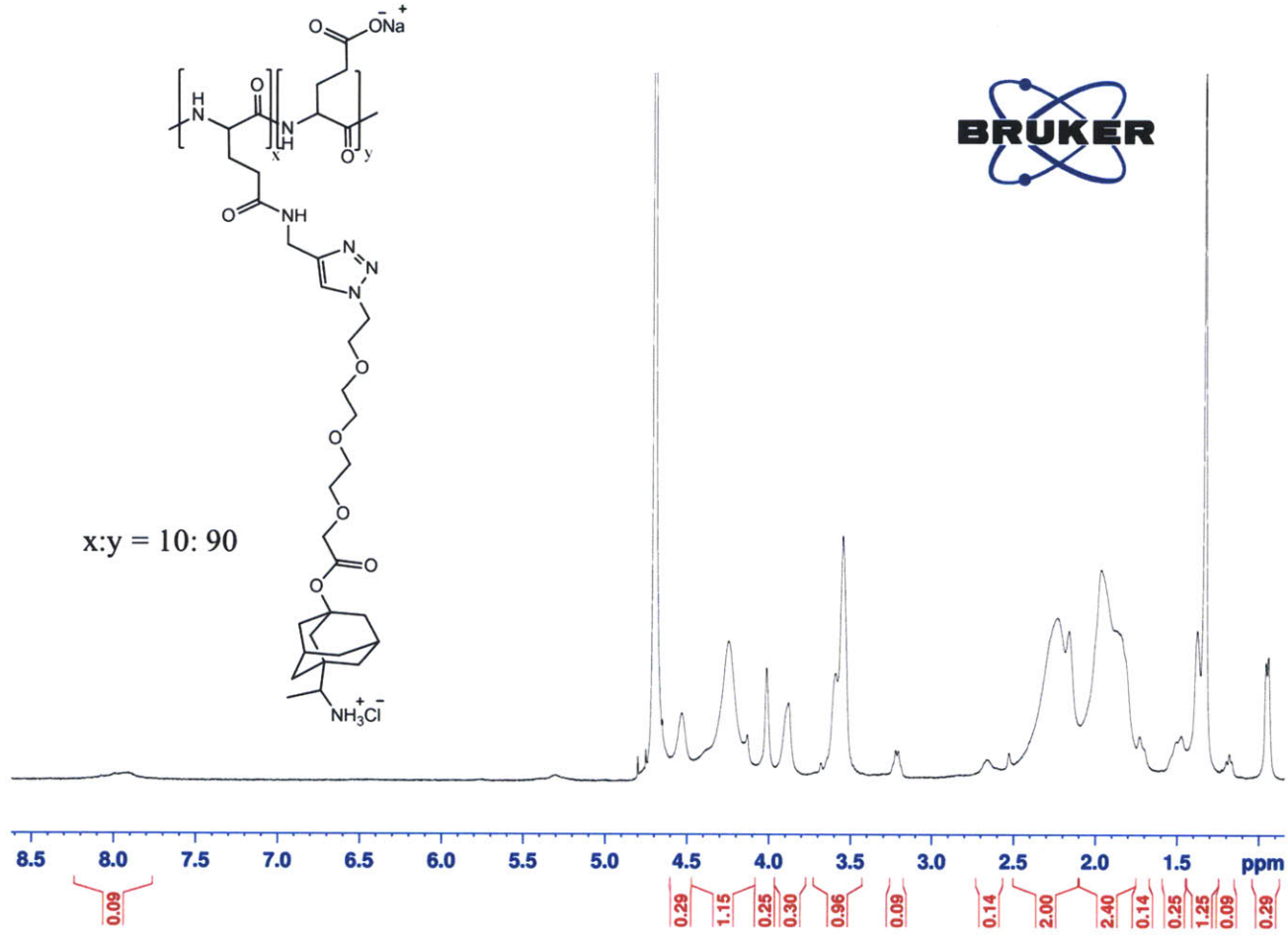


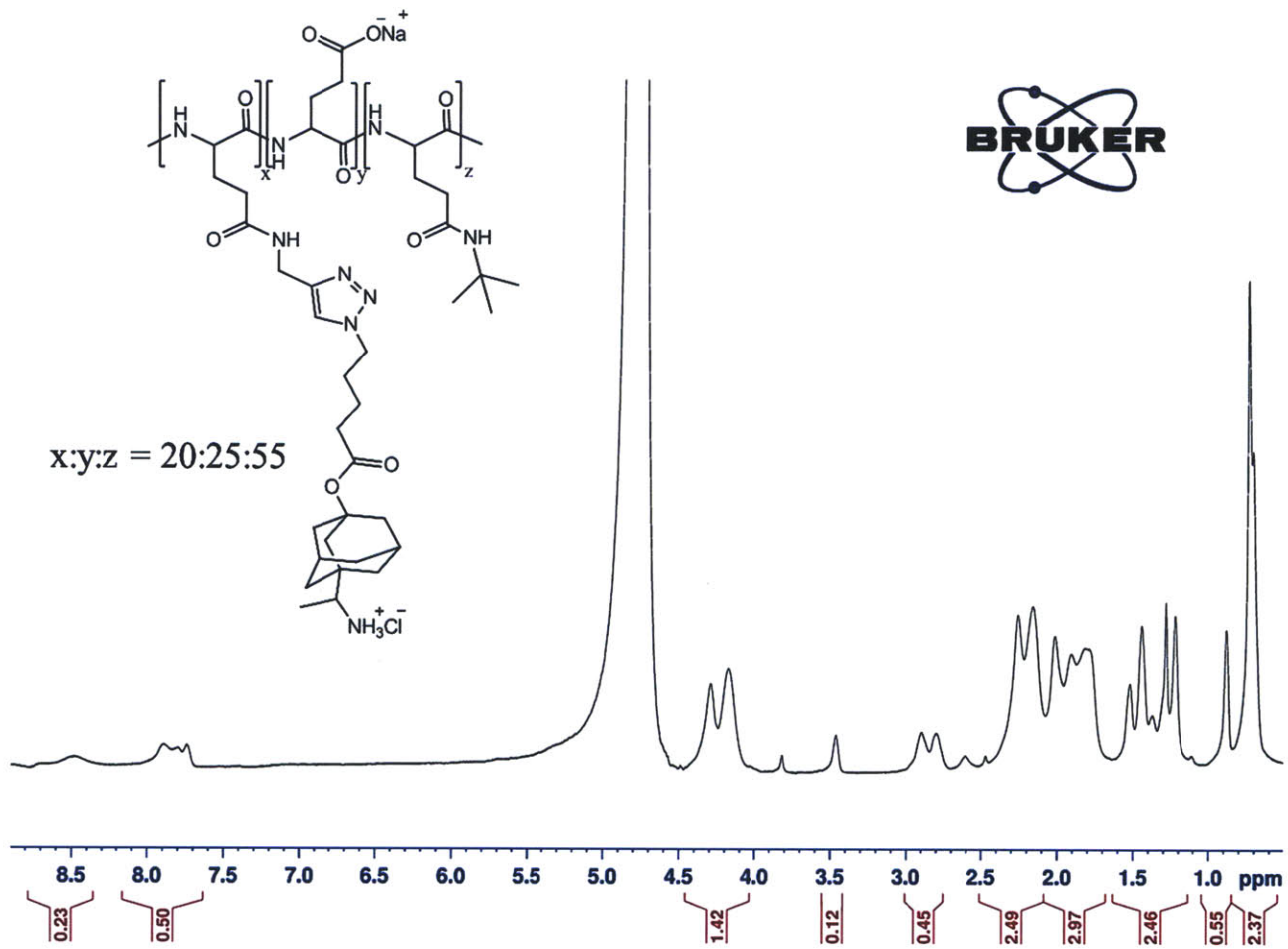


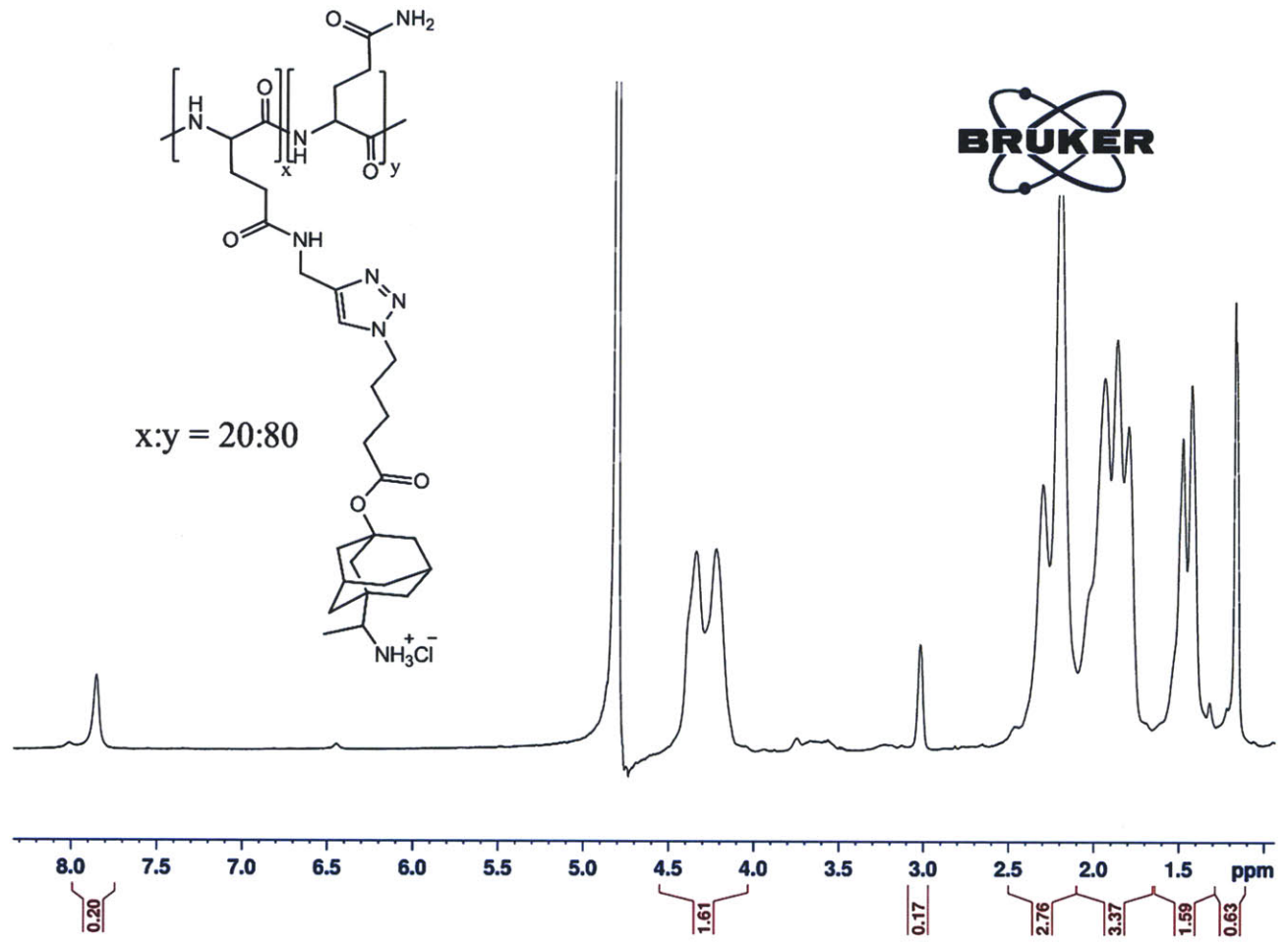


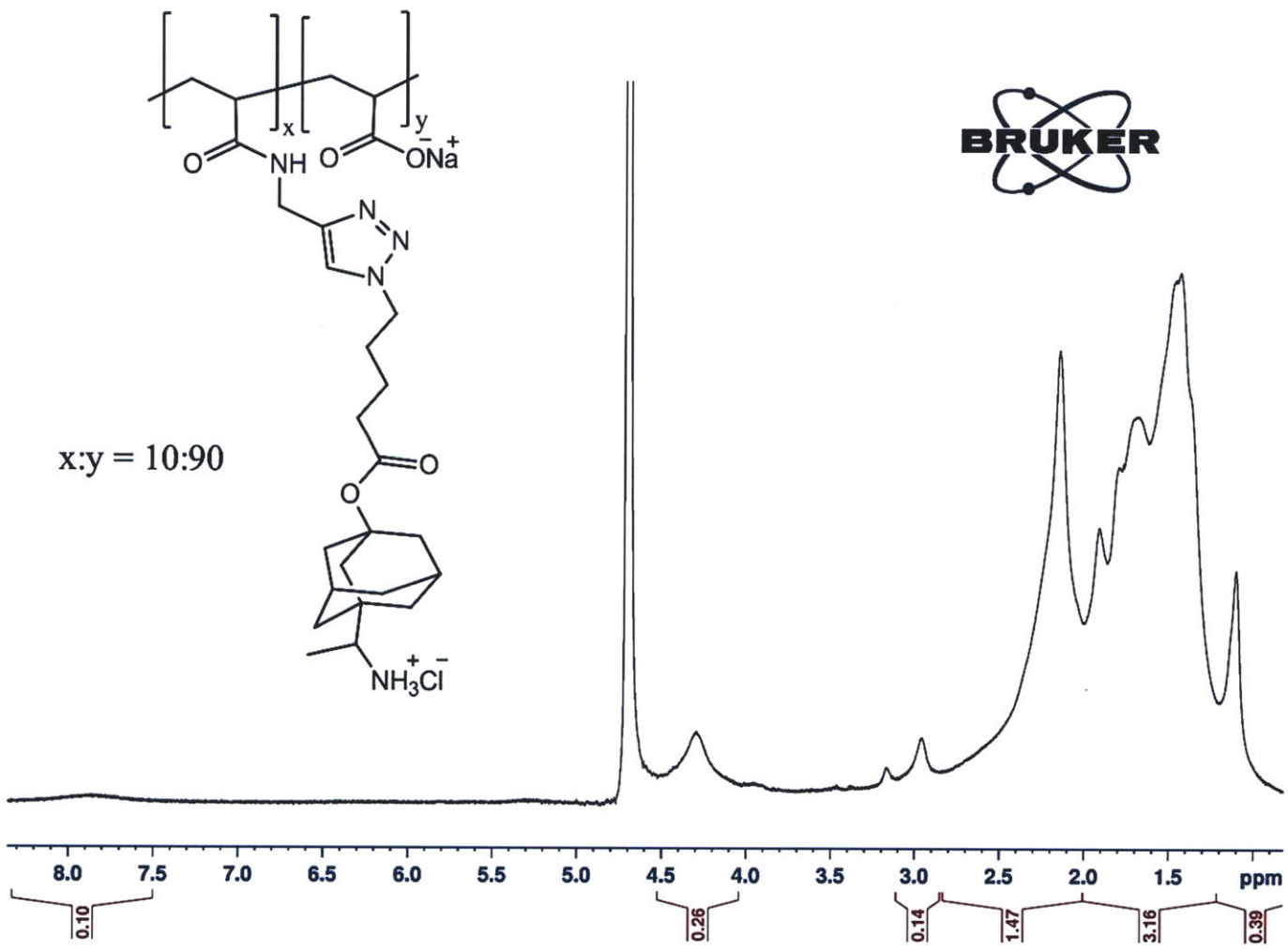


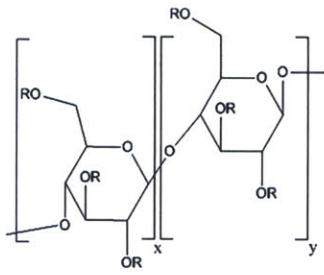








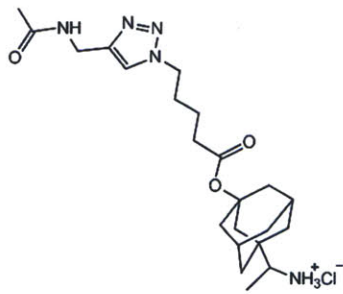




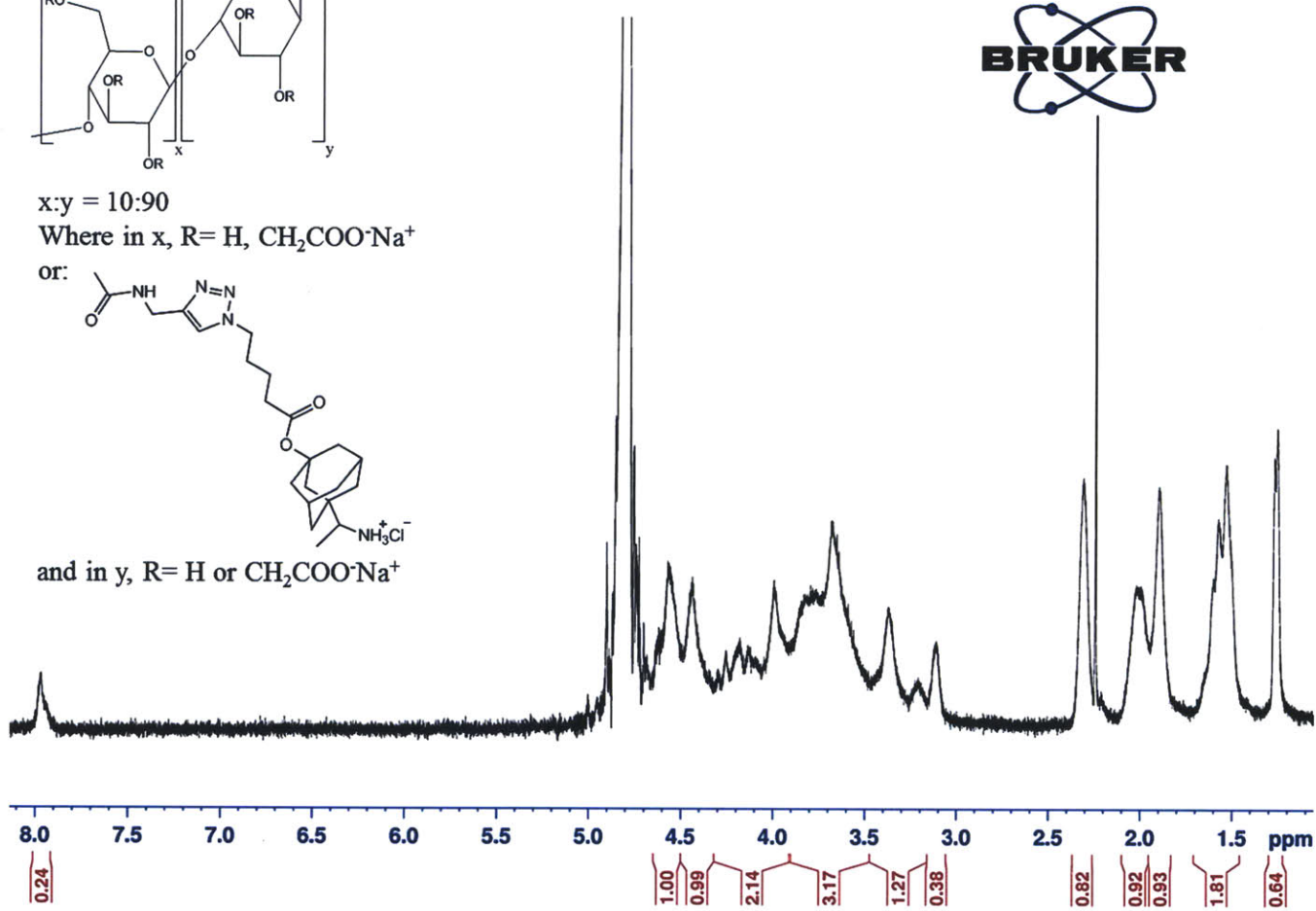
$x:y = 10:90$

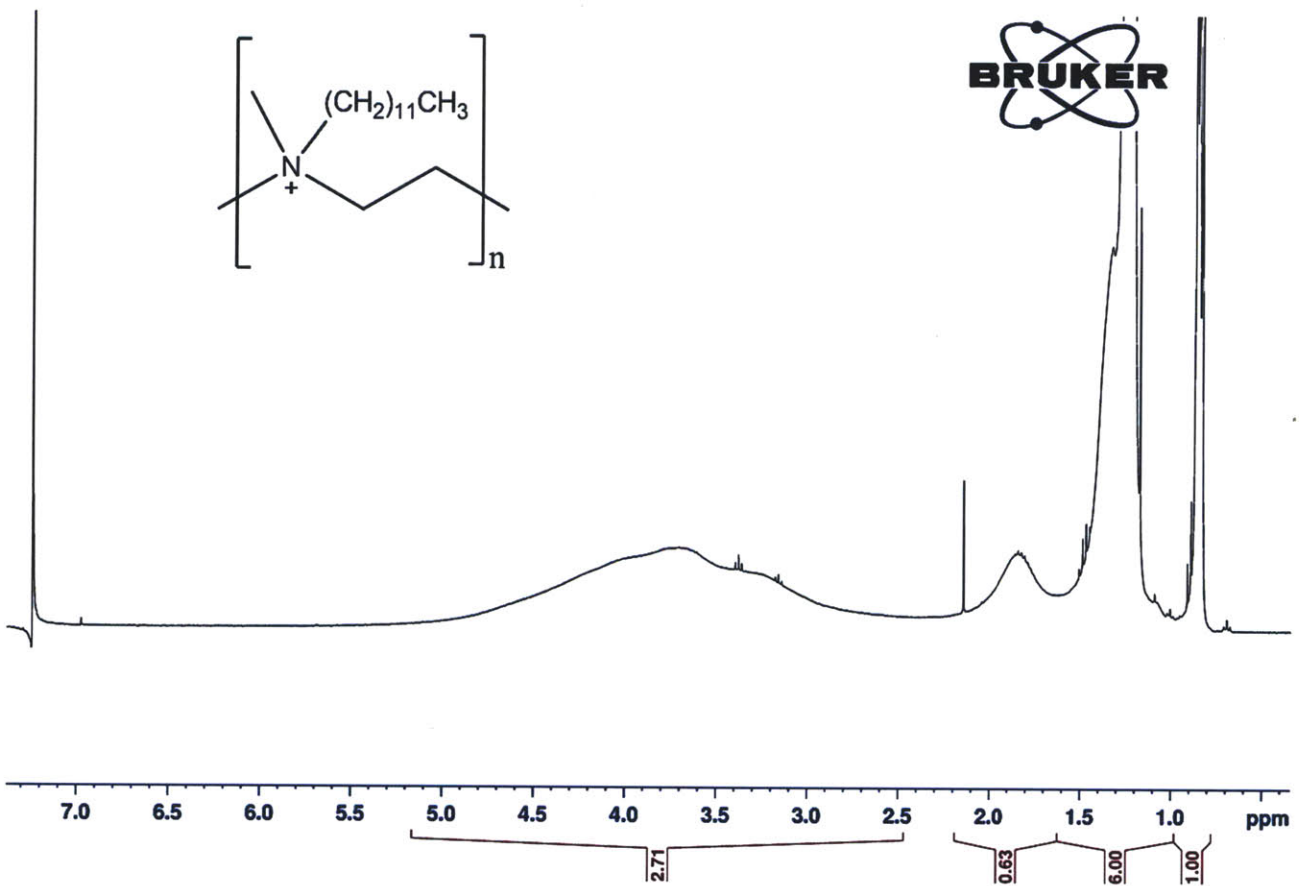
Where in x,  $R = H, CH_2COO^-Na^+$

or:

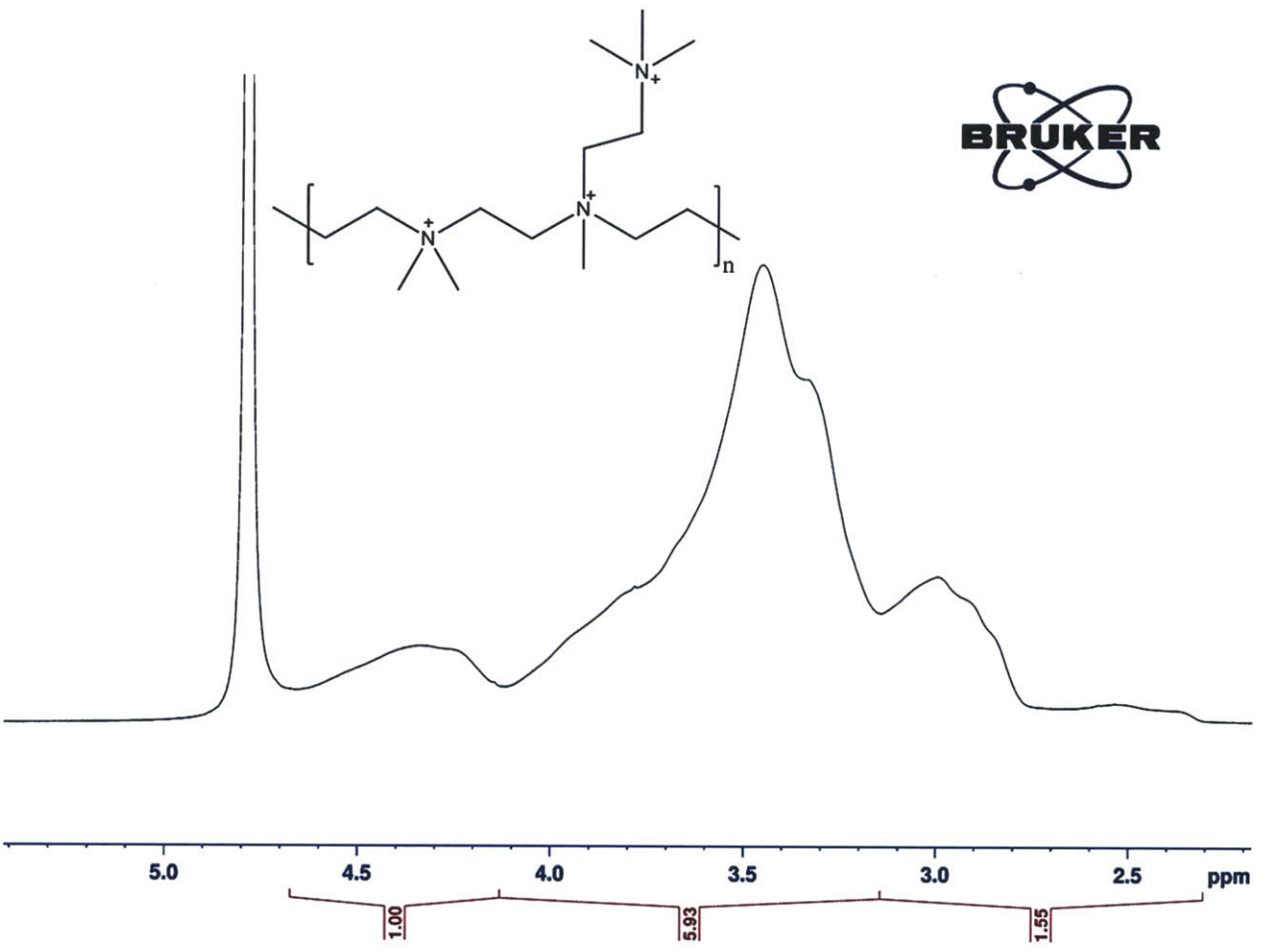


and in y,  $R = H$  or  $CH_2COO^-Na^+$









# CURRICULUM VITAE

## EDUCATION

• **Massachusetts Institute of Technology**, Cambridge, MA (September 2008-June 2013 anticipated)

**Ph.D. in Biochemistry**

Advisor: Professor Alexander M. Klibanov

• **University of California, Santa Barbara**, Santa Barbara, CA (September 2004-June 2008)

**Bachelor of Science in Biochemistry, Minor in Earth Sciences, Graduated with High Honors**

## EXPERIMENTAL AND LABORATORY SKILLS

### • Biological Skills:

- Tissue culture with mammalian cells
- Propagating and titering viruses
- Bacterial culture
- Bacterial protein expression in *E. coli*
- Site-directed mutagenesis, PCR
- Protein purification
- DNA and protein gel electrophoresis

### • Chemistry Skills:

- Polymer derivatization
- Glass surface derivatization
- Conjugation chemistry
- Copper-catalyzed click chemistry
- NMR characterization of small molecules and polymers

## RESEARCH EXPERIENCE

• **Massachusetts Institute of Technology**, Cambridge, MA (September 2008- present)

Research Assistant in the laboratories of Professor Alexander M Klibanov and Professor Jianzhu Chen  
Exploring mechanistically (i) the potency of polymer-attached inhibitors of influenza viruses, and (ii) antimicrobial action of surface-immobilized hydrophobic polycations based on alkylated polyethylenimine (PEI).

- Designed and synthesized polymer-attached inhibitors of influenza virus with a potency of over 200-fold greater than that of their monomeric precursors.
- Discovered the disinfecting effect of *N,N*-dodecyl,methyl-PEI against solutions of poliovirus, rotavirus, and herpes simplex viruses.
- Formulated polymer-attached adamantane influenza inhibitors that overcame some drug resistance in adamantane-resistant influenza strains.
- Communicated scientific results in first-author publications and oral presentations.

• **University of British Columbia**, Vancouver, Canada (August 2007)

Summer student researcher in the laboratory of Professor Lindsay Eltis

- Analyzed and compared propane monooxygenase gene sequences from various isolated bacteria.

• **Universität Bremen**, Bremen, Germany (June 2006-August 2006)

Summer student fellow in the lab of Professor Jorn Peckmann

- Extracted and analyzed lipid biomarkers in marine sediment collected from regions of coastal upwelling.

• **University of California, Santa Barbara**, Santa Barbara, CA (June 2005-June 2008)

Undergraduate researcher in the laboratory of Professor David Valentine

- Researched seawater advection into hydrocarbon seeps and analyzed propane monooxygenase genes from microbes isolated from hydrocarbon seeps.

## PUBLICATIONS

**Larson, A.M.**, Chen, J., Klibanov A.M. Conjugation to polymeric chains of influenza drugs targeting M2 ion channels partially restores their inhibition of drug-resistant mutants. Submitted to the *Journal of Pharmaceutical Sciences*

**Larson, A.M.**, Klibanov A.M. Biocidal packaging of pharmaceuticals, foods, and other perishables. *Annual Reviews of Chemical and Biomedical Engineering*, accepted for publication.

Gerrard, S.E., **Larson, A.M.**, Klibanov, A.M., Slater, N.K.H., Hanson, C.V., Abrams, B.F., Morris, M.K. Reducing infectivity of HIV upon exposure to surfaces coated with *N,N*-dodecyl,methyl-polyethylenimine. *Biotechnology and Bioengineering*, accepted for publication.

Park, D., **Larson, A.M.**, Klibanov, A.M., Wang, Y. Antiviral and antibacterial polyurethanes of various modalities. *Applied Biochemistry and Biotechnology*. Vol. 169, pp. 1134-1146, 2013.

**Larson, A.M.**, Oh, H., Knipe, D.M., Klibanov, A.M. Decreasing herpes simplex viral infectivity in solution by surface-immobilized and suspended *N,N*-dodecyl, methyl-polyethylenimine. *Pharmaceutical Research*. Vol. 30, pp. 25-31, 2013.

**Larson, A.M.**, Wang, H., Cao, Y., Jiang, T., Chen, J., Klibanov, A.M. Conjugating drug candidates to polymeric chains does not necessarily enhance anti-influenza activity. *Journal of Pharmaceutical Sciences*. Vol. 101, pp. 3896-3905, 2012.

**Larson, A.M.**, Hsu, B.B., Rautaray, D., Haldar, J., Chen, J., Klibanov, A.M. Hydrophobic polycationic coatings disinfect poliovirus and rotavirus solutions. *Biotechnology and Bioengineering*. Vol. 108, pp. 720-723, 2011.

Arning, E., Birgel, D., Schulz-Vogt, H., Holmkvist, L. Jørgensen, B., **Larson, A.**, Peckmann, J. Lipid Biomarker Patterns of Phosphogenic Sediments from Upwelling Regions. *Geomicrobiology Journal*. Vol. 25, pp. 69-82, 2008.

## ORAL PRESENTATIONS

American Chemical Society 244<sup>th</sup> National Meeting, Philadelphia, Pennsylvania. August 23, 2012.  
Division of Polymeric Materials.

American Chemical Society 241<sup>st</sup> National Meeting, Anaheim, California. March 27, 2011. Division of Polymeric Materials.

## AWARDS AND ACCOMPLISHMENTS

- **Massachusetts Institute of Technology**, Cambridge, MA
  - G.E.M.S. (Graduate Education in Medical Sciences) Scholar (2010-present)
  - Martin Family Society Fellow for Sustainability (2011-2012)
  - Graduate Student Teaching Certificate Program (2011)
  - Department of Chemistry Award for Outstanding Graduate Student Teaching (2009)
  - Completed 32 hour basic mediation skills training through Mediation@MIT
- **University of California, Santa Barbara**, Santa Barbara, CA
  - U.R.C.A. (Undergraduate Research and Creative Activities) grant (2007-2008)

## LEADERSHIP AND SERVICE

- **NeXXt Scholars Program** (through the New York Academy of Sciences-Inaugural group). Mentor (September 2012-Present)
- **MIT Chemistry Career Panel Series**- Founding member (2012)
- **Volunteer Consulting Group** (through the consulting club at MIT) (June 2011-August 2011)
- **Department of Chemistry Resources for Easing Friction and Stress (chemREFS)**: Mediator (June 2010- Present)
- **Environmental Health and Safety Committee for the MIT Chemistry Department**: Student representative (December 2009- Present)
- **Women in Chemistry**: Member: (June 2009-Present; Co-president: August 2011-August 2012)
- **MIT Chemistry Graduate Student Council**: Member (February 2009-Present; Secretary: June 2009-August 2010; Co-president: August 2010-August 2011)

## TEACHING EXPERIENCE

- **Massachusetts Institute of Technology**, Cambridge, MA (September 2008- December 2012)  
Teaching Assistant: Biological Chemistry (5.07), Biological Chemistry Laboratory (undergraduate) (5.36), and Biological Chemistry Laboratory (graduate) (5.52).
- **University of California, Santa Barbara**, Santa Barbara, CA (September 2006- June 2008)  
Campus Learning Assistance Services (C.L.A.S.) tutor: General Chemistry (1a, 1b, and 1c), Geology 1.